Published for SISSA by Springer

Received: *April 30, 2017*
Accepted: *August 29, 2017*
Published: *September 19, 2017*

Search for new phenomena in a lepton plus high jet multiplicity final state with the ATLAS experiment using $\sqrt{s} = 13$ TeV proton-proton collision data

The ATLAS collaboration

E-mail: atlas.publications@cern.ch

Abstract: A search for new phenomena in final states characterized by high jet multiplicity, an isolated lepton (electron or muon) and either zero or at least three b-tagged jets is presented. The search uses 36.1 fb^{-1} of $\sqrt{s} = 13$ TeV proton-proton collision data collected by the ATLAS experiment at the Large Hadron Collider in 2015 and 2016. The dominant sources of background are estimated using parameterized extrapolations, based on observables at medium jet multiplicity, to predict the b-tagged jet multiplicity distribution at the higher jet multiplicities used in the search. No significant excess over the Standard Model expectation is observed and 95% confidence-level limits are extracted constraining four simplified models of R-parity-violating supersymmetry that feature either gluino or top-squark pair production. The exclusion limits reach as high as 2.1 TeV in gluino mass and 1.2 TeV in top-squark mass in the models considered. In addition, an upper limit is set on the cross-section for Standard Model $t\bar{t}t\bar{t}$ production of 60 fb (6.5 $\times$ the Standard Model prediction) at 95% confidence level. Finally, model-independent limits are set on the contribution from new phenomena to the signal-region yields.

Keywords: Beyond Standard Model, Hadron-Hadron scattering (experiments)

ArXiv ePrint: 1704.08493

https://doi.org/10.1007/JHEP09(2017)088

JHEP09(2017)088

Contents

1 Introduction

The ATLAS experiment at the Large Hadron Collider (LHC) has carried out a large number of searches for beyond the Standard Model (BSM) physics. These searches cover a broad range of different final-state particles and kinematics. However, one gap in the search coverage, as pointed out in refs. [1, 2], is in final states with one or more leptons, many jets and no-or-little missing transverse momentum (the magnitude of which is denoted by

JHEP09(2017)088

$E_{\mathrm{T}}^{\mathrm{miss}}$). Such a search is presented in this article, considering final states with an isolated lepton (electron or muon), at least eight to twelve jets (depending on the jet transverse momentum threshold), either zero or many b-tagged jets, and with no requirement on $E_{\mathrm{T}}^{\mathrm{miss}}$.

This search has potential sensitivity to a large number of BSM physics models. In this article, model-independent limits on the possible contribution of BSM physics to several single-bin signal regions are presented. In addition, four R-parity-violating (RPV) supersymmetric (SUSY [3–8]) benchmark models are used to interpret the results. In this case, a multi-bin fit to the two-dimensional space of jet-multiplicity and b-tagged jet multiplicity is used to constrain the models. The dominant Standard Model (SM) background arises from top-quark pair production and W/Z+jets production, with at least one lepton produced in the vector boson decay. The theoretical modelling of these backgrounds at high jet multiplicity suffers from large uncertainties, so they are estimated from the data by extrapolating the b-tagged jet multiplicity distribution extracted at moderate jet multiplicities to the high jet multiplicities of the search region. Previous searches targeting similar RPV SUSY models have been carried out by the ATLAS and CMS collaborations [9–12].

The result is also used to search for SM four-top-quark production. Previous searches for four-top-quark production were carried out by the ATLAS [13] and CMS [14] collaborations.

2 ATLAS detector

The ATLAS detector [15] is a multipurpose detector with a forward-backward symmetric cylindrical geometry and nearly 4π coverage in solid angle.[1] The inner detector (ID) tracking system consists of silicon pixel and microstrip detectors covering the pseudorapidity region $|\eta| < 2.5$, surrounded by a transition radiation tracker which improves electron identification in the region $|\eta| < 2.0$. The innermost pixel layer, the insertable B-layer [16], was added between Run 1 and Run 2 of the LHC, at a radius of 33 mm around a new, narrower and thinner, beam pipe. The ID is surrounded by a thin superconducting solenoid providing an axial 2 T magnetic field and by a fine-granularity lead/liquid-argon (LAr) electromagnetic calorimeter covering $|\eta| < 3.2$. A steel/scintillator-tile calorimeter provides hadronic calorimetry in the central pseudorapidity range ($|\eta| < 1.7$). The endcap and forward regions ($1.5 < |\eta| < 4.9$) of the hadronic calorimeter are made of LAr active layers with either copper or tungsten as the absorber material. A muon spectrometer with an air-core toroidal magnet system surrounds the calorimeters. Three layers of high-precision tracking chambers provide coverage in the range $|\eta| < 2.7$, while dedicated chambers allow triggering in the region $|\eta| < 2.4$.

The ATLAS trigger system [17] consists of two levels; the first level is a hardware-based system, while the second is a software-based system called the High-Level Trigger.

[1] ATLAS uses a right-handed coordinate system with its origin at the nominal interaction point in the centre of the detector. The positive x-axis is defined by the direction from the interaction point to the centre of the LHC ring, with the positive y-axis pointing upwards, while the beam direction defines the z-axis. Cylindrical coordinates (r, ϕ) are used in the transverse plane, ϕ being the azimuthal angle around the z-axis. The pseudorapidity η is defined in terms of the polar angle θ by $\eta = -\ln\tan(\theta/2)$. The transverse momentum p_{T} is defined in the x-y plane. Rapidity is defined as $y = 0.5\ln[(E+p_z)/(E-p_z)]$ where E denotes the energy and p_z is the component of the momentum along the beam direction.

JHEP09(2017)088

3 Data and simulated event samples

3.1 Data sample

After applying beam, detector and data-quality criteria, the data sample analysed comprises 36.1 fb^{-1} of $\sqrt{s}$ = 13 TeV proton-proton (pp) collision data (3.2 fb^{-1} collected in 2015 and 32.9 fb^{-1} collected in 2016) with a minimum pp bunch spacing of 25 ns. In this data set, the mean number of pp interactions per proton-bunch crossing (pile-up) is $\langle\mu\rangle$ = 23.7. The luminosity and its uncertainty of 3.2% are derived following a methodology similar to that detailed in ref. [18] from a preliminary calibration of the luminosity scale using a pair of x–y beam separation scans performed in August 2015 and June 2016.

Events are recorded online using a single-electron or single-muon trigger with thresholds that give a constant efficiency as a function of lepton-p_{T} of ≈90% (≈80%) for electrons (muons) for the event selection used. For the determination of the multi-jet background, alternative lepton triggers, using less stringent lepton isolation requirements with respect to the nominal ones, are considered, as discussed in section 6. Single-photon and multi-jet triggers are also employed to select data samples used in the validation of the background estimation technique.

3.2 Simulated event samples

Samples of Monte Carlo (MC) simulated events are used to model the signal and to validate the background estimation procedure for the dominant background contributions. In addition, simulated events are used to model the sub-dominant background processes. The response of the detector to particles is modelled with a full ATLAS detector simulation [19] based on GEANT4 [20], or with a fast simulation based on a parameterization of the response of the ATLAS electromagnetic and hadronic calorimeters [21] and on GEANT4 elsewhere. All simulated events are overlaid with pile-up collisions simulated with the soft strong interaction processes of PYTHIA 8.186 [22] using the A2 set of tunable parameters (tune) [23] and the MSTW2008LO [24] parton distribution function (PDF) set. The simulated events are reconstructed in the same way as the data, and are reweighted so that the distribution of the expected number of collisions per bunch crossing matches the one in the data.

For all MC samples used, except those produced by the SHERPA event generator, the EVTGEN 1.2.0 program [25] is used to model the properties of bottom and charm hadron decays.

3.2.1 Simulated signal events

Simulated signal events from four SUSY benchmark models are used to guide the analysis selections and to estimate the expected signal yields for different signal-mass hypotheses used to interpret the analysis results. In all models, the RPV couplings and the SUSY particle masses are chosen to ensure prompt decays of the SUSY particles. Diagrams of the first three benchmark simplified models, which involve gluino pair production, are shown in figures 1(a), 1(b), and 1(c). In the first model, each gluino decays via a virtual top squark to two top quarks and the lightest neutralino ($\tilde{\chi}_1^0$) which is the lightest supersymmetric

JHEP09(2017)088

particle (LSP). The $\tilde{\chi}_1^0$ decays to three light quarks ($\tilde{\chi}_1^0 \to uds$) via the RPV coupling λ''_{112}. For this model, $\tilde{\chi}_1^0$ masses below 10 GeV are not considered in order to avoid the effect of the limited phase space in the $\tilde{\chi}_1^0$ decay. In the second model, each gluino decays to a top quark and a top squark LSP, with the top squark decaying to an s-quark and a b-quark via a non-zero λ''_{323} RPV coupling.[2] The third model involves the gluino decaying to two first or second generation quarks ($q \equiv (u, d, s, c)$) and the $\tilde{\chi}_1^0$ LSP, which then decays to two additional first or second generation quarks and a charged lepton or a neutrino ($\tilde{\chi}_1^0 \to q\bar{q}'\ell$ or $\tilde{\chi}_1^0 \to q\bar{q}\nu$, labelled as $\tilde{\chi}_1^0 \to q\bar{q}\ell/\nu$). The decay proceeds via a λ' RPV coupling, where each RPV decay can produce any of the four first- and second-generation leptons ($e^{\pm}, \mu^{\pm}, \nu_e, \nu_\mu$) with equal probability. For this model, $\tilde{\chi}_1^0$ masses below 50 GeV are not considered.

The fourth scenario considered involves right-handed top-squark pair production with the top squark decaying to a bino or higgsino LSP and a top or bottom quark. The LSP decays through the non-zero RPV coupling $\lambda''_{323} \approx \mathcal{O}(10^{-2}\text{–}10^{-1})$, with the value chosen to ensure prompt decays for the particle masses considered[3] and to avoid more complex patterns of RPV decays that are not considered here. Figure 1(d) shows the production and possible decays considered. The different decay modes depend on the nature of the LSP and have a small dependence on the top-squark mass, with the top squark decaying as: $\tilde{t} \to t\tilde{\chi}_1^0$ for a bino-like LSP and as $\tilde{t} \to t\tilde{\chi}_2^0$ (≈25%), $\tilde{t} \to t\tilde{\chi}_1^0$ (≈25%), $\tilde{t} \to b\tilde{\chi}_1^+$ (≈50%) for higgsino-like LSPs. With the chosen model parameters, the electroweakinos decay as $\tilde{\chi}_{1/2}^0 \to tbs$ or $\tilde{\chi}_1^{\pm} \to bbs$. The search results are interpreted in this model, with the assumption of either a pure higgsino ($\tilde{H}$) or pure bino ($\tilde{B}$) LSP. In the case of a wino LSP, the search has no sensitivity as the top squark decays directly as $\tilde{t} \to \bar{b}\bar{s}$ with no leptons produced in the final state.[4]

Event samples for the first signal model ($\tilde{g} \to t\bar{t}\tilde{\chi}_1^0 \to t\bar{t}uds$) are produced using the Herwig++ 2.7.1 [29] event generator with the CTEQ6L1 [30] PDF set, and the UEEE5 tune [31]. For the other three models, the MG5_aMC@NLO v2.3.3 [32] event generator interfaced to Pythia 8.210 is used. For these cases, signal events are produced with either one ($\tilde{g} \to t\bar{t}\tilde{t} \to t\bar{t}b\bar{s}$ model) or two ($\tilde{g} \to q\bar{q}\tilde{\chi}_1^0 \to q\bar{q}q\bar{q}\ell/\nu$ and $\tilde{t} \to t\tilde{H}/\tilde{B}$ models) additional partons in the matrix element and using the A14 [33] tune. The parton luminosities are provided by the NNPDF23LO [34] PDF set.

Signal cross-sections are calculated to next-to-leading order in the strong coupling constant, adding the resummation of soft-gluon emission at next-to-leading-logarithmic accuracy (NLO+NLL) [35–39]. The nominal cross-section and its uncertainty are taken from an envelope of cross-section predictions using different PDF sets as well as different factorization and renormalization scales, as described in ref. [40].

The analysis is also used to search for SM four-top-quark production. In this case, the $t\bar{t}t\bar{t}$ sample is generated with the MG5_aMC@NLO 2.2.2 event generator interfaced to Pythia 8.186 using the NNPDF23LO PDF set and the A14 tune.

[2]The same final state can be produced by requiring a non-zero λ''_{313} RPV coupling, however the minimal flavour violation hypothesis [26] favours a large λ''_{323} coupling [27].

[3]LSP masses below 200 GeV are not considered as in this case non-prompt RPV decays can occur.

[4]For this case, a dedicated ATLAS search [28] excludes top-squark masses up to 315 GeV.

JHEP09(2017)088

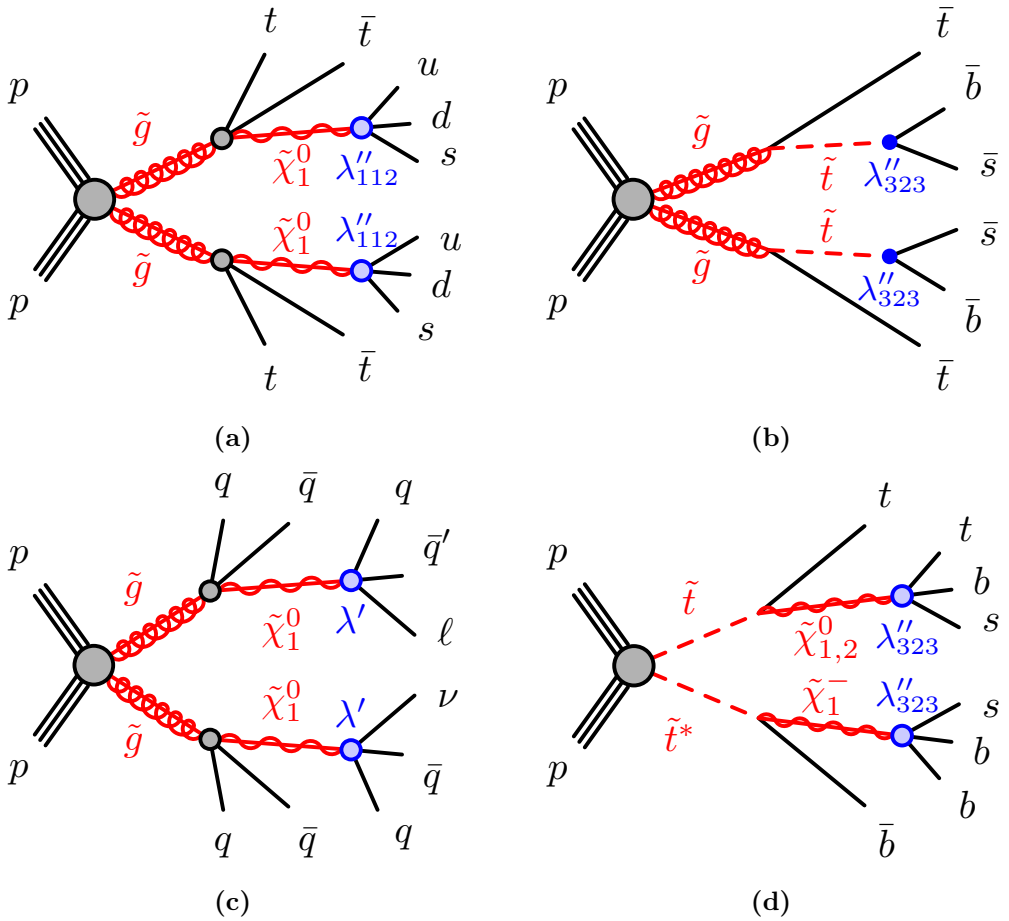

Figure 1. Diagrams of the four simplified signal benchmark models considered. The first three models involve pair production of gluinos with each gluino decaying as (a) $\tilde{g} \to t\bar{t}\tilde{\chi}_1^0 \to t\bar{t}uds$, (b) $\tilde{g} \to \bar{t}\tilde{t} \to \bar{t}b\bar{s}$, (c) $\tilde{g} \to q\bar{q}\tilde{\chi}_1^0 \to q\bar{q}q\bar{q}\ell/\nu$. The fourth model (d) involves pair production of top squarks with the decay $\tilde{t} \to t\tilde{\chi}_{1/2}^0$ or $\tilde{t} \to b\tilde{\chi}_1^+$ and with the LSP decays $\tilde{\chi}_{1/2}^0 \to tbs$ or $\tilde{\chi}_1^+ \to \bar{b}\bar{b}\bar{s}$; the specific decay depends on the nature of the LSP. In all signal scenarios, anti-squarks decay into the charge-conjugate final states of those indicated for the corresponding squarks, and each gluino decays with equal probabilities into the given final state or its charge conjugate.

3.2.2 Simulated background events

The dominant backgrounds from top-quark pair production and W/Z+jets production are estimated from the data as described in section 6, whereas the expected yields for minor backgrounds are taken from MC simulation. In addition, the background estimation procedure is validated with simulated events, and some of the systematic uncertainties are estimated using simulated event samples. The samples used are shown in table 1 and more details of the event generator configurations can be found in refs. [41–44].

4 Event reconstruction

For a given event, primary vertex candidates are required to be consistent with the luminous region and to have at least two associated tracks with $p_{\mathrm{T}} > 400$ MeV. The vertex with the largest $\sum p_{\mathrm{T}}^2$ of the associated tracks is chosen as the primary vertex of the event.

JHEP09(2017)088

Physics process	Event generator	Parton-shower modelling	Cross-section normalization	PDF set	Tune
$W(\to \ell\nu)$ + jets	Sherpa 2.2.1 [45]	Sherpa 2.2.1	NNLO [46]	NLO CT10 [47]	Sherpa default
$W(\to \ell\nu)$ + jets (*)	MG5_aMC@NLO 2.2.2	Pythia 8.186	NNLO	NNPDF2.3LO	A14
$W(\to \ell\nu)$ + jets (*)	Alpgen v2.14 [48]	Pythia 6.426 [49]	NNLO	CTEQ6L1	Perugia2012 [50]
$Z/\gamma^*(\to \ell\ell)$ + jets	Sherpa 2.2.1	Sherpa 2.2.1	NNLO [46]	NLO CT10	Sherpa default
$t\bar{t}$ + jets	powheg-box v2 [51]	Pythia 6.428	NNLO+NNLL [52–57]	NLO CT10	Perugia2012
$t\bar{t}$ + jets (*)	MG5_aMC@NLO 2.2.2	Pythia 8.186	NNLO+NNLL	NNPDF2.3LO	A14
Single-top (t-channel)	powheg-box v1	Pythia 6.428	NNLO+NNLL [58]	NLO CT10f4	Perugia2012
Single-top (s- and Wt-channel)	powheg-box v2	Pythia 6.428	NNLO+NNLL [59, 60]	NLO CT10	Perugia2012
$t\bar{t}+W/Z/WW$	MG5_aMC@NLO 2.2.2	Pythia 8.186	NLO [32]	NNPDF2.3LO	A14
WW, WZ and ZZ	Sherpa 2.2.1	Sherpa 2.2.1	NLO	NLO CT10	Sherpa default
$t\bar{t}H$	MG5_aMC@NLO 2.3.2	Pythia 8.186	NLO [61]	NNPDF2.3LO	A14
$t\bar{t}t\bar{t}$	MG5_aMC@NLO 2.2.2	Pythia 8.186	NLO [32]	NNPDF2.3LO	A14

Table 1. Simulated background event samples: the corresponding event generator, parton-shower modelling, cross-section normalization, PDF set and underlying-event tune are shown. The samples marked with (*) are alternative samples used to validate the background estimation method.

Jet candidates are reconstructed using the anti-k_t jet clustering algorithm [62, 63] with a radius parameter of 0.4 starting from energy deposits in clusters of calorimeter cells [64]. The jets are corrected for energy deposits from pile-up collisions using the method suggested in ref. [65] and calibrated with ATLAS data in ref. [66]: a contribution equal to the product of the jet area and the median energy density of the event is subtracted from the jet energy. Further corrections derived from MC simulation and data are used to calibrate on average the energies of jets to the scale of their constituent particles [67]. In the search, three jet p_{T} thresholds of 40 GeV, 60 GeV and 80 GeV are used, with all jets required to have $|\eta| < 2.4$. To minimize the contribution from jets arising from pile-up interactions, the selected jets must satisfy a loose jet vertex tagger (JVT) requirement [68], where JVT is an algorithm that uses tracking and primary vertex information to determine if a given jet originates from the primary vertex. The chosen working point has an efficiency of 94% at a jet p_{T} of 40 GeV and is nearly fully efficient above 60 GeV for jets originating from the hard parton-parton scatter. This selection reduces the number of jets originating from, or heavily contaminated by, pile-up interactions, to a negligible level. Events with jet candidates originating from detector noise or non-collision background are rejected if any of the jet candidates satisfy the 'LooseBad' quality criteria, described in ref. [69]. The coverage of the calorimeter and the jet reconstruction techniques allow high-jet-multiplicity final states to be reconstructed efficiently. For example, 12 jets take up only about one fifth of the available solid angle.

Jets containing a b-hadron (b-jets) are identified by a multivariate algorithm using information about the impact parameters of ID tracks matched to the jet, the presence of displaced secondary vertices, and the reconstructed flight paths of b- and c-hadrons inside the jet [70]. The operating point used corresponds to an efficiency of 78% in simulated $t\bar{t}$ events, along with a rejection factor of approximately 110 for jets induced by gluons or light quarks and of 8 for charm jets [71], and is configured to give a constant b-tagging efficiency as a function of jet p_{T}.

JHEP09(2017)088

Since there is no requirement on $E_{\mathrm{T}}^{\mathrm{miss}}$ or any $E_{\mathrm{T}}^{\mathrm{miss}}$ derived quantity the search is particularly sensitive to fake or non-prompt leptons in multi-jet events. In order to suppress this background to an acceptable level, stringent lepton identification and isolation requirements are used.

Muon candidates are formed by combining information from the muon spectrometer and the ID and must satisfy the 'Medium' quality criteria described in ref. [72]. They are required to have $p_{\mathrm{T}} > 30$ GeV and $|\eta| < 2.4$. Furthermore, they must satisfy requirements on the significance of the transverse impact parameter with respect to the primary vertex, $|d_0^{\mathrm{PV}}|/\sigma(d_0^{\mathrm{PV}}) < 3$, the longitudinal impact parameter with respect to the primary vertex, $|z_0^{\mathrm{PV}}\sin(\theta)| < 0.5$ mm, and the 'Gradient' isolation requirements, described in ref. [72], relying on a set of η- and p_{T}-dependent criteria based on tracking- and calorimeter-related variables.

Electron candidates are reconstructed from isolated energy deposits in the electromagnetic calorimeter matched to ID tracks and are required to have $p_{\mathrm{T}} > 30$ GeV, $|\eta| < 2.47$, and to satisfy the 'Tight' likelihood-based identification criteria described in ref. [73]. Electron candidates that fall in the transition region between the barrel and endcap calorimeters ($1.37 < |\eta| < 1.52$) are rejected. They are also required to have $|d_0^{\mathrm{PV}}|/\sigma(d_0^{\mathrm{PV}}) < 5$, $|z_0^{\mathrm{PV}}\sin(\theta)| < 0.5$ mm, and to satisfy isolation requirements described in ref. [73].

An overlap removal procedure is carried out to resolve ambiguities between candidate jets (with $p_{\mathrm{T}} > 20$ GeV) and baseline leptons[5] as follows: first, any non-b-tagged jet candidate[6] lying within an angular distance $\Delta R \equiv \sqrt{(\Delta y)^2 + (\Delta\phi)^2} = 0.2$ of a baseline electron is discarded. Furthermore, non-b-tagged jets within $\Delta R = 0.4$ of baseline muons are removed if the number of tracks associated with the jet is less than three or the ratio of muon p_{T} to jet p_{T} is greater than 0.5. Finally, any baseline lepton candidate remaining within a distance $\Delta R = 0.4$ of any surviving jet candidate is discarded.

Corrections derived from data control samples are applied to account for differences between data and simulation for the lepton trigger, reconstruction, identification and isolation efficiencies, the lepton momentum/energy scale and resolution [72, 73], and for the efficiency and mis-tag rate of the b-tagging algorithm [70].

5 Event selection and analysis strategy

Events are selected online using a single-electron or single-muon trigger. For the analysis selection, at least one electron or muon, matched to the trigger lepton, is required in the event. The analysis is carried out with three sets of jet p_{T} thresholds to provide sensitivity to a broad range of possible signals. These thresholds are applied to all jets in the event and are $p_{\mathrm{T}} = 40$ GeV, 60 GeV, and 80 GeV. The jet multiplicity is binned from a minimum of five jets to a maximum number that depends on the p_{T} threshold. The last bin is inclusive,

[5] Baseline leptons are reconstructed as described above, but with a looser p_{T} requirement ($p_{\mathrm{T}} > 10$ GeV), no isolation or impact parameter requirements, and, in the case of electrons, the 'Loose' lepton identification criteria [74].

[6] In this case, a b-tagging working point corresponding to an efficiency of identifying b-jets in a simulated $t\bar{t}$ sample of 85% is used.

JHEP09(2017)088

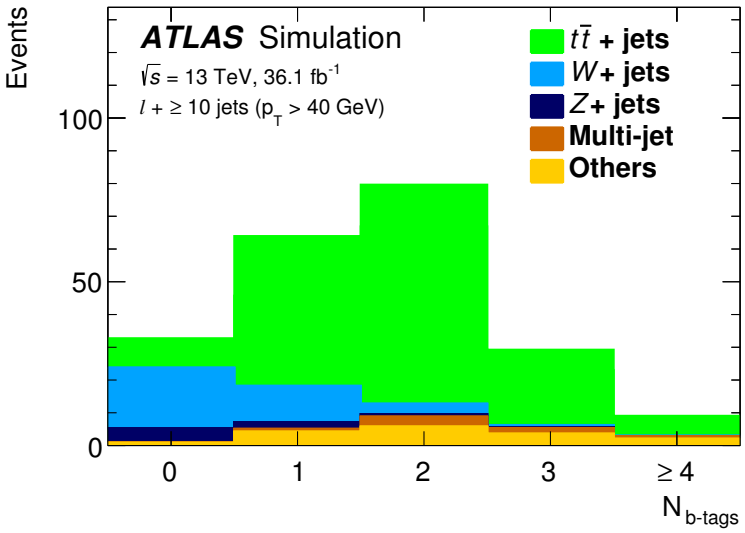

Figure 2. The expected background from MC simulation in the different b-tag bins, with a selection of at least ten jets (with $p_{\mathrm{T}} > 40$ GeV).

so that it also includes all events with more jets than the bin number. This bin corresponds to 12 or more jets for the 40 GeV requirement, and 10 or more jets for the 60 GeV and 80 GeV thresholds. There are five bins in the b-tagged jet multiplicity (exclusive bins from zero to three with an additional inclusive four-or-more bin). In this article, the notation $N_{j,b}^{\mathrm{process}}$ is used to denote the number of events predicted by the background fit model, with j jets and b b-tagged jets for a given process, e.g. $N_{j,b}^{t\bar{t}+\mathrm{jets}}$ for $t\bar{t}$+jets events. The number of events summed over all b-tag multiplicity bins for a given number of jets is denoted by N_{j}^{process}, and is also referred to as a jet slice.

For probing a specific BSM model, all of these bins in data are simultaneously fit to constrain the model, in what is labeled a model-dependent fit. In the search for a hypothetical BSM signal, dedicated signal regions (SRs) are defined which could be populated by a signal, and where the SM contribution is expected to be small. The background in these SRs is estimated from a fit in which some of the bins can be excluded to limit the effect of signal contamination biasing the background estimate; this set-up is labeled a model-independent fit. More details of the SR definitions are given in section 7.

An example of the expected background contributions from MC simulation for the different b-tag bins, with a selection of at least ten jets, can be seen in figure 2. This figure shows that the background in the zero b-tag bin is dominated by W/Z+jets and $t\bar{t}$+jets, whereas in the other b-tag bins it is dominated by $t\bar{t}$+jets. The contribution from other processes is very small in all bins.

The estimation of the dominant background processes of $t\bar{t}$+jets and W/Z+jets production is carried out using a combined fit to the jet and b-tagged jet multiplicity bins described above. For these backgrounds, the normalization per jet slice is derived using parameterized extrapolations from lower jet multiplicities. The b-tag multiplicity shape per jet slice is taken from simulation for the W/Z+jets background, whereas for the $t\bar{t}$+jets

JHEP09(2017)088

background it is predicted from the data using a parameterized extrapolation based on observables at medium jet multiplicities. A separate likelihood fit is carried out for each jet p_{T} threshold, with the fit parameters of the background model determined separately in each fit. The assumptions used in the parameterization are validated using data and MC simulation. Regarding the model-independent results, it is to be noted that possible signal leakage to the control regions can produce a bias in the background estimation. Such limits have been hence obtained assuming negligible signal contributions to events with five, six or seven jets. Signal processes with final states that the search is targeting, generally have negligible leakage into these jet slices, as is the case for the benchmark models considered.

6 Background estimation

6.1 W/Z+jets

A partially data-driven approach is used to estimate the W/Z+jets background. Since the selected W/Z+jets background events usually have no b-jets, the shapes of the b-tag multiplicity distributions are taken from simulated events, whereas the normalization in each jet slice is derived from the data. The estimate of the normalization relies on assuming a functional form to describe the evolution of the number of W/Z+jets events as a function of the jet multiplicity, $r(j) \equiv N_{j+1}^{W/Z+\mathrm{jets}}/N_j^{W/Z+\mathrm{jets}}$.

Above a certain number of jets, $r(j)$ can be assumed to be constant, implying a fixed probability of additional jet radiation, referred to as "staircase scaling" [75–78]. This behaviour has been observed by the ATLAS [79, 80] and CMS [81] collaborations. For lower jet multiplicities, a different scaling is expected with $r(j) = k/(j+1)$ where k is a constant, referred to as "Poisson scaling" [78].[7]

For the kinematic phase space relevant for this search, a combination of the two scalings is found to describe the data in dedicated validation regions (described later in this section), as well as in simulated W/Z+jets event samples with an integrated luminosity much larger than the one of the data. This combined scaling is parameterized as

$$r(j) = c_0 + c_1/(j+1), \tag{6.1}$$

where c_0 and c_1 are constants that are extracted from the data. Studies using simulated event samples, both at generator level and after event reconstruction, demonstrate that the flexibility of this parameterization is also able to absorb reconstruction effects related to the decrease in event reconstruction efficiency with increasing jet multiplicity, which are mainly due to the lepton-jet overlap and lepton isolation requirements.

The number of W+jets or Z+jets events with different jet and b-jet multiplicities, $N_{j,b}^{W/Z+\mathrm{jets}}$, is then parameterized as follows:

$$N_{j,b}^{W/Z+\mathrm{jets}} = \frac{MC_{j,b}^{W/Z+\mathrm{jets}}}{MC_j^{W/Z+\mathrm{jets}}} \cdot N_5^{W/Z+\mathrm{jets}} \cdot \prod_{j'=5}^{j'=j-1} r(j'),$$

[7] The transition between these scaling behaviours depends on the jet kinematic selections.

JHEP09(2017)088

where $MC_{j,b}^{W/Z+\text{jets}}$ and $MC_{j}^{W/Z+\text{jets}}$ are the predicted numbers of W/Z + j jets events with b b-tags and inclusive in b-tags, respectively, both taken from MC simulation, and $N_5^{W/Z+\text{jets}}$ is the absolute normalization in five-jet events. The term $N_5^{W/Z+\text{jets}} \cdot \prod_{j'=5}^{j'=j-1} r(j')$ gives the number of b-tag inclusive events in jet slice j, and the ratio $MC_{j,b}^{W/Z+\text{jets}}/MC_{j}^{W/Z+\text{jets}}$ is the fraction of b b-tagged events in this jet slice. The four parameters $N_5^{W+\text{jets}}$, $N_5^{Z+\text{jets}}$, c_0, and c_1 are left floating in the fit and are therefore extracted from the data along with the other background contributions.

Due to different b-tagged-jet multiplicity distributions in W+jets and Z+jets events, the b-tag distribution is modelled separately for the two processes. The normalization and scaling parameters $N_5^{W/Z+\text{jets}}$, c_0, and c_1 are determined using control regions with five, six or seven jets and zero b-tags. For the Z+jets background determination, the control regions are defined by selecting events with two oppositely charged same-flavour leptons fulfilling an invariant-mass requirement around the Z-boson mass ($81 \leq m_{\ell\ell} \leq 101$ GeV), as well as the requirement of exactly five, exactly six or exactly seven jets, and zero b-tags. The determination of the W+jets background relies on control regions containing the remaining events with exactly five, six or seven jets, and zero b-tags, which, for each jet multiplicity, are split according to the electric charge of the highest-p_{T} lepton. The expected charge asymmetry in W+jets events is taken from MC simulation separately for five-jet, six-jet and seven-jet events and used to constrain the W+jets normalization from the data using these control regions. Although all parameters are determined in a global likelihood fit, the most powerful constraint on the absolute normalization comes from the five-jet control regions, and the dominant constraints on the c_0 and c_1 parameters originate from the combination of the five-jet, six-jet and seven-jet control regions. The contamination by $t\bar{t}$ events in the Z+jets two-lepton control regions is negligible, whereas in the control regions used to estimate the W+jets normalization it is significant and is discussed in section 6.2. Once the W+jets and Z+jets backgrounds are normalized, they are extrapolated to higher jet multiplicities using the same common scaling function $r(j)$. While independent scalings could be used, tests in data show no significant difference and therefore a common function is used.

The jet-scaling assumption is validated in data using γ+jets and multi-jet events, and simulated W+jets and Z+jets samples are also found to be consistent with this assumption. The γ+jets events are selected using a photon trigger, and an isolated photon [82] with $p_{\text{T}} > 145$ GeV is required in the event selection, whereas the multi-jet events are selected using prescaled and unprescaled multi-jet triggers. In both cases, selections are applied to ensure these control regions probe a kinematic phase-space region similar to the one relevant for the analysis.

Figure 3 shows the $r(j)$ ratio for various processes used to validate the jet-scaling parameterization. Each panel shows the ratio for data or MC simulation with the fitted parameterization overlaid as a line. In the case of pure "staircase scaling", the shown ratio would be a constant.

Since the last jet-multiplicity bin used in the analysis is inclusive in the number of jets, the W/Z+jets background model is used to predict this by iterating to higher jet

JHEP09(2017)088

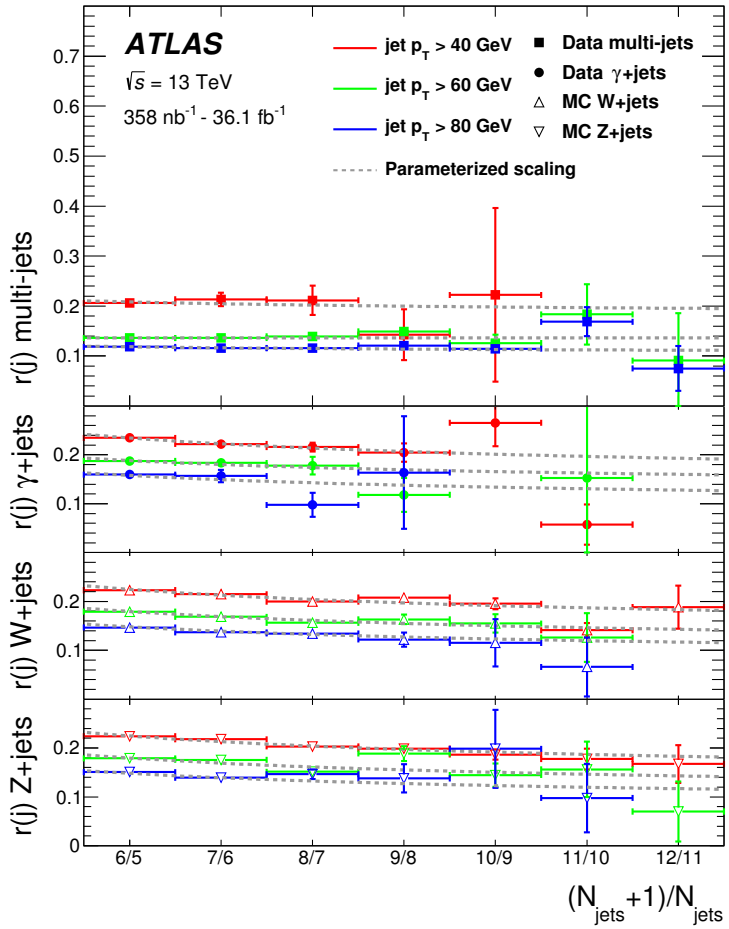

Figure 3. The ratio of the number of events with $(j+1)$ jets to the number with j jets for various processes used to validate the jet-scaling parameterization. Each panel shows the ratio for data or MC simulation with the fitted parameterization overlaid as a line. In the case of pure "staircase scaling", the shown ratio would be a constant. For the multi-jet data points, the 40 GeV jet p_{T} selection uses a prescaled trigger corresponding to an integrated luminosity of 358 nb^{-1}; all other selections use unprescaled triggers corresponding to the full data set. The uncertainties shown are statistical.

multiplicities and summing the contribution for each jet multiplicity above the maximum used in the analysis, and therefore gives the correct inclusive yield in this bin.

6.2 $t\bar{t}$+jets

A data-driven model is used to estimate the number of events from $t\bar{t}$+jets production in a given jet and b-tag multiplicity bin. The basic concept of this model is based on the extraction of an initial template of the b-tag multiplicity distribution in events with five jets and the parameterization of the evolution of this template to higher jet multiplicities. The absolute normalization for each jet slice is constrained in the fit as discussed later in this section. Figure 4 shows the b-tag multiplicity distributions in $t\bar{t}$+jets MC simulation, for

JHEP09(2017)088

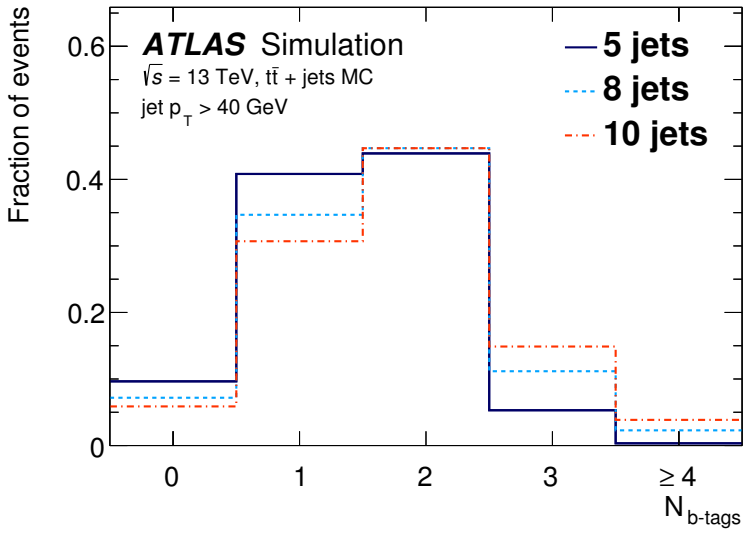

Figure 4. The normalized b-tag multiplicity distribution from $t\bar{t}$+jets MC simulation events with five, eight and ten jets (with $p_{\mathrm{T}} > 40$ GeV).

five-, eight- and ten-jet events, demonstrating how the distributions evolve as the number of jets increases. The background estimation parameterizes this effect and extracts the parameters describing the evolution from a fit to the data.

The extrapolation of the b-tag multiplicity distribution to higher jet multiplicities starts from the assumption that the difference between the b-tag multiplicity distribution in events with j and $j+1$ jets arises mainly from the production of additional jets, and can be described by a fixed probability that the additional jet is b-tagged. Given the small mis-tag rate, this probability is dominated by the probability that the additional jet is a heavy-flavour jet which is b-tagged. In order to account for acceptance effects due to the different kinematics in events with high jet multiplicity, the probability of further b-tagged jets entering the acceptance is also taken into account. The extrapolation to one additional jet can be parameterized as:

$$\begin{aligned} N_{j,b}^{t\bar{t}+\mathrm{jets}} &= N_{j}^{t\bar{t}+\mathrm{jets}} \cdot f_{j,b}, \\ f_{(j+1),b} &= f_{j,b} \cdot x_0 + f_{j,(b-1)} \cdot x_1 + f_{j,(b-2)} \cdot x_2, \end{aligned} \tag{6.2}$$

where $N_{j}^{t\bar{t}+\mathrm{jets}}$ is the number of $t\bar{t}$+jets events with j jets and $f_{j,b}$ is the fraction of $t\bar{t}$ events with j jets of which b are b-tagged. The parameters x_i describe the probability of one additional jet to be either not b-tagged (x_0), b-tagged (x_1), or b-tagged and causing a second b-tagged jet to move into the fiducial acceptance (x_2). The latter is dominated by cases where the extra jet is a b-jet, influencing the event kinematics such that an additional b-jet, below the jet p_{T} threshold, enters the acceptance. Given that the x_i parameters describe probabilities, the sum $\sum_i x_i$ is normalized to unity. Subsequent application of this parameterization produces a b-tag template for arbitrarily high jet multiplicities.

Studies based on MC simulated events with sample sizes corresponding to very large equivalent luminosities, as well as studies using fully efficient generator-level b-tagging, in-

JHEP09(2017)088

dicate the necessity to add a fit parameter that allows for correlated production of two b-tagged jets as may be expected with b-jet production from gluon splitting. This is implemented by changing the evolution described in eq. (6.2) such that any term with $x_1 \cdot x_1$ is replaced by $x_1 \cdot x_1 \cdot \rho_{11}$, where ρ_{11} describes the correlated production of two b-tagged jets.

The initial b-tag multiplicity template is extracted from data events with five jets after subtracting all non-$t\bar{t}$ background processes, and is denoted by $f_{5,b}$ and scaled by the absolute normalization $N_5^{t\bar{t}+\text{jets}}$ in order to obtain the model in the five-jet bin:

$$N_{5,b}^{t\bar{t}+\text{jets}} = N_5^{t\bar{t}+\text{jets}} \cdot f_{5,b},$$

where the sum of $f_{5,b}$ over the five b-tag bins is normalized to unity.

The model described above is based on the assumption that any change of the b-tag multiplicity distribution is due to additional jet radiation with a certain probability to lead to b-tagged jets. There is, however, also a small increase in the acceptance for b-jets produced in the decay of the $t\bar{t}$ system, when increasing the jet multiplicity, due to the higher jet momentum on average. The effect amounts to up to 5% in the one- and two-b-tag bins for high jet multiplicities, and is taken into account using a correction to the initial template extracted from simulated $t\bar{t}$ events.

As is the case for the W/Z+jets background, the normalization of the $t\bar{t}$ background in each jet slice is constrained using a scaling behaviour similar to that in eq. (6.1). The parameterization is slightly modified to:

$$N_{j+1}^{t\bar{t}+\text{jets}}/N_j^{t\bar{t}+\text{jets}} \equiv r^{t\bar{t}+\text{jets}}(j) = c_0^{t\bar{t}+\text{jets}} + c_1^{t\bar{t}+\text{jets}}/(j + c_2^{t\bar{t}+\text{jets}}),$$

where the three parameters $c_0^{t\bar{t}+\text{jets}}$, $c_1^{t\bar{t}+\text{jets}}$ and $c_2^{t\bar{t}+\text{jets}}$ are extracted from a fit to the data. In this case, since j is the total number of jets in the event, and not the number of jets produced in addition to the $t\bar{t}$ system, the denominator $(j+1)$ in eq. (6.1) is replaced by $(j + c_2^{t\bar{t}+\text{jets}})$ to take into account the ambiguity in the counting of additional jets due to acceptance effects for the $t\bar{t}$ decay products.

The scaling behaviour is tested in $t\bar{t}$+jets MC simulation (both with the nominal sample and the alternative sample described in table 1), and also in data with a dileptonic $t\bar{t}$+jets control sample. This sample is selected by requiring an electron candidate and a muon candidate in the event, with at least three jets of which at least one is b-tagged, and the small background predicted by MC simulation is subtracted. In this control region, the scaling behaviour can be tested for up to eight jets, but this corresponds to ten jets for a semileptonic $t\bar{t}$+jets sample (which is the dominant component of the $t\bar{t}$+jets background). Figure 5 presents a comparison of the scaling behaviour in data and MC simulation compared to a fit of the parameterization used and shows that the assumed function describes the data and MC simulation well for the jet-multiplicity range relevant to this search.

As for the W/Z+jets background estimate, the $t\bar{t}$+jets background model is used to predict the yield in the highest jet-multiplicity bin by iterating to higher jet multiplicities and summing these contributions to give the inclusive yield.

The zero-b-tag component of the initial $t\bar{t}$ template, which is extracted from events with five jets, exhibits an anti-correlation with the absolute W+jets normalization, which

JHEP09(2017)088

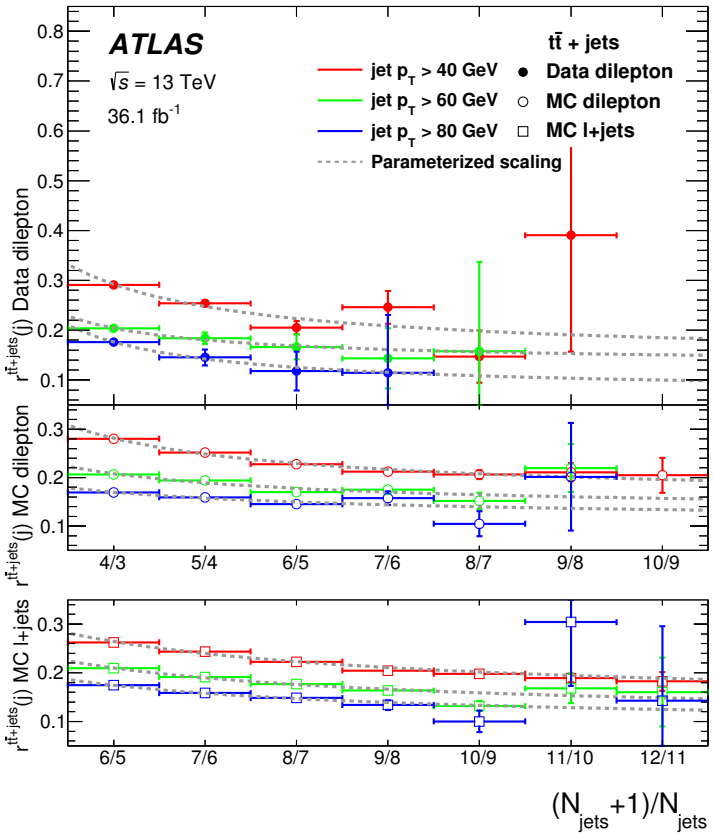

Figure 5. The ratio of the number of events with $(j + 1)$ jets to the number with j jets in dileptonic and semileptonic $t\bar{t}$+jets events, used to validate the jet-scaling parameterization. Each panel shows the ratio for data or MC simulation with the fitted parameterization overlaid as a line. In the case of pure "staircase scaling", the shown ratio would be a constant. The uncertainties shown are statistical.

is extracted in the same bin. The control regions separated in leading-lepton charge, detailed in section 6.1, provide a handle to extract the absolute W+jets normalization. The remaining anti-correlation does not affect the total background estimate. For these control regions, the $t\bar{t}$+jets process is assumed to be charge symmetric and the model is simply split into two halves for these bins.

6.3 Multi-jet events

The contribution from multi-jet production with a fake or non-prompt (FNP) lepton (such as hadrons misidentified as leptons, leptons originating from the decay of heavy-flavour hadrons, and electrons from photon conversions), constitutes a minor but non-negligible background, especially in the lower jet slices. It is estimated from the data with a matrix method similar to that described in ref. [83]. In this method, two types of lepton identification criteria are defined: "tight", corresponding to the default lepton criteria described in section 4, and "loose", corresponding to baseline leptons after overlap removal. The matrix

JHEP09(2017)088

method relates the number of events containing prompt or FNP leptons to the number of observed events with tight or loose-not-tight leptons using the probability for loose-prompt or loose-FNP leptons to satisfy the tight criteria. The probability for loose-prompt leptons to satisfy the tight selection criteria is obtained using a $Z \to \ell\ell$ data sample and is modelled as a function of the lepton p_{T}. The probability for loose FNP leptons to satisfy the tight selection criteria is determined from a data control region enriched in non-prompt leptons requiring a loose lepton, multiple jets, low $E_{\mathrm{T}}^{\mathrm{miss}}$ [84, 85] and low transverse mass.[8] The efficiencies are measured as a function of lepton candidate p_{T} after subtracting the contribution from prompt-lepton processes and are assumed to be independent of the jet multiplicity.[9]

6.4 Small backgrounds

The small background contributions from diboson production, single-top production, $t\bar{t}$ production in association with a vector/Higgs boson (labeled $t\bar{t}V/H$) and SM four-top-quark production are estimated using MC simulation. In all but the highest jet slices considered, the sum of these backgrounds contributes not more than 10% of the SM expectation in any of the b-tag bins; for the highest jet slices this can rise up to 35% .

7 Fit configuration and validation

For each jet p_{T} threshold, the search results are determined from a simultaneous likelihood fit. The likelihood is built as the product of Poisson probability terms describing the observed numbers of events in the different bins and Gaussian distributions constraining the nuisance parameters associated with the systematic uncertainties. The widths of the Gaussian distributions correspond to the sizes of these uncertainties. Poisson distributions are used to constrain the nuisance parameters for MC simulation and data control region statistical uncertainties. Correlations of a given nuisance parameter between the different background sources and the signal are taken into account when relevant. The systematic uncertainties are not constrained by the data in the fit procedure.

The likelihood is configured differently for the model-dependent and model-independent hypothesis tests. The former is used to derive exclusion limits for a specific BSM model, and the full set of bins (for example 5 to 12-inclusive jet multiplicity bins, and 0 to 4-inclusive b-jet bins for the 40 GeV jet p_{T} threshold) is employed in the likelihood. The signal contribution, as predicted by the given BSM model, is considered in all bins and is scaled by one common signal-strength parameter. The number of freely floating parameters in the background model is 15. There are four parameters in the W/Z+jets model: the two jet-scaling parameters (c_0, c_1), and the normalizations of the W+jets and Z+jets events in the five-jet region ($N_5^{W+\mathrm{jets}}$, $N_5^{Z+\mathrm{jets}}$). In addition, there are 11 parameters in the $t\bar{t}$+jets background model: one for the normalization in the five-jet slice ($N_5^{t\bar{t}+\mathrm{jets}}$), three

[8] The transverse mass of the lepton-$E_{\mathrm{T}}^{\mathrm{miss}}$ system is defined as: $m_{\mathrm{T}}^2 = 2p_{\mathrm{T}}^{\ell} E_{\mathrm{T}}^{\mathrm{miss}}(1 - \cos(\Delta\phi(\ell, E_{\mathrm{T}}^{\mathrm{miss}})))$.

[9] To minimize the dependence on the number of jets, the event selection considers only the leading-p_{T} baseline lepton when checking the more stringent identification and isolation criteria of the "tight" lepton definitions.

JHEP09(2017)088

for the normalization scaling ($c_0^{t\bar{t}+\text{jets}}$, $c_1^{t\bar{t}+\text{jets}}$, $c_2^{t\bar{t}+\text{jets}}$), four for the initial b-tag multiplicity template ($f_{5,b}$, $b = 1$–4), and three for the evolution parameters (x_1, x_2 and ρ_{11}), taking into account the constraints: $x_0 = 1 - x_1 - x_2$, and $f_{5,0} = 1 - \sum_{b=1}^{\geq 4} f_{5,b}$. The number of fitted bins[10] varies between 36 and 46 depending on the highest jet-multiplicity bin used, leading to an over-constrained system in all cases.

The model-independent test is used to search for, and to set generic exclusion limits on, the potential contribution from a hypothetical BSM signal in the phase-space region probed by this analysis. For this purpose, dedicated signal regions are defined which could be populated by such a signal, and where the SM contribution is expected to be small. The SR selections are defined as requiring exactly zero or at least three b-tags (labelled 0b, or 3b respectively) for a given minimum number of jets J, and for a jet p_{T} threshold X, with each SR labelled as X-0b-J or X-3b-J. For each jet p_{T} threshold, six SRs are defined as follows:

- For the 40 GeV jet p_{T} threshold: 40-0b-10, 40-3b-10, 40-0b-11, 40-3b-11, 40-0b-12, 40-3b-12.
- For the 60 GeV jet p_{T} threshold: 60-0b-8, 60-3b-8, 60-0b-9, 60-3b-9, 60-0b-10, 60-3b-10.
- For the 80 GeV jet p_{T} threshold: 80-0b-8, 80-3b-8, 80-0b-9, 80-3b-9, 80-0b-10, 80-3b-10.

The SRs therefore overlap and an event can enter more than one SR. Due to the efficiency of the b-tagging algorithm used, signal models with large b-tag multiplicities can have significant contamination in the two-b-tag bins, which can bias the $t\bar{t}$+jets background estimate and reduce the sensitivity of the search. To reduce this effect, for the SRs with ≥ 3 b-tags, the two-b-tag bin is not included in the fit for the highest jet slice in each SR.[11]

For the model-independent hypothesis tests, a separate likelihood fit is performed for each SR. A potential signal contribution is considered in the given SR bin only. The number of freely floating parameters in the background model is 15, whereas the number of observables varies between 23 (for SRs 60-3b-8 and 80-3b-8) and 45 (for SR 40-0b-12), so the system is also always over-constrained.

The fit set-up was extensively tested using MC simulated events, and was demonstrated to give a negligible bias in the fitted yields, both in the case where the background-only distributions are fit, or when a signal is injected into the fitted data. These tests were carried out with the nominal MC samples as well as the alternative samples described in table 1. In addition, when fitting the data the fitted parameter values and their inter-correlations were studied in detail and found to be in agreement with the expectation based

[10]For example, for the 60 and 80 GeV jet p_{T} thresholds, there are five b-tag multiplicity bins in the eight-to-ten-jet slices, and seven bins (the zero-b-tag bin is split into three bins for each of the W/Z control regions) in the five-, six- and seven-jet slices, giving 36 bins in total.

[11]For example, for the 60-0b-8 and 80-0b-8 SRs all bins with five, six or seven jets are included in the fit, as well as the one-, two-, three- and four-or-more-b-tag bins with at least eight jets. Whereas for the 60-3b-8 and 80-3b-8 SRs all bins with five, six or seven jets are included in the fit, as well as the zero- and one-b-tag bins with at least eight jets.

JHEP09(2017)088

on MC simulation. The jet-reconstruction stability at high multiplicities was validated by comparing jets with track-jets that are clustered from ID tracks with a radius parameter of 0.2. The ratio of the multiplicities of track-jets and jets, which is sensitive to jet-merging effects, was found to be stable up to the highest jet multiplicities studied. The estimate of the multi-jet background was validated in data regions enriched in FNP leptons, and was found to describe the data within the quoted uncertainties.

8 Systematic uncertainties

The dominant backgrounds are estimated from the data without the use of MC simulation, and therefore the main systematic uncertainties related to the estimation of these backgrounds arise from the assumptions made in the W/Z+jets, $t\bar{t}$+jets and multi-jet background estimates. Uncertainties related to the theoretical modelling of the specific processes and due to the modelling of the detector response in simulated events are only relevant for the minor backgrounds, which are taken from MC simulation, and for the estimates of the signal yields after selections.

For the W/Z+jets background estimation, the uncertainty related to the assumed scaling behaviour is taken from studies of this behaviour in W+jets and Z+jets MC simulation, as well as in γ+jets and multi-jet data control regions chosen to be kinematically similar to the search selection (see figure 3). No evidence is seen for a deviation from the assumed scaling behaviour and the statistical precision of these methods is used as an uncertainty (up to 18% for the highest jet-multiplicity bins). The expected uncertainty of the charge asymmetry for W+jets production is 3–5% from PDF variations [86], but in the seven-jet region, the uncertainty is dominated by the limited number of MC events (up to 10% for the 80 GeV jet p_{T} threshold). The uncertainty in the shape of the b-tag multiplicity distribution in W+jets and Z+jets events is derived by comparing different MC generator set-ups (e.g. varying the renormalization and factorization scale and the parton-shower model parameters). It is seen to grow as a function of jet multiplicity and is about 50% for events with five jets, after which the MC statistical uncertainty becomes very large. A conservative uncertainty of 100% is therefore assigned to the fractional contribution from $W+b$ and $W+c$ events for all jet slices considered, which has a very small impact on the final result as the background from W boson production with additional heavy flavour jets is small compared to that from top quark pair production. In addition, the uncertainties related to the b-tagging efficiency and mis-tag rate are taken into account in the uncertainty in the W/Z+jets b-tag template.

The uncertainties related to the $t\bar{t}$+jets background estimation primarily relate to the number of events in the data regions used for the fit. As mentioned in section 6.2, the method shows good closure using simulated events, so no systematic uncertainty related to these studies is assigned. There is a small uncertainty related to the acceptance correction for the initial b-tag multiplicity template, which is derived by varying the MC generator set-up for the $t\bar{t}$ sample used to estimate the correction. This leads to a 3% uncertainty in the correction and has no significant effect on the final uncertainty. The uncertainty related to the parameterization of the scaling of the $t\bar{t}$+jets background with jet multiplicity is

JHEP09(2017)088

determined with MC simulation closure tests. The validation of the method presented in figure 5 shows that the parameterization describes the data and MC simulation well. The uncertainties assigned vary from 3% (at 8 jets) to 33% (at 12 jets) for the 40 GeV jet p_{T} threshold, and from 10% (at 8 jets) to 60% (at 10 jets) for the 80 GeV jet p_{T} threshold. These are estimated by studying the closure of the method in different MC samples (including using alternative MC generators, and varying the event selection) and are of similar size to the statistical uncertainty from the data validation.

The dominant uncertainties in the multi-jet background estimate arise from the number of data events in the control regions, uncertainties related to the subtraction of electroweak backgrounds from these control regions (here a 20% uncertainty is applied to the expected yield of the backgrounds in the control regions) and uncertainties to cover the possible dependencies of the real- and fake-lepton efficiencies [83] on variables other than lepton p_{T} (for example the dependence on the number of jets in the event). The total uncertainty in the multi-jet background yields is about 50%.

The uncertainty in the expected yields of the minor backgrounds includes theoretical uncertainties in the cross-sections and in the modelling of the kinematics by the MC generator, as well as experimental uncertainties related to the modelling of the detector response in the simulation. The uncertainties assigned to cover the theoretical estimate of these backgrounds in the relevant regions are 50%, 100% and 30% for diboson, single top-quark, and $t\bar{t}V/H$ production, respectively.

The final uncertainty in the background estimate in the SRs is dominated by the statistical uncertainty related to the number of data events in the different bins, and other systematic uncertainties do not contribute significantly.

The uncertainties assigned to the expected signal yield for the SUSY benchmark processes considered include the experimental uncertainties related to the detector modelling, which are dominated by the modelling of the jet energy scale and the b-tagging efficiencies and mis-tagging rates. For example, for a signal model with four b-quarks the b-tagging uncertainties are ≈10%, and the jet related uncertainties are typically ≈5%. The uncertainty in the signal cross-sections used is discussed in section 3.2.1. The uncertainty in the signal yields related to the modelling of additional jet radiation is studied by varying the factorization, renormalization, and jet-matching scales as well as the parton-shower tune in the simulation. The corresponding uncertainty is small for most of the signal parameter space, but increases to up to 25% for very light or very heavy LSPs where the contribution from additional jet radiation is relevant.

9 Results

Results are provided both as model-independent limits on the contribution from BSM physics to the dedicated signal regions and in the context of the four SUSY benchmark models discussed in section 3.2.1. As previously mentioned, different fit set-ups are used for these two sets of results. In all cases, the profile-likelihood-ratio test [87] is used to establish 95% confidence intervals using the $\mathrm{CL_s}$ prescription [88].

JHEP09(2017)088

Figures 6, 7 and 8 show the observed numbers of data events compared to the fitted background model, for the three jet p_{T} thresholds, respectively. The likelihood fit is configured using the model-dependent set-up where all bins are input to the fit, and fixing the signal-strength parameter to zero. An example signal model is also shown to illustrate the separation between the signal and the background achieved, as well as the level of signal-event leakage into lower b-tag and jet-multiplicity bins. The bottom panel of each figure shows the background prediction using MC simulation. For high b-tag multiplicities (≥ 3), the MC simulation strongly underestimates the background contributions compared to the data-driven background estimation. This effect has been observed before [89, 90] and shows that the MC simulations are not able to correctly describe final states with high b-jet multiplicity. In addition, the MC simulation predicts too many events at low b-jet multiplicity, which is likely to be due to a mismodelling of the W+jets production at high jet multiplicity. Since the background prediction from MC simulation does not reflect the expected background contribution, in all cases the expected limit is computed using the background prediction from a fit to all bins in the data with no signal component included in the fit model.

9.1 Model-independent results

The model-independent results are calculated from the observed number of events, and the expected background in the SRs. Tables 2, 3, and 4 show the expected background in the SRs from these fits together with the observed numbers of events for the sets of SRs with the 40 GeV, 60 GeV and 80 GeV jet p_{T} thresholds. In addition, the p_0 values are shown, which quantify the probability that a background-only experiment results in a fluctuation giving an event yield equal to or larger than the one observed in the data. The background estimate describes the observed data in the SRs well, with the largest excesses over the background estimate corresponding to 0.8 standard deviations in SRs 40-3b-11 and 40-3b-12.

Model-independent upper limits at 95% confidence level (CL) on the number of BSM events, N_{BSM}, that may contribute to the signal regions, are computed from the observed number of events and the fitted background. Normalizing these results by the integrated luminosity L of the data sample, they can be interpreted as upper limits on the visible BSM cross-section σ_{vis}, defined as the product $\sigma_{\mathrm{prod}} \times A \times \epsilon = N_{\mathrm{BSM}}/L$ of production cross-section (σ_{prod}), acceptance (A) and reconstruction efficiency (ϵ). These limits are presented in table 5.

For a hypothetical signal with three or four b-jets, the analysis sensitivity is reduced because of the leakage of signal events into lower b-tag jet multiplicity bins due to the b-tagging efficiency of about 78%, which would bias the normalization of the $t\bar{t}$+jets background. This is partially mitigated by excluding the two-b-tag bin in the background determination for the highest jet slice probed, and by the constraint on the scaling of the $t\bar{t}$+jets background as a function of jet multiplicity.

JHEP09(2017)088

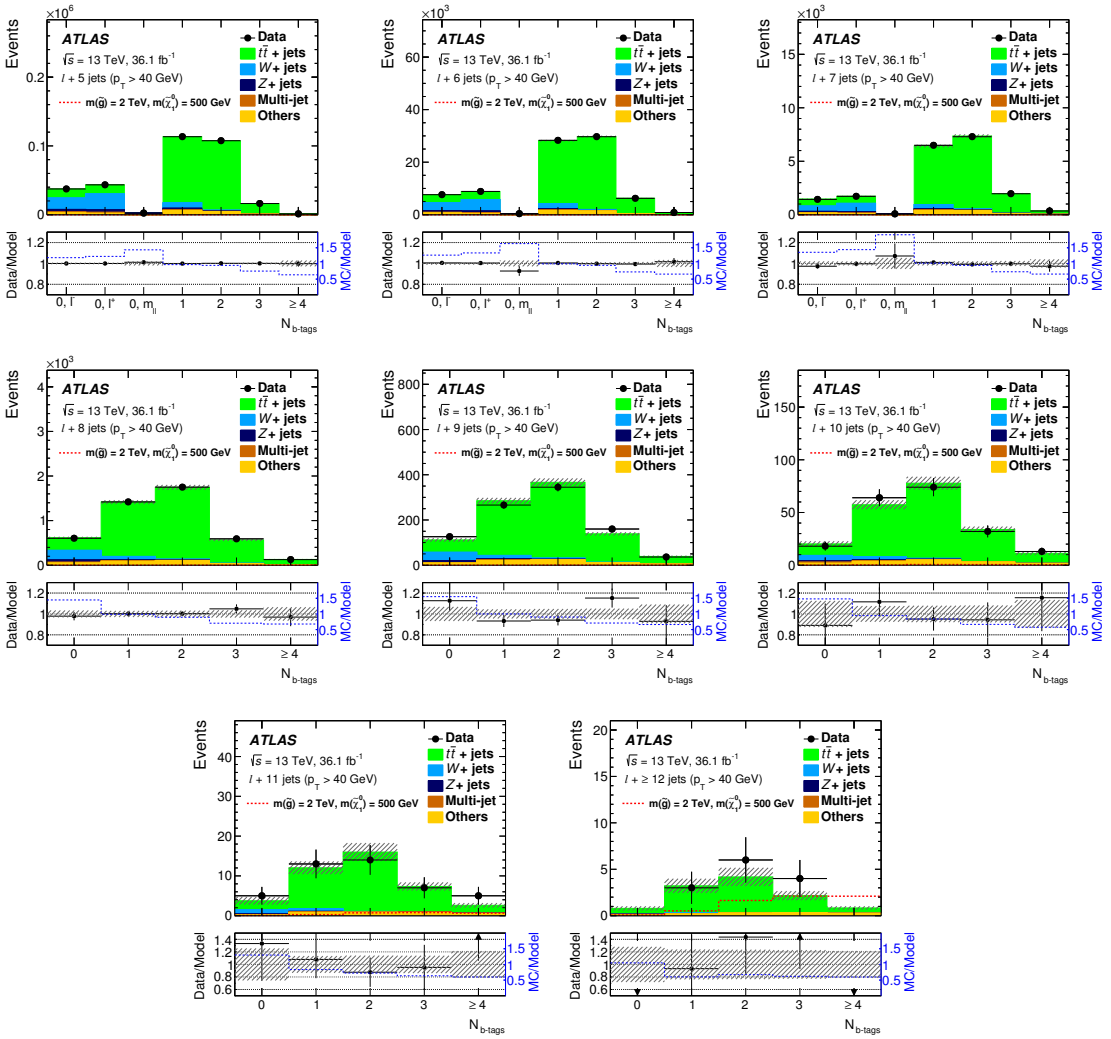

Figure 6. The expected background and observed data in the different jet and b-tag multiplicity bins for the 40 GeV jet p_{T} threshold. The background shown is estimated by including all bins in the fit. For the five-, six- and seven-jet slices the control regions used to estimate the W+jets and Z+jets normalizations are also shown (labelled ℓ^-, ℓ^+, and $m_{\ell\ell}$). An example signal for the $\tilde{g} \to t\bar{t}\tilde{\chi}_1^0 \to t\bar{t}uds$ model with $m_{\tilde{g}} = 2000$ GeV and $m_{\tilde{\chi}_1^0} = 500$ GeV is also overlaid (although its contribution is very small with this jet p_{T} threshold). The bottom panels show the ratio of the observed data to the expected background, as well as the ratio of the prediction from MC simulation to the expected background. All uncertainties, which can be correlated across the bins, are included in the error bands (shaded regions).

JHEP09(2017)088

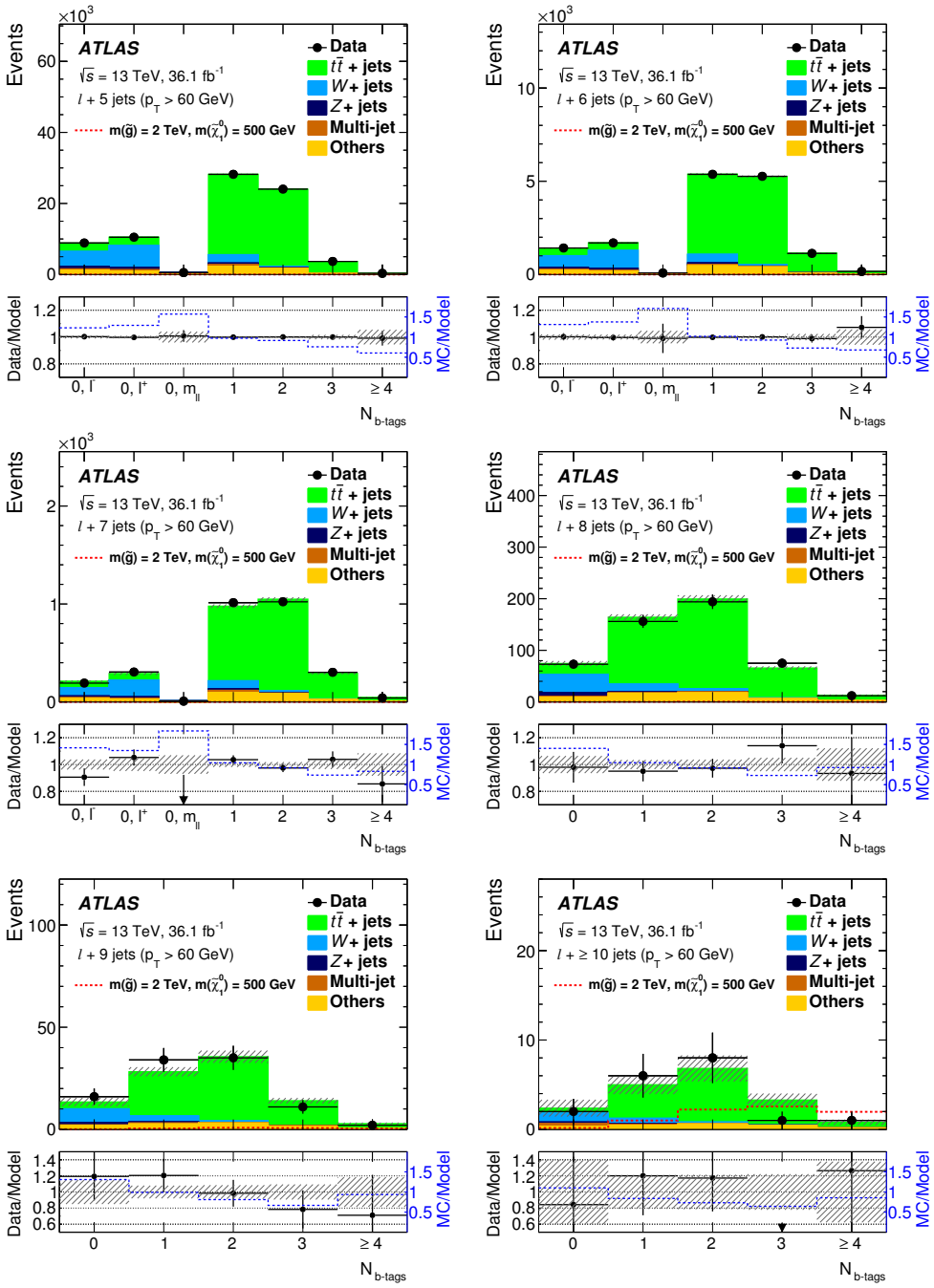

Figure 7. The expected background and observed data in the different jet and b-tag multiplicity bins for the 60 GeV jet p_{T} threshold. The background shown is estimated by including all bins in the fit. For the five-, six- and seven-jet slices the control regions used to estimate the W+jets and Z+jets normalizations are also shown (labelled ℓ^-, ℓ^+, and $m_{\ell\ell}$). An example signal for the $\tilde{g} \to t\bar{t}\tilde{\chi}_1^0 \to t\bar{t}uds$ model with $m_{\tilde{g}} = 2000$ GeV and $m_{\tilde{\chi}_1^0} = 500$ GeV is also overlaid (although its contribution is very small in most of the jet multiplicity slices shown). The bottom panels show the ratio of the observed data to the expected background, as well as the ratio of the prediction from MC simulation to the expected background. All uncertainties, which can be correlated across the bins, are included in the error bands (shaded regions).

JHEP09(2017)088

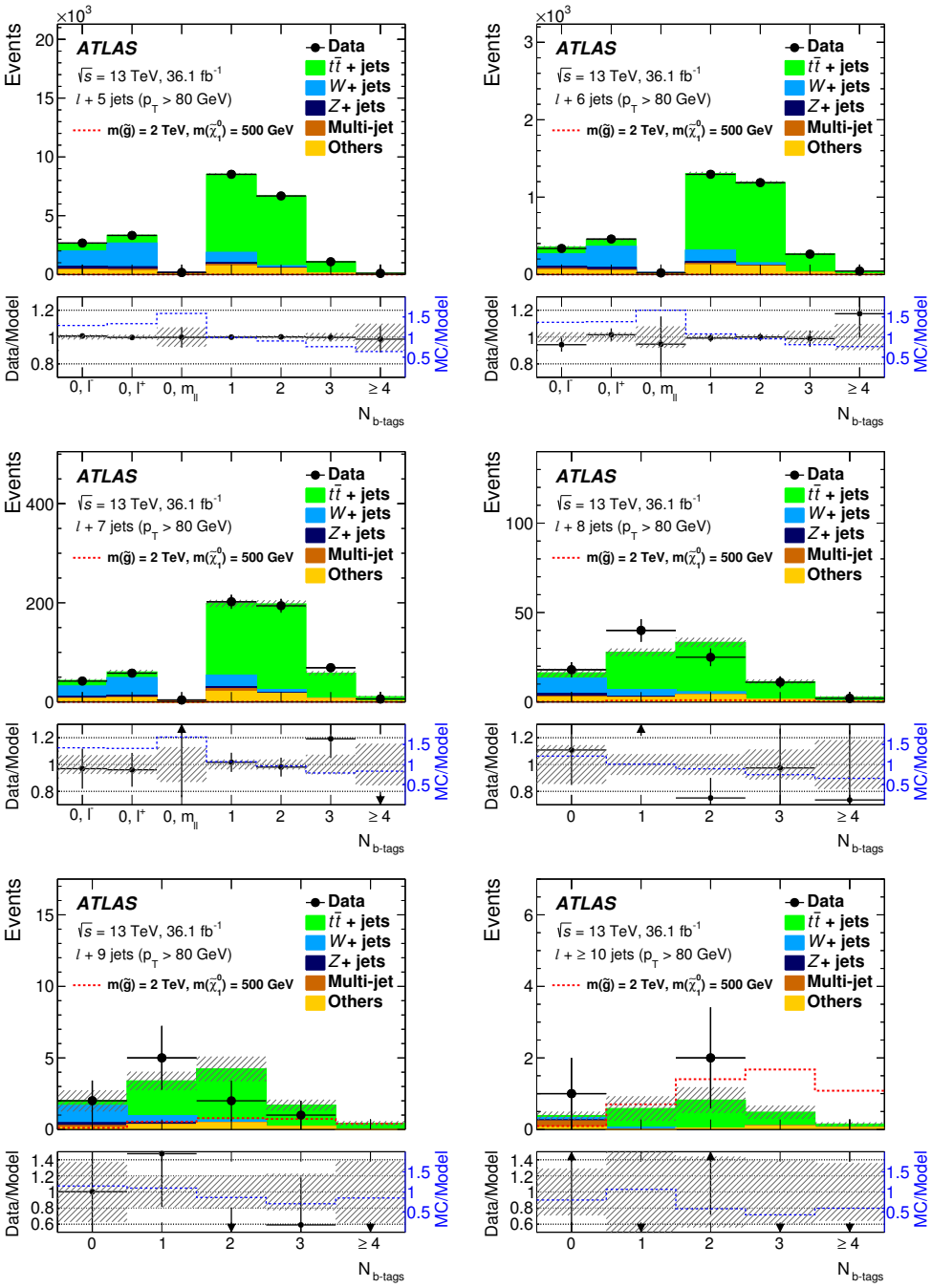

Figure 8. The expected background and observed data in the different jet and b-tag multiplicity bins for the 80 GeV jet p_{T} threshold. The background shown is estimated by including all bins in the fit. For the five-, six- and seven-jet slices the control regions used to estimate the W+jets and Z+jets normalizations are also shown (labelled ℓ^-, ℓ^+, and $m_{\ell\ell}$). An example signal for the $\tilde{g} \to t\bar{t}\tilde{\chi}_1^0 \to t\bar{t}uds$ model with $m_{\tilde{g}} = 2000$ GeV and $m_{\tilde{\chi}_1^0} = 500$ GeV is also overlaid (although its contribution is very small in most of the jet multiplicity slices shown). The bottom panels show the ratio of the observed data to the expected background, as well as the ratio of the prediction from MC simulation to the expected background. All uncertainties, which can be correlated across the bins, are included in the error bands (shaded regions).

JHEP09(2017)088

	≥ 10 jets		≥ 11 jets		≥ 12 jets	
Process	0 b	≥ 3 b	0 b	≥ 3 b	0 b	≥ 3 b
$t\bar{t}$+jets	14.3 ± 2.9	53 ± 6	3.0 ± 0.7	10.5 ± 1.8	0.58 ± 0.20	1.9 ± 0.6
W+jets	7 ± 4	0.22 ± 0.08	0.9 ± 0.9	0.04 ± 0.03	0.1 ± 0.1	< 0.01
Others	1.9 ± 0.6	6.3 ± 1.8	0.19 ± 0.06	1.7 ± 0.6	0.05 ± 0.02	0.57 ± 0.20
Z+jets	1.7 ± 0.9	0.10 ± 0.03	0.25 ± 0.22	0.02 ± 0.01	0.03 ± 0.04	< 0.01
Multi-jet	1.3 ± 0.7	0.48 ± 0.20	0.15 ± 0.08	0.27 ± 0.12	0.12 ± 0.07	< 0.01
Total Bkd.	26 ± 4	60 ± 6	4.5 ± 1.0	12.6 ± 1.9	0.87 ± 0.23	2.5 ± 0.7
Data	23	61	5	16	0	4
p_0 (σ)	0.5 (0)	0.46 (0.1)	0.42 (0.2)	0.21 (0.8)	0.5 (0)	0.21 (0.8)

Table 2. Fitted background yields in the different b-tag multiplicity bins for jet $p_{\mathrm{T}} > 40$ GeV in the different signal regions. The parameters of the model are determined in a fit to a reduced set of bins, corresponding to the model-independent fit discussed in the text. The individual background uncertainties can be larger than the total uncertainty due to correlations between parameters. The p_0 value quantifies the probability that a background-only experiment results in a fluctuation giving an event yield equal to or larger than the one observed in the data, and is capped at 0.5.

	≥ 8 jets		≥ 9 jets		≥ 10 jets	
Process	0 b	≥ 3 b	0 b	≥ 3 b	0 b	≥ 3 b
$t\bar{t}$+jets	26 ± 11	88 ± 17	4.0 ± 1.9	20.7 ± 3.4	0.56 ± 0.33	4.1 ± 1.7
W+jets	42 ± 9	1.18 ± 0.31	7.1 ± 2.4	0.24 ± 0.09	1.2 ± 1.1	0.02 ± 0.02
Others	11 ± 4	12 ± 4	2.2 ± 0.8	3.0 ± 0.9	0.34 ± 0.11	0.77 ± 0.26
Z+jets	8.0 ± 1.3	0.32 ± 0.04	1.3 ± 0.4	0.09 ± 0.02	0.23 ± 0.19	0.02 ± 0.02
Multi-jet	3.0 ± 1.5	0.50 ± 0.24	0.56 ± 0.27	0.27 ± 0.13	0.32 ± 0.15	< 0.01
Total Bkd.	90 ± 9	102 ± 17	15.1 ± 2.5	24.4 ± 3.3	2.7 ± 1.2	4.9 ± 1.7
Data	91	102	18	15	2	2
p_0 (σ)	0.46 (0.1)	0.5 (0)	0.27 (0.6)	0.5 (0)	0.5 (0)	0.5 (0)

Table 3. Fitted background yields in the different b-tag multiplicity bins for jet $p_{\mathrm{T}} > 60$ GeV in the different signal regions. The parameters of the model are determined in a fit to a reduced set of bins, corresponding to the model-independent fit discussed in the text. The individual background uncertainties can be larger than the total uncertainty due to correlations between parameters. The p_0 value quantifies the probability that a background-only experiment results in a fluctuation giving an event yield equal to or larger than the one observed in the data, and is capped at 0.5.

9.2 Model-dependent results

For each signal model probed, the fit is configured using the model-dependent set-up, as detailed in section 7. All bins are included in the fit and the expected signal contribution in each bin is taken into account. Figure 9 shows the observed and expected exclusion limits for the three benchmark signal models featuring gluino pair production, as a function of the gluino mass and neutralino or top-squark mass. Figure 10 shows exclusion limits in the top-squark production model where the limit for pure bino and higgsino LSPs are shown separately, taking into account the processes discussed in section 3.2.1. For the gluino production models, all the probed model points have the best expected sensitivity when using the 80 GeV jet p_{T} threshold, whereas for the top-squark production model, the

JHEP09(2017)088

	≥ 8 jets		≥ 9 jets		≥ 10 jets	
Process	0 b	≥ 3 b	0 b	≥ 3 b	0 b	≥ 3 b
$t\bar{t}$+jets	4.0 ± 1.7	15.7 ± 2.3	0.44 ± 0.21	2.7 ± 0.7	0.06 ± 0.04	0.38 ± 0.27
W+jets	9.0 ± 2.9	0.18 ± 0.07	1.2 ± 0.7	0.02 ± 0.02	0.05 ± 0.07	< 0.01
Others	2.3 ± 0.9	2.4 ± 0.7	0.16 ± 0.05	0.45 ± 0.15	0.06 ± 0.03	0.14 ± 0.05
Z+jets	1.7 ± 0.5	0.06 ± 0.02	0.23 ± 0.14	0.03 ± 0.01	0.02 ± 0.03	< 0.01
Multi-jet	0.8 ± 0.4	< 0.01	0.30 ± 0.15	< 0.01	0.16 ± 0.08	< 0.01
Total Bkd.	17.8 ± 2.9	18.4 ± 2.2	2.3 ± 0.9	3.2 ± 0.7	0.35 ± 0.13	0.52 ± 0.27
Data	21	14	3	1	1	0
p_0 (σ)	0.27 (0.6)	0.5 (0)	0.34 (0.4)	0.5 (0)	0.18 (0.9)	0.5 (0)

Table 4. Fitted background yields in the different b-tag multiplicity bins for jet $p_{\mathrm{T}} > 80$ GeV in the different signal regions. The parameters of the model are determined in a fit to a reduced set of bins, corresponding to the model-independent fit discussed in the text. The individual background uncertainties can be larger than the total uncertainty due to correlations between parameters. The p_0 value quantifies the probability that a background-only experiment results in a fluctuation giving an event yield equal to or larger than the one observed in the data, and is capped at 0.5.

Jet multiplicity	0 b obs. [fb]	0 b exp. [fb]	≥ 3 b obs. [fb]	≥ 3 b exp. [fb]
≥ 10 jets ($p_{\mathrm{T}} > 40$ GeV)	0.32	$0.36^{+0.16}_{-0.10}$	0.57	$0.54^{+0.24}_{-0.15}$
≥ 11 jets ($p_{\mathrm{T}} > 40$ GeV)	0.17	$0.16^{+0.08}_{-0.05}$	0.33	$0.25^{+0.12}_{-0.07}$
≥ 12 jets ($p_{\mathrm{T}} > 40$ GeV)	0.08	$0.09^{+0.05}_{-0.01}$	0.17	$0.13^{+0.07}_{-0.04}$
≥ 8 jets ($p_{\mathrm{T}} > 60$ GeV)	0.73	$0.71^{+0.27}_{-0.20}$	1.02	$1.03^{+0.39}_{-0.29}$
≥ 9 jets ($p_{\mathrm{T}} > 60$ GeV)	0.35	$0.28^{+0.12}_{-0.08}$	0.19	$0.32^{+0.15}_{-0.09}$
≥ 10 jets ($p_{\mathrm{T}} > 60$ GeV)	0.12	$0.14^{+0.07}_{-0.04}$	0.11	$0.15^{+0.08}_{-0.04}$
≥ 8 jets ($p_{\mathrm{T}} > 80$ GeV)	0.38	$0.31^{+0.14}_{-0.09}$	0.21	$0.28^{+0.13}_{-0.08}$
≥ 9 jets ($p_{\mathrm{T}} > 80$ GeV)	0.15	$0.13^{+0.07}_{-0.04}$	0.09	$0.13^{+0.07}_{-0.04}$
≥ 10 jets ($p_{\mathrm{T}} > 80$ GeV)	0.10	$0.08^{+0.04}_{-0.00}$	0.08	$0.08^{+0.04}_{-0.00}$

Table 5. Observed and expected 95% CL model-independent upper limits on the product of cross-section, acceptance and efficiency (in fb) for each signal region. The limits are determined by fitting the background model in a reduced set of bins as described in the text.

60 GeV jet p_{T} threshold gives the best expected sensitivity, and these thresholds are used to set the exclusion limits.

In the model with an RPV decay of the $\tilde{\chi}_1^0$ to three light-quark jets, gluino masses up to 2.10 TeV are excluded, with weaker limits for light and heavy $\tilde{\chi}_1^0$. For the benchmark model with $\tilde{g} \to t\bar{t}\tilde{t}$ and $\tilde{t} \to \bar{b}\bar{s}$, gluino masses up to 1.65 TeV are excluded. In this case, the observed limit is about two standard deviations stronger than the expected limit. This is due to a difference between the observed data and the expected background in the three- and four-b-tag bins in the eight-, nine- and ten-jet slices (see figure 8), which are the most sensitive bins for this model. An exclusion limit is also derived for the same model but with a virtual top squark (with mass set to 2 TeV) where gluinos of mass up to 1.62 TeV

JHEP09(2017)088

are excluded (with an expected exclusion up to 1.50 TeV). The analysis excludes gluinos with masses up to 1.80 TeV in the $\tilde{g} \to q\bar{q}\tilde{\chi}_1^0 \to q\bar{q}q\bar{q}\ell/\nu$ model.

For the top-squark pair production model, top-squark masses up to 1.10 TeV and 1.25 TeV are excluded for higgsino and bino LSPs respectively. There is greater sensitivity in the case of the bino LSP because the lepton and jet multiplicities are higher than in the higgsino LSP scenario.[12]

Typical acceptance times efficiency ($A \times \epsilon$) values for the relevant SR for each of the benchmark signal models are:

- 8% for the $\tilde{g} \to t\bar{t}\tilde{\chi}_1^0 \to t\bar{t}uds$ model for the 80-3b-10 SR,
- 3% for the $\tilde{g} \to \bar{\tilde{t}}\tilde{t} \to \bar{t}\bar{b}\bar{s}$ model for the 80-3b-8 SR,
- 13% for the $\tilde{g} \to q\bar{q}\tilde{\chi}_1^0 \to q\bar{q}q\bar{q}\ell/\nu$ model for the 80-0b-8 SR,
- 2% (6%) for the top-squark production model with a higgsino (bino) LSP for the 60-3b-10 SR.

These values correspond to the case where the produced SUSY particle is close to the exclusion limit, and for intermediate LSP masses. In general, the acceptance falls for light or heavy LSPs as some of the produced jets or leptons become softer.

9.3 Limits on four-top-quark production

The analysis is also used to search for SM four-top-quark production. In this case, the small contribution to the background from four-top-quark production is removed, and a model-dependent fit is carried out with the four-top-quark simulated sample used as the signal. The best expected sensitivity is achieved with the 60 GeV jet p_{T} threshold, which leads to a cross-section upper limit at 95% CL on the four-top-quark signal of 60 fb (whereas 84 fb is expected), which is 6.5 times the SM cross-section for this process.[13]

10 Conclusion

A search for beyond the Standard Model physics in events with an isolated lepton (electron or muon), high jet multiplicity and no, or many, b-tagged jets is presented. Unlike many previous searches in similar final states, no requirement on the missing transverse momentum in the event is applied. A novel data-driven technique is used to estimate the dominant backgrounds from $t\bar{t}$+jets and W/Z+jets production. The analysis is performed with proton-proton collision data at $\sqrt{s} = 13$ TeV collected in 2015 and 2016 with the ATLAS detector at the Large Hadron Collider corresponding to an integrated luminosity of 36.1 fb^{-1}. With no significant excess over the Standard Model expectation observed, results are interpreted in the framework of simplified models featuring gluino or top-squark

[12] In the bino case, every top-squark decay produces a top quark whereas for higgsino LSPs top quarks are produced in only about half of the cases.

[13] No uncertainty in the theoretical modelling of the four-top-quark process is included when setting the cross-section limit, although uncertainties related to the b-tagging, jet and lepton reconstruction are taken into account.

JHEP09(2017)088

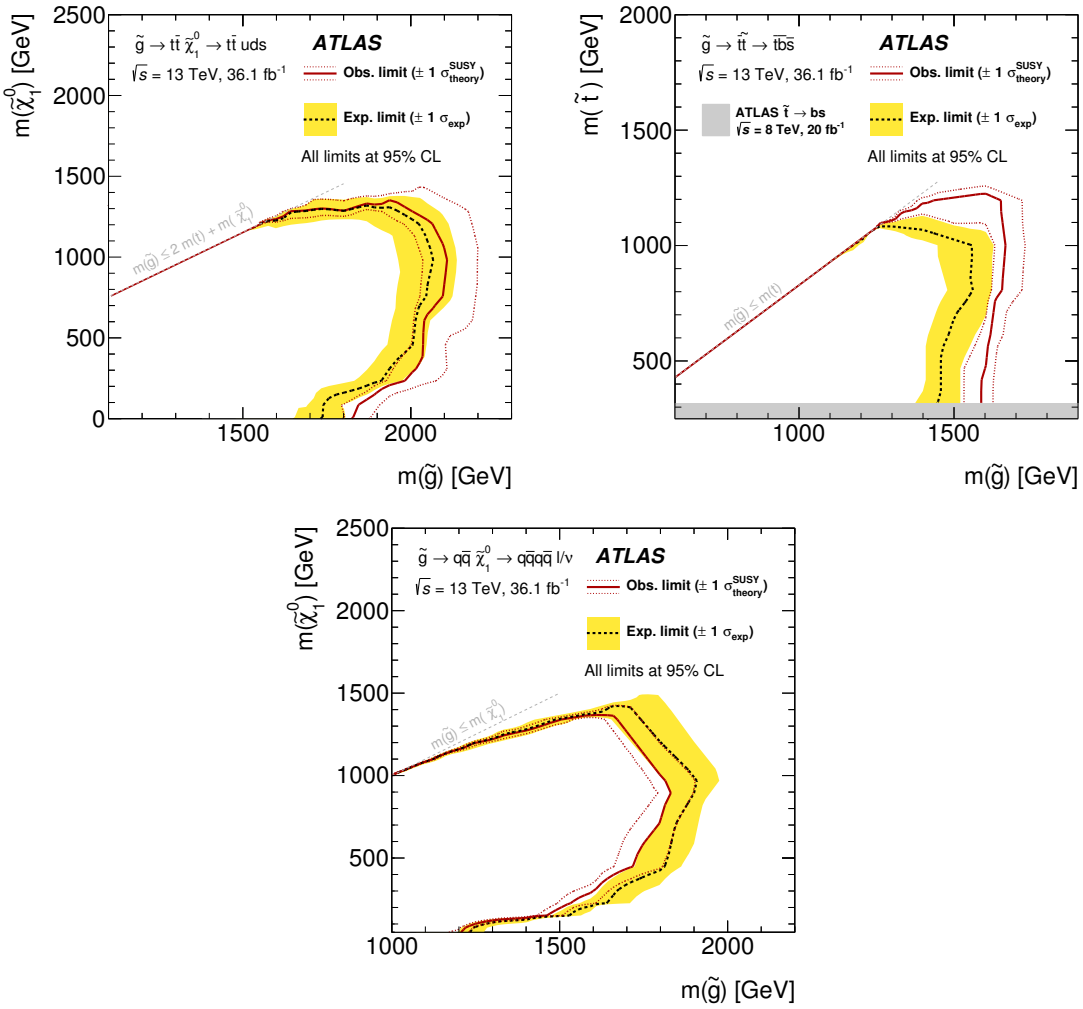

Figure 9. Observed and expected exclusion contours on the $\tilde{g}$ and $\tilde{\chi}_1^0$ or $\tilde{t}$ masses in the context of the RPV SUSY scenarios probed, with simplified mass spectra featuring $\tilde{g}\tilde{g}$ pair production with exclusive decay modes. The contours of the band around the expected limit are the $\pm 1\sigma$ variations, including all uncertainties except theoretical uncertainties in the signal cross-section. The dotted lines around the observed limit illustrate the change in the observed limit as the nominal signal cross-section is scaled up and down by the theoretical uncertainty. All limits are computed at 95% CL. The diagonal line indicates the kinematic limit for the decays in each specified scenario. For the $\tilde{g} \to \bar{t}\tilde{t} \to \bar{t}b\bar{s}$ model, the limit on the top-squark mass from ref. [28] is also shown.

pair production in R-parity-violating supersymmetry scenarios. In a benchmark model with $\tilde{g} \to t\bar{t}\tilde{\chi}_1^0 \to t\bar{t}uds$, gluino masses up to 2.10 TeV are excluded at 95% confidence level. In a model with $\tilde{g} \to \bar{t}\tilde{t}$ and $\tilde{t} \to \bar{b}\bar{s}$, gluino masses up to 1.65 TeV are excluded, whereas in a model with $\tilde{g} \to q\bar{q}\tilde{\chi}_1^0 \to q\bar{q}q\bar{q}\ell/\nu$, gluino masses up to 1.80 TeV are excluded. A model with direct top-squark production and R-parity-violating decays of higgsino or bino LSPs excludes top squarks with masses up to 1.10 TeV and 1.25 TeV respectively. These results improve the previously existing limits for the gluino production models considered, whereas they represent the first limits for the top squark production model. In addition, an upper

JHEP09(2017)088

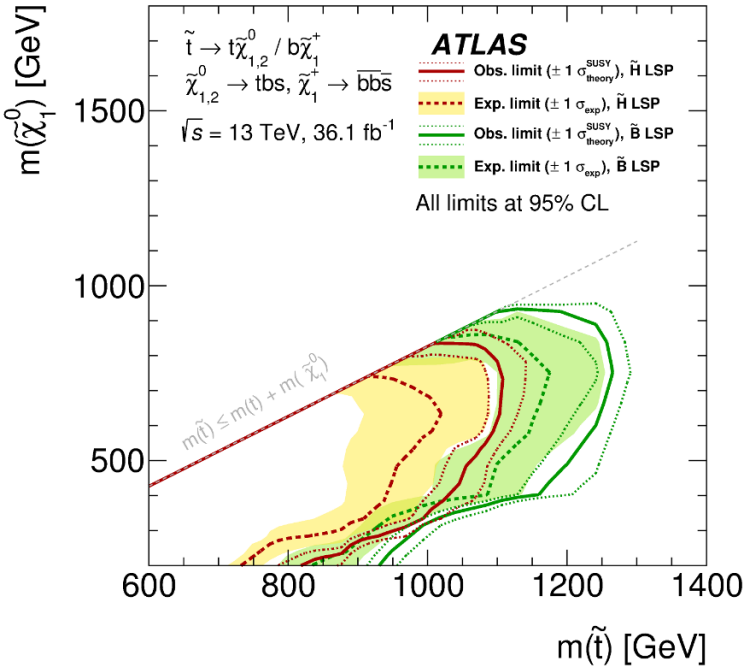

Figure 10. Observed and expected exclusion contours on the $\tilde{t}$ and $\tilde{\chi}^0_1$ masses in the context of top-squark production model with RPV decays of the LSP. Limits are shown in the case of pure bino ($\tilde{B}$) or pure higgsino ($\tilde{H}$) LSPs. The contours of the band around the expected limit are the $\pm 1\sigma$ variations, including all uncertainties except theoretical uncertainties in the signal cross-section. The dotted lines around the observed limit illustrate the change in the observed limit as the nominal signal cross-section is scaled up and down by the theoretical uncertainty. All limits are computed at 95% CL. The diagonal line indicates the kinematic limit for the decays in the considered scenario.

limit of 60 fb is set on the cross-section of Standard Model four-top-quark production, improving on the previous strongest limit of 69 fb [14]. Finally, model-independent limits are set on the contribution of new phenomena to the signal-region yields.

Acknowledgments

We thank CERN for the very successful operation of the LHC, as well as the support staff from our institutions without whom ATLAS could not be operated efficiently.

We acknowledge the support of ANPCyT, Argentina; YerPhI, Armenia; ARC, Australia; BMWFW and FWF, Austria; ANAS, Azerbaijan; SSTC, Belarus; CNPq and FAPESP, Brazil; NSERC, NRC and CFI, Canada; CERN; CONICYT, Chile; CAS, MOST and NSFC, China; COLCIENCIAS, Colombia; MSMT CR, MPO CR and VSC CR, Czech Republic; DNRF and DNSRC, Denmark; IN2P3-CNRS, CEA-DSM/IRFU, France; SRNSF, Georgia; BMBF, HGF, and MPG, Germany; GSRT, Greece; RGC, Hong Kong SAR, China; ISF, I-CORE and Benoziyo Center, Israel; INFN, Italy; MEXT and JSPS, Japan; CNRST, Morocco; NWO, Netherlands; RCN, Norway; MNiSW and NCN, Poland;

JHEP09(2017)088

FCT, Portugal; MNE/IFA, Romania; MES of Russia and NRC KI, Russian Federation; JINR; MESTD, Serbia; MSSR, Slovakia; ARRS and MIZŠ, Slovenia; DST/NRF, South Africa; MINECO, Spain; SRC and Wallenberg Foundation, Sweden; SERI, SNSF and Cantons of Bern and Geneva, Switzerland; MOST, Taiwan; TAEK, Turkey; STFC, United Kingdom; DOE and NSF, United States of America. In addition, individual groups and members have received support from BCKDF, the Canada Council, CANARIE, CRC, Compute Canada, FQRNT, and the Ontario Innovation Trust, Canada; EPLANET, ERC, ERDF, FP7, Horizon 2020 and Marie Skłodowska-Curie Actions, European Union; Investissements d'Avenir Labex and Idex, ANR, Région Auvergne and Fondation Partager le Savoir, France; DFG and AvH Foundation, Germany; Herakleitos, Thales and Aristeia programmes co-financed by EU-ESF and the Greek NSRF; BSF, GIF and Minerva, Israel; BRF, Norway; CERCA Programme Generalitat de Catalunya, Generalitat Valenciana, Spain; the Royal Society and Leverhulme Trust, United Kingdom.

The crucial computing support from all WLCG partners is acknowledged gratefully, in particular from CERN, the ATLAS Tier-1 facilities at TRIUMF (Canada), NDGF (Denmark, Norway, Sweden), CC-IN2P3 (France), KIT/GridKA (Germany), INFN-CNAF (Italy), NL-T1 (Netherlands), PIC (Spain), ASGC (Taiwan), RAL (U.K.) and BNL (U.S.A.), the Tier-2 facilities worldwide and large non-WLCG resource providers. Major contributors of computing resources are listed in ref. [91].

References

[1] M. Lisanti, P. Schuster, M. Strassler and N. Toro, *Study of LHC searches for a lepton and many jets*, *JHEP* **11** (2012) 081 [arXiv:1107.5055] [INSPIRE].

[2] J.A. Evans, Y. Kats, D. Shih and M.J. Strassler, *Toward full LHC coverage of natural supersymmetry*, *JHEP* **07** (2014) 101 [arXiv:1310.5758] [INSPIRE].

[3] Yu. A. Golfand and E.P. Likhtman, *Extension of the algebra of Poincaré group generators and violation of p invariance*, *JETP Lett.* **13** (1971) 323 [*Pisma Zh. Eksp. Teor. Fiz.* **13** (1971) 452] [INSPIRE].

[4] D.V. Volkov and V.P. Akulov, *Is the neutrino a goldstone particle?*, *Phys. Lett.* **B 46** (1973) 109 [INSPIRE].

[5] J. Wess and B. Zumino, *Supergauge transformations in four-dimensions*, *Nucl. Phys.* **B 70** (1974) 39 [INSPIRE].

[6] J. Wess and B. Zumino, *Supergauge invariant extension of quantum electrodynamics*, *Nucl. Phys.* **B 78** (1974) 1 [INSPIRE].

[7] S. Ferrara and B. Zumino, *Supergauge invariant Yang-Mills theories*, *Nucl. Phys.* **B 79** (1974) 413 [INSPIRE].

[8] A. Salam and J.A. Strathdee, *Supersymmetry and nonabelian gauges*, *Phys. Lett.* **B 51** (1974) 353 [INSPIRE].

JHEP09(2017)088

[9] ATLAS collaboration, *Search for massive supersymmetric particles decaying to many jets using the ATLAS detector in pp collisions at* $\sqrt{s} = 8$ *TeV*, *Phys. Rev.* **D 91** (2015) 112016 [arXiv:1502.05686].

[10] CMS collaboration, *Search for new phenomena in events with high jet multiplicity and low missing transverse momentum in proton-proton collisions at* $\sqrt{s} = 8$ *TeV*, *Phys. Lett.* **B 770** (2017) 257 [arXiv:1608.01224].

[11] CMS collaboration, *Searches for R-parity-violating supersymmetry in pp collisions at* $\sqrt{s} = 8$ *TeV in final states with 0-4 leptons*, *Phys. Rev.* **D 94** (2016) 112009 [arXiv:1606.08076].

[12] ATLAS collaboration, *Search for supersymmetry in final states with two same-sign or three leptons and jets using* $36\,fb^{-1}$ *of* $\sqrt{s} = 13$ *TeV pp collision data with the ATLAS detector*, arXiv:1706.03731 [INSPIRE].

[13] ATlAS collaboration, *Search for production of vector-like quark pairs and of four top quarks in the lepton-plus-jets final state in pp collisions at* $\sqrt{s} = 8$ *TeV with the ATLAS detector*, *JHEP* **08** (2015) 105 [arXiv:1505.04306].

[14] CMS collaboration, *Search for standard model production of four top quarks in proton-proton collisions at* $\sqrt{s} = 13$ *TeV*, *Phys. Lett.* **B 772** (2017) 336 [arXiv:1702.06164] [INSPIRE].

[15] ATLAS collaboration, *The ATLAS experiment at the CERN Large Hadron Collider*, 2008 *JINST* **3** S08003 [INSPIRE].

[16] ATLAS collaboration, *ATLAS insertable B-layer technical design report addendum*, ATLAS-TDR-19 (2010), addendum ATLAS-TDR-19-ADD-1 (2012).

[17] ATLAS collaboration, *Performance of the ATLAS trigger system in 2015*, *Eur. Phys. J.* **C 77** (2017) 317 [arXiv:1611.09661] [INSPIRE].

[18] ATLAS collaboration, *Luminosity determination in pp collisions at* $\sqrt{s} = 8$ *TeV using the ATLAS detector at the LHC*, *Eur. Phys. J.* **C 76** (2016) 653 [arXiv:1608.03953] [INSPIRE].

[19] ATLAS collaboration, *The ATLAS simulation infrastructure*, *Eur. Phys. J.* **C 70** (2010) 823 [arXiv:1005.4568] [INSPIRE].

[20] GEANT4 collaboration, S. Agostinelli et al., *GEANT4 — a Simulation toolkit*, *Nucl. Instrum. Meth.* **A 506** (2003) 250 [INSPIRE].

[21] ATLAS collaboration, *The simulation principle and performance of the ATLAS fast calorimeter simulation FastCaloSim*, ATL-PHYS-PUB-2010-013 (2010).

[22] T. Sjöstrand, S. Mrenna and P.Z. Skands, *A brief introduction to PYTHIA 8.1*, *Comput. Phys. Commun.* **178** (2008) 852 [arXiv:0710.3820] [INSPIRE].

[23] ATLAS collaboration, *Further ATLAS tunes of PYTHIA6 and PYTHIA 8*, ATL-PHYS-PUB-2011-014 (2011).

[24] A. Sherstnev and R.S. Thorne, *Parton distributions for LO generators*, *Eur. Phys. J.* **C 55** (2008) 553 [arXiv:0711.2473] [INSPIRE].

[25] D.J. Lange, *The EvtGen particle decay simulation package*, *Nucl. Instrum. Meth.* **A 462** (2001) 152 [INSPIRE].

[26] G. D'Ambrosio, G.F. Giudice, G. Isidori and A. Strumia, *Minimal flavor violation: an effective field theory approach*, *Nucl. Phys.* **B 645** (2002) 155 [hep-ph/0207036] [INSPIRE].

JHEP09(2017)088

[27] C. Csáki, Y. Grossman and B. Heidenreich, *MFV SUSY: a natural theory for R-parity violation*, *Phys. Rev.* **D 85** (2012) 095009 [arXiv:1111.1239] [INSPIRE].

[28] ATLAS collaboration, *A search for top squarks with R-parity-violating decays to all-hadronic final states with the ATLAS detector in* $\sqrt{s} = 8$ *TeV proton-proton collisions*, *JHEP* **06** (2016) 067 [arXiv:1601.07453].

[29] G. Corcella et al., *HERWIG 6: an event generator for hadron emission reactions with interfering gluons (including supersymmetric processes)*, *JHEP* **01** (2001) 010 [hep-ph/0011363] [INSPIRE].

[30] J. Pumplin et al., *New generation of parton distributions with uncertainties from global QCD analysis*, *JHEP* **07** (2002) 012 [hep-ph/0201195] [INSPIRE].

[31] S. Gieseke, C. Rohr and A. Siodmok, *Colour reconnections in HERWIG++*, *Eur. Phys. J.* **C 72** (2012) 2225 [arXiv:1206.0041] [INSPIRE].

[32] J. Alwall et al., *The automated computation of tree-level and next-to-leading order differential cross sections and their matching to parton shower simulations*, *JHEP* **07** (2014) 079 [arXiv:1405.0301] [INSPIRE].

[33] ATLAS collaboration, *ATLAS Pythia 8 tunes to* 7 *TeV data*, ATL-PHYS-PUB-2014-021 (2014).

[34] R.D. Ball et al., *Parton distributions with LHC data*, *Nucl. Phys.* **B 867** (2013) 244 [arXiv:1207.1303] [INSPIRE].

[35] W. Beenakker, R. Hopker, M. Spira and P.M. Zerwas, *Squark and gluino production at hadron colliders*, *Nucl. Phys.* **B 492** (1997) 51 [hep-ph/9610490] [INSPIRE].

[36] A. Kulesza and L. Motyka, *Threshold resummation for squark-antisquark and gluino-pair production at the LHC*, *Phys. Rev. Lett.* **102** (2009) 111802 [arXiv:0807.2405] [INSPIRE].

[37] A. Kulesza and L. Motyka, *Soft gluon resummation for the production of gluino-gluino and squark-antisquark pairs at the LHC*, *Phys. Rev.* **D 80** (2009) 095004 [arXiv:0905.4749] [INSPIRE].

[38] W. Beenakker et al., *Soft-gluon resummation for squark and gluino hadroproduction*, *JHEP* **12** (2009) 041 [arXiv:0909.4418] [INSPIRE].

[39] W. Beenakker et al., *Squark and Gluino Hadroproduction*, *Int. J. Mod. Phys.* **A 26** (2011) 2637 [arXiv:1105.1110] [INSPIRE].

[40] C. Borschensky, M. Krämer, A. Kulesza, M. Mangano, S. Padhi, T. Plehn et al., *Squark and gluino production cross sections in pp collisions at* $\sqrt{s}$ *= 13, 14, 33 and 100 TeV*, *Eur. Phys. J.* **C 74** (2014) 3174 [arXiv:1407.5066] [INSPIRE].

[41] ATLAS collaboration, *Simulation of top-quark production for the ATLAS experiment at* $\sqrt{s} = 13$ *TeV*, ATL-PHYS-PUB-2016-004 (2016).

[42] ATLAS collaboration, *Monte Carlo Generators for the Production of a* W *or* Z/γ^* *Boson in Association with Jets at ATLAS in Run 2*, ATL-PHYS-PUB-2016-003 (2016).

[43] ATLAS collabration, *Multi-boson simulation for* 13 *TeV ATLAS analyses* ATL-PHYS-PUB-2016-002 (2016).

[44] ATLAS collaboration, *Modelling of the* $t\bar{t}H$ *and* $t\bar{t}V(V = W, Z)$ *processes for* $\sqrt{s} = 13$ *TeV ATLAS analyses*, ATL-PHYS-PUB-2016-005 (2016).

JHEP09(2017)088

[45] T. Gleisberg et al., *Event generation with SHERPA 1.1*, *JHEP* **02** (2009) 007 [arXiv:0811.4622] [INSPIRE].

[46] S. Catani, L. Cieri, G. Ferrera, D. de Florian and M. Grazzini, *Vector boson production at hadron colliders: a fully exclusive QCD calculation at NNLO*, *Phys. Rev. Lett.* **103** (2009) 082001 [arXiv:0903.2120] [INSPIRE].

[47] H.-L. Lai et al., *New parton distributions for collider physics*, *Phys. Rev.* **D 82** (2010) 074024 [arXiv:1007.2241] [INSPIRE].

[48] M.L. Mangano, M. Moretti, F. Piccinini, R. Pittau and A.D. Polosa, *ALPGEN, a generator for hard multiparton processes in hadronic collisions*, *JHEP* **07** (2003) 001 [hep-ph/0206293] [INSPIRE].

[49] T. Sjöstrand, S. Mrenna and P.Z. Skands, *PYTHIA 6.4 physics and manual*, *JHEP* **05** (2006) 026 [hep-ph/0603175] [INSPIRE].

[50] P.Z. Skands, *Tuning Monte Carlo generators: the Perugia tunes*, *Phys. Rev.* **D 82** (2010) 074018 [arXiv:1005.3457] [INSPIRE].

[51] S. Alioli, P. Nason, C. Oleari and E. Re, *A general framework for implementing NLO calculations in shower Monte Carlo programs: the POWHEG BOX*, *JHEP* **06** (2010) 043 [arXiv:1002.2581] [INSPIRE].

[52] M. Czakon, P. Fiedler and A. Mitov, *Total top-quark pair-production cross section at hadron colliders through $O(\alpha_S^4)$*, *Phys. Rev. Lett.* **110** (2013) 252004 [arXiv:1303.6254] [INSPIRE].

[53] M. Czakon and A. Mitov, *NNLO corrections to top pair production at hadron colliders: the quark-gluon reaction*, *JHEP* **01** (2013) 080 [arXiv:1210.6832] [INSPIRE].

[54] M. Czakon and A. Mitov, *NNLO corrections to top-pair production at hadron colliders: the all-fermionic scattering channels*, *JHEP* **12** (2012) 054 [arXiv:1207.0236] [INSPIRE].

[55] P. Bärnreuther, M. Czakon and A. Mitov, *Percent level precision physics at the Tevatron: first genuine NNLO QCD corrections to $q\bar{q} \to t\bar{t} + X$*, *Phys. Rev. Lett.* **109** (2012) 132001 [arXiv:1204.5201] [INSPIRE].

[56] M. Cacciari et al., *Top-pair production at hadron colliders with next-to-next-to-leading logarithmic soft-gluon resummation*, *Phys. Lett.* **B 710** (2012) 612 [arXiv:1111.5869] [INSPIRE].

[57] M. Czakon and A. Mitov, *Top++: a program for the calculation of the top-pair cross-section at hadron colliders*, *Comput. Phys. Commun.* **185** (2014) 2930 [arXiv:1112.5675] [INSPIRE].

[58] N. Kidonakis, *Next-to-next-to-leading-order collinear and soft gluon corrections for t-channel single top quark production*, *Phys. Rev.* **D 83** (2011) 091503 [arXiv:1103.2792] [INSPIRE].

[59] N. Kidonakis, *Two-loop soft anomalous dimensions for single top quark associated production with a W^- or H^-*, *Phys. Rev.* **D 82** (2010) 054018 [arXiv:1005.4451] [INSPIRE].

[60] N. Kidonakis, *NNLL resummation for s-channel single top quark production*, *Phys. Rev.* **D 81** (2010) 054028 [arXiv:1001.5034] [INSPIRE].

[61] LHC Higgs Cross section Working Group collaboration, S. Dittmaier et al., *Handbook of LHC Higgs cross sections: 1. Inclusive observables*, arXiv:1101.0593 [INSPIRE].

[62] M. Cacciari, G.P. Salam and G. Soyez, *The anti-k_t jet clustering algorithm*, *JHEP* **04** (2008) 063 [arXiv:0802.1189] [INSPIRE].

JHEP09(2017)088

[63] M. Cacciari and G.P. Salam, *Dispelling the N^3 myth for the k_t jet-finder*, *Phys. Lett.* **B 641** (2006) 57 [hep-ph/0512210] [INSPIRE].

[64] ATLAS collaboration, *Topological cell clustering in the ATLAS calorimeters and its performance in LHC Run 1*, *Eur. Phys. J.* **C 77** (2017) 490 [arXiv:1603.02934] [INSPIRE].

[65] M. Cacciari and G.P. Salam, *Pileup subtraction using jet areas*, *Phys. Lett.* **B 659** (2008) 119 [arXiv:0707.1378] [INSPIRE].

[66] ATLAS collaboration, *Pile-up subtraction and suppression for jets in ATLAS*, ATLAS-CONF-2013-083 (2013).

[67] ATLAS collaboration, *Jet energy scale measurements and their systematic uncertainties in proton-proton collisions at $\sqrt{s} = 13$ TeV with the ATLAS detector*, arXiv:1703.09665 [INSPIRE].

[68] ATLAS collaboration, *Tagging and suppression of pileup jets with the ATLAS detector*, ATLAS-CONF-2014-018 (2014).

[69] ATLAS collaboration, *Selection of jets produced in 13 TeV proton-proton collisions with the ATLAS detector*, ATLAS-CONF-2015-029 (2015).

[70] ATLAS collaboration, *Performance of b-jet identification in the ATLAS experiment*, 2016 *JINST* **11** P04008 [arXiv:1512.01094] [INSPIRE].

[71] ATLAS collaboration, *Optimisation of the ATLAS b-tagging performance for the 2016 LHC Run*, ATL-PHYS-PUB-2016-012 (2016).

[72] ATLAS collaboration, *Muon reconstruction performance of the ATLAS detector in proton-proton collision data at $\sqrt{s} = 13$ TeV*, *Eur. Phys. J.* **C 76** (2016) 292 [arXiv:1603.05598] [INSPIRE].

[73] ATLAS collaboration, *Electron efficiency measurements with the ATLAS detector using the 2015 LHC proton-proton collision data*, ATLAS-CONF-2016-024 (2016).

[74] ATLAS collaboration, *Electron identification measurements in ATLAS using $\sqrt{s} = 13$ TeV data with 50 ns bunch spacing*, ATL-PHYS-PUB-2015-041 (2015).

[75] S.D. Ellis, R. Kleiss and W.J. Stirling, *W's, Z's and jets*, *Phys. Lett.* **B 154** (1985) 435 [INSPIRE].

[76] F.A. Berends, W.T. Giele, H. Kuijf, R. Kleiss and W.J. Stirling, *Multi-jet production in W, Z events at $p\bar{p}$ colliders*, *Phys. Lett.* **B 224** (1989) 237 [INSPIRE].

[77] W.T. Giele and W.J. Stirling, *Top search at Fermilab: multi-jet signals and backgrounds*, *Nucl. Phys.* **B 343** (1990) 14 [INSPIRE].

[78] E. Gerwick, T. Plehn, S. Schumann and P. Schichtel, *Scaling patterns for QCD jets*, *JHEP* **10** (2012) 162 [arXiv:1208.3676] [INSPIRE].

[79] ATLAS collaboration, *Measurement of the production cross section of jets in association with a Z boson in pp collisions at $\sqrt{s} = 7$ TeV with the ATLAS detector*, *JHEP* **07** (2013) 032 [arXiv:1304.7098].

[80] ATLAS collaboration, *Measurements of the production cross section of a Z boson in association with jets in pp collisions at $\sqrt{s} = 13$ TeV with the ATLAS detector*, *Eur. Phys. J.* **C 77** (2017) 361 [arXiv:1702.05725] [INSPIRE].

[81] CMS collaboration, *Jet production rates in association with W and Z bosons in pp collisions at $\sqrt{s} = 7$ TeV*, *JHEP* **01** (2012) 010 [arXiv:1110.3226] [INSPIRE].

JHEP09(2017)088

[82] ATLAS collaboration, *Measurements of the photon identification efficiency with the ATLAS detector using* $4.9\,fb^{-1}$ *of pp collision data collected in 2011*, ATLAS-CONF-2012-123 (2012).

[83] ATLAS collaboration, *Search for supersymmetry at* $\sqrt{s} = 13$ *TeV in final states with jets and two same-sign leptons or three leptons with the ATLAS detector*, *Eur. Phys. J.* **C 76** (2016) 259 [arXiv:1602.09058] [INSPIRE].

[84] ATLAS collaboration, *Performance of missing transverse momentum reconstruction with the ATLAS detector in the first proton-proton collisions at* $\sqrt{s} = 13$ *TeV*, ATL-PHYS-PUB-2015-027 (2015).

[85] ATLAS collaboration, *Expected performance of missing transverse momentum reconstruction for the ATLAS detector at* $\sqrt{s} = 13$ *TeV*, ATL-PHYS-PUB-2015-023 (2015).

[86] M. Botje et al., *The PDF4LHC working group interim recommendations*, arXiv:1101.0538 [INSPIRE].

[87] G. Cowan, K. Cranmer, E. Gross and O. Vitells, *Asymptotic formulae for likelihood-based tests of new physics*, *Eur. Phys. J.* **C 71** (2011) 1554 [*Erratum ibid.* **C 73** (2013) 2501] [arXiv:1007.1727] [INSPIRE].

[88] A.L. Read, *Presentation of search results: The* CL_s *technique*, *J. Phys.* **G 28** (2002) 2693 [INSPIRE].

[89] CMD collaboration, *Measurement of the cross section ratio* $\sigma_{t\bar{t}b\bar{b}}/\sigma_{t\bar{t}jj}$ *in pp collisions at* $\sqrt{s} = 8$ *TeV*, *Phys. Lett.* **B 746** (2015) 132 [arXiv:1411.5621].

[90] ATLAS collaboration, *Search for the Standard Model Higgs boson produced in association with top quarks and decaying into* $b\bar{b}$ *in pp collisions at* $\sqrt{s} = 8$ *TeV with the ATLAS detector*, *Eur. Phys. J.* **C 75** (2015) 349 [arXiv:1503.05066] [INSPIRE].

[91] ATLAS collaboration, *ATLAS computing acknowledgements 2016-2017*, ATL-GEN-PUB-2016-002 (2016).

JHEP09(2017)088

The ATLAS collaboration

M. Aaboud[137d], G. Aad[88], B. Abbott[115], O. Abdinov[12,*], B. Abeloos[119], S.H. Abidi[161], O.S. AbouZeid[139], N.L. Abraham[151], H. Abramowicz[155], H. Abreu[154], R. Abreu[118], Y. Abulaiti[148a,148b], B.S. Acharya[167a,167b,a], S. Adachi[157], L. Adamczyk[41a], J. Adelman[110], M. Adersberger[102], T. Adye[133], A.A. Affolder[139], T. Agatonovic-Jovin[14], C. Agheorghiesei[28c], J.A. Aguilar-Saavedra[128a,128f], S.P. Ahlen[24], F. Ahmadov[68,b], G. Aielli[135a,135b], S. Akatsuka[71], H. Akerstedt[148a,148b], T.P.A. Åkesson[84], E. Akilli[52], A.V. Akimov[98], G.L. Alberghi[22a,22b], J. Albert[172], P. Albicocco[50], M.J. Alconada Verzini[74], M. Aleksa[32], I.N. Aleksandrov[68], C. Alexa[28b], G. Alexander[155], T. Alexopoulos[10], M. Alhroob[115], B. Ali[130], M. Aliev[76a,76b], G. Alimonti[94a], J. Alison[33], S.P. Alkire[38], B.M.M. Allbrooke[151], B.W. Allen[118], P.P. Allport[19], A. Aloisio[106a,106b], A. Alonso[39], F. Alonso[74], C. Alpigiani[140], A.A. Alshehri[56], M. Alstaty[88], B. Alvarez Gonzalez[32], D. Álvarez Piqueras[170], M.G. Alviggi[106a,106b], B.T. Amadio[16], Y. Amaral Coutinho[26a], C. Amelung[25], D. Amidei[92], S.P. Amor Dos Santos[128a,128c], A. Amorim[128a,128b], S. Amoroso[32], G. Amundsen[25], C. Anastopoulos[141], L.S. Ancu[52], N. Andari[19], T. Andeen[11], C.F. Anders[60b], J.K. Anders[77], K.J. Anderson[33], A. Andreazza[94a,94b], V. Andrei[60a], S. Angelidakis[9], I. Angelozzi[109], A. Angerami[38], A.V. Anisenkov[111,c], N. Anjos[13], A. Annovi[126a,126b], C. Antel[60a], M. Antonelli[50], A. Antonov[100,*], D.J. Antrim[166], F. Anulli[134a], M. Aoki[69], L. Aperio Bella[32], G. Arabidze[93], Y. Arai[69], J.P. Araque[128a], V. Araujo Ferraz[26a], A.T.H. Arce[48], R.E. Ardell[80], F.A. Arduh[74], J-F. Arguin[97], S. Argyropoulos[66], M. Arik[20a], A.J. Armbruster[145], L.J. Armitage[79], O. Arnaez[161], H. Arnold[51], M. Arratia[30], O. Arslan[23], A. Artamonov[99], G. Artoni[122], S. Artz[86], S. Asai[157], N. Asbah[45], A. Ashkenazi[155], L. Asquith[151], K. Assamagan[27], R. Astalos[146a], M. Atkinson[169], N.B. Atlay[143], K. Augsten[130], G. Avolio[32], B. Axen[16], M.K. Ayoub[119], G. Azuelos[97,d], A.E. Baas[60a], M.J. Baca[19], H. Bachacou[138], K. Bachas[76a,76b], M. Backes[122], M. Backhaus[32], P. Bagnaia[134a,134b], M. Bahmani[42], H. Bahrasemani[144], J.T. Baines[133], M. Bajic[39], O.K. Baker[179], E.M. Baldin[111,c], P. Balek[175], F. Balli[138], W.K. Balunas[124], E. Banas[42], Sw. Banerjee[176,e], A.A.E. Bannoura[178], L. Barak[32], E.L. Barberio[91], D. Barberis[53a,53b], M. Barbero[88], T. Barillari[103], M-S Barisits[32], T. Barklow[145], N. Barlow[30], S.L. Barnes[36c], B.M. Barnett[133], R.M. Barnett[16], Z. Barnovska-Blenessy[36a], A. Baroncelli[136a], G. Barone[25], A.J. Barr[122], L. Barranco Navarro[170], F. Barreiro[85], J. Barreiro Guimarães da Costa[35a], R. Bartoldus[145], A.E. Barton[75], P. Bartos[146a], A. Basalaev[125], A. Bassalat[119,f], R.L. Bates[56], S.J. Batista[161], J.R. Batley[30], M. Battaglia[139], M. Bauce[134a,134b], F. Bauer[138], H.S. Bawa[145,g], J.B. Beacham[113], M.D. Beattie[75], T. Beau[83], P.H. Beauchemin[165], P. Bechtle[23], H.P. Beck[18,h], H.C. Beck[57], K. Becker[122], M. Becker[86], M. Beckingham[173], C. Becot[112], A.J. Beddall[20e], A. Beddall[20b], V.A. Bednyakov[68], M. Bedognetti[109], C.P. Bee[150], T.A. Beermann[32], M. Begalli[26a], M. Begel[27], J.K. Behr[45], A.S. Bell[81], G. Bella[155], L. Bellagamba[22a], A. Bellerive[31], M. Bellomo[154], K. Belotskiy[100], O. Beltramello[32], N.L. Belyaev[100], O. Benary[155,*], D. Benchekroun[137a], M. Bender[102], K. Bendtz[148a,148b], N. Benekos[10], Y. Benhammou[155], E. Benhar Noccioli[179], J. Benitez[66], D.P. Benjamin[48], M. Benoit[52], J.R. Bensinger[25], S. Bentvelsen[109], L. Beresford[122], M. Beretta[50], D. Berge[109], E. Bergeaas Kuutmann[168], N. Berger[5], J. Beringer[16], S. Berlendis[58], N.R. Bernard[89], G. Bernardi[83], C. Bernius[145], F.U. Bernlochner[23], T. Berry[80], P. Berta[131], C. Bertella[35a], G. Bertoli[148a,148b], F. Bertolucci[126a,126b], I.A. Bertram[75], C. Bertsche[45], D. Bertsche[115], G.J. Besjes[39], O. Bessidskaia Bylund[148a,148b], M. Bessner[45], N. Besson[138], C. Betancourt[51], A. Bethani[87], S. Bethke[103], A.J. Bevan[79], J. Beyer[103], R.M. Bianchi[127], O. Biebel[102], D. Biedermann[17], R. Bielski[87], K. Bierwagen[86], N.V. Biesuz[126a,126b], M. Biglietti[136a], T.R.V. Billoud[97], H. Bilokon[50], M. Bindi[57], A. Bingul[20b], C. Bini[134a,134b], S. Biondi[22a,22b], T. Bisanz[57], C. Bittrich[47], D.M. Bjergaard[48], C.W. Black[152], J.E. Black[145], K.M. Black[24], R.E. Blair[6], T. Blazek[146a], I. Bloch[45], C. Blocker[25], A. Blue[56], W. Blum[86,*], U. Blumenschein[79], S. Blunier[34a], G.J. Bobbink[109], V.S. Bobrovnikov[111,c], S.S. Bocchetta[84], A. Bocci[48], C. Bock[102], M. Boehler[51], D. Boerner[178], D. Bogavac[102], A.G. Bogdanchikov[111], C. Bohm[148a], V. Boisvert[80], P. Bokan[168,i], T. Bold[41a], A.S. Boldyrev[101], A.E. Bolz[60b], M. Bomben[83], M. Bona[79], M. Boonekamp[138], A. Borisov[132], G. Borissov[75], J. Bortfeldt[32], D. Bortoletto[122],

JHEP09(2017)088

V. Bortolotto[62a,62b,62c], D. Boscherini[22a], M. Bosman[13], J.D. Bossio Sola[29], J. Boudreau[127], J. Bouffard[2], E.V. Bouhova-Thacker[75], D. Boumediene[37], C. Bourdarios[119], S.K. Boutle[56], A. Boveia[113], J. Boyd[32], I.R. Boyko[68], J. Bracinik[19], A. Brandt[8], G. Brandt[57], O. Brandt[60a], U. Bratzler[158], B. Brau[89], J.E. Brau[118], W.D. Breaden Madden[56], K. Brendlinger[45], A.J. Brennan[91], L. Brenner[109], R. Brenner[168], S. Bressler[175], D.L. Briglin[19], T.M. Bristow[49], D. Britton[56], D. Britzger[45], F.M. Brochu[30], I. Brock[23], R. Brock[93], G. Brooijmans[38], T. Brooks[80], W.K. Brooks[34b], J. Brosamer[16], E. Brost[110], J.H Broughton[19], P.A. Bruckman de Renstrom[42], D. Bruncko[146b], A. Bruni[22a], G. Bruni[22a], L.S. Bruni[109], BH Brunt[30], M. Bruschi[22a], N. Bruscino[23], P. Bryant[33], L. Bryngemark[45], T. Buanes[15], Q. Buat[144], P. Buchholz[143], A.G. Buckley[56], I.A. Budagov[68], F. Buehrer[51], M.K. Bugge[121], O. Bulekov[100], D. Bullock[8], T.J. Burch[110], S. Burdin[77], C.D. Burgard[51], A.M. Burger[5], B. Burghgrave[110], K. Burka[42], S. Burke[133], I. Burmeister[46], J.T.P. Burr[122], E. Busato[37], D. Büscher[51], V. Büscher[86], P. Bussey[56], J.M. Butler[24], C.M. Buttar[56], J.M. Butterworth[81], P. Butti[32], W. Buttinger[27], A. Buzatu[35c], A.R. Buzykaev[111,c], S. Cabrera Urbán[170], D. Caforio[130], V.M. Cairo[40a,40b], O. Cakir[4a], N. Calace[52], P. Calafiura[16], A. Calandri[88], G. Calderini[83], P. Calfayan[64], G. Callea[40a,40b], L.P. Caloba[26a], S. Calvente Lopez[85], D. Calvet[37], S. Calvet[37], T.P. Calvet[88], R. Camacho Toro[33], S. Camarda[32], P. Camarri[135a,135b], D. Cameron[121], R. Caminal Armadans[169], C. Camincher[58], S. Campana[32], M. Campanelli[81], A. Camplani[94a,94b], A. Campoverde[143], V. Canale[106a,106b], M. Cano Bret[36c], J. Cantero[116], T. Cao[155], M.D.M. Capeans Garrido[32], I. Caprini[28b], M. Caprini[28b], M. Capua[40a,40b], R.M. Carbone[38], R. Cardarelli[135a], F. Cardillo[51], I. Carli[131], T. Carli[32], G. Carlino[106a], B.T. Carlson[127], L. Carminati[94a,94b], R.M.D. Carney[148a,148b], S. Caron[108], E. Carquin[34b], S. Carrá[94a,94b], G.D. Carrillo-Montoya[32], J. Carvalho[128a,128c], D. Casadei[19], M.P. Casado[13,j], M. Casolino[13], D.W. Casper[166], R. Castelijn[109], V. Castillo Gimenez[170], N.F. Castro[128a,k], A. Catinaccio[32], J.R. Catmore[121], A. Cattai[32], J. Caudron[23], V. Cavaliere[169], E. Cavallaro[13], D. Cavalli[94a], M. Cavalli-Sforza[13], V. Cavasinni[126a,126b], E. Celebi[20a], F. Ceradini[136a,136b], L. Cerda Alberich[170], A.S. Cerqueira[26b], A. Cerri[151], L. Cerrito[135a,135b], F. Cerutti[16], A. Cervelli[18], S.A. Cetin[20d], A. Chafaq[137a], D. Chakraborty[110], S.K. Chan[59], W.S. Chan[109], Y.L. Chan[62a], P. Chang[169], J.D. Chapman[30], D.G. Charlton[19], C.C. Chau[161], C.A. Chavez Barajas[151], S. Che[113], S. Cheatham[167a,167c], A. Chegwidden[93], S. Chekanov[6], S.V. Chekulaev[163a], G.A. Chelkov[68,l], M.A. Chelstowska[32], C. Chen[67], H. Chen[27], S. Chen[35b], S. Chen[157], X. Chen[35c,m], Y. Chen[70], H.C. Cheng[92], H.J. Cheng[35a], A. Cheplakov[68], E. Cheremushkina[132], R. Cherkaoui El Moursli[137e], E. Cheu[7], K. Cheung[63], L. Chevalier[138], V. Chiarella[50], G. Chiarelli[126a,126b], G. Chiodini[76a], A.S. Chisholm[32], A. Chitan[28b], Y.H. Chiu[172], M.V. Chizhov[68], K. Choi[64], A.R. Chomont[37], S. Chouridou[156], V. Christodoulou[81], D. Chromek-Burckhart[32], M.C. Chu[62a], J. Chudoba[129], A.J. Chuinard[90], J.J. Chwastowski[42], L. Chytka[117], A.K. Ciftci[4a], D. Cinca[46], V. Cindro[78], I.A. Cioara[23], C. Ciocca[22a,22b], A. Ciocio[16], F. Cirotto[106a,106b], Z.H. Citron[175], M. Citterio[94a], M. Ciubancan[28b], A. Clark[52], B.L. Clark[59], M.R. Clark[38], P.J. Clark[49], R.N. Clarke[16], C. Clement[148a,148b], Y. Coadou[88], M. Cobal[167a,167c], A. Coccaro[52], J. Cochran[67], L. Colasurdo[108], B. Cole[38], A.P. Colijn[109], J. Collot[58], T. Colombo[166], P. Conde Muiño[128a,128b], E. Coniavitis[51], S.H. Connell[147b], I.A. Connelly[87], S. Constantinescu[28b], G. Conti[32], F. Conventi[106a,n], M. Cooke[16], A.M. Cooper-Sarkar[122], F. Cormier[171], K.J.R. Cormier[161], M. Corradi[134a,134b], F. Corriveau[90,o], A. Cortes-Gonzalez[32], G. Cortiana[103], G. Costa[94a], M.J. Costa[170], D. Costanzo[141], G. Cottin[30], G. Cowan[80], B.E. Cox[87], K. Cranmer[112], S.J. Crawley[56], R.A. Creager[124], G. Cree[31], S. Crépé-Renaudin[58], F. Crescioli[83], W.A. Cribbs[148a,148b], M. Cristinziani[23], V. Croft[108], G. Crosetti[40a,40b], A. Cueto[85], T. Cuhadar Donszelmann[141], A.R. Cukierman[145], J. Cummings[179], M. Curatolo[50], J. Cúth[86], P. Czodrowski[32], G. D'amen[22a,22b], S. D'Auria[56], L. D'eramo[83], M. D'Onofrio[77], M.J. Da Cunha Sargedas De Sousa[128a,128b], C. Da Via[87], W. Dabrowski[41a], T. Dado[146a], T. Dai[92], O. Dale[15], F. Dallaire[97], C. Dallapiccola[89], M. Dam[39], J.R. Dandoy[124], M.F. Daneri[29], N.P. Dang[176], A.C. Daniells[19], N.S. Dann[87], M. Danninger[171], M. Dano Hoffmann[138], V. Dao[150], G. Darbo[53a], S. Darmora[8], J. Dassoulas[3], A. Dattagupta[118], T. Daubney[45], W. Davey[23],

JHEP09(2017)088

C. David[45], T. Davidek[131], D.R. Davis[48], P. Davison[81], E. Dawe[91], I. Dawson[141], K. De[8], R. de Asmundis[106a], A. De Benedetti[115], S. De Castro[22a,22b], S. De Cecco[83], N. De Groot[108], P. de Jong[109], H. De la Torre[93], F. De Lorenzi[67], A. De Maria[57], D. De Pedis[134a], A. De Salvo[134a], U. De Sanctis[135a,135b], A. De Santo[151], K. De Vasconcelos Corga[88], J.B. De Vivie De Regie[119], W.J. Dearnaley[75], R. Debbe[27], C. Debenedetti[139], D.V. Dedovich[68], N. Dehghanian[3], I. Deigaard[109], M. Del Gaudio[40a,40b], J. Del Peso[85], D. Delgove[119], F. Deliot[138], C.M. Delitzsch[52], A. Dell'Acqua[32], L. Dell'Asta[24], M. Dell'Orso[126a,126b], M. Della Pietra[106a,106b], D. della Volpe[52], M. Delmastro[5], C. Delporte[119], P.A. Delsart[58], D.A. DeMarco[161], S. Demers[179], M. Demichev[68], A. Demilly[83], S.P. Denisov[132], D. Denysiuk[138], D. Derendarz[42], J.E. Derkaoui[137d], F. Derue[83], P. Dervan[77], K. Desch[23], C. Deterre[45], K. Dette[46], M.R. Devesa[29], P.O. Deviveiros[32], A. Dewhurst[133], S. Dhaliwal[25], F.A. Di Bello[52], A. Di Ciaccio[135a,135b], L. Di Ciaccio[5], W.K. Di Clemente[124], C. Di Donato[106a,106b], A. Di Girolamo[32], B. Di Girolamo[32], B. Di Micco[136a,136b], R. Di Nardo[32], K.F. Di Petrillo[59], A. Di Simone[51], R. Di Sipio[161], D. Di Valentino[31], C. Diaconu[88], M. Diamond[161], F.A. Dias[39], M.A. Diaz[34a], E.B. Diehl[92], J. Dietrich[17], S. Díez Cornell[45], A. Dimitrievska[14], J. Dingfelder[23], P. Dita[28b], S. Dita[28b], F. Dittus[32], F. Djama[88], T. Djobava[54b], J.I. Djuvsland[60a], M.A.B. do Vale[26c], D. Dobos[32], M. Dobre[28b], C. Doglioni[84], J. Dolejsi[131], Z. Dolezal[131], M. Donadelli[26d], S. Donati[126a,126b], P. Dondero[123a,123b], J. Donini[37], J. Dopke[133], A. Doria[106a], M.T. Dova[74], A.T. Doyle[56], E. Drechsler[57], M. Dris[10], Y. Du[36b], J. Duarte-Campderros[155], A. Dubreuil[52], E. Duchovni[175], G. Duckeck[102], A. Ducourthial[83], O.A. Ducu[97,p], D. Duda[109], A. Dudarev[32], A.Chr. Dudder[86], E.M. Duffield[16], L. Duflot[119], M. Dührssen[32], M. Dumancic[175], A.E. Dumitriu[28b], A.K. Duncan[56], M. Dunford[60a], H. Duran Yildiz[4a], M. Düren[55], A. Durglishvili[54b], D. Duschinger[47], B. Dutta[45], M. Dyndal[45], C. Eckardt[45], K.M. Ecker[103], R.C. Edgar[92], T. Eifert[32], G. Eigen[15], K. Einsweiler[16], T. Ekelof[168], M. El Kacimi[137c], R. El Kosseifi[88], V. Ellajosyula[88], M. Ellert[168], S. Elles[5], F. Ellinghaus[178], A.A. Elliot[172], N. Ellis[32], J. Elmsheuser[27], M. Elsing[32], D. Emeliyanov[133], Y. Enari[157], O.C. Endner[86], J.S. Ennis[173], J. Erdmann[46], A. Ereditato[18], M. Ernst[27], S. Errede[169], M. Escalier[119], C. Escobar[127], B. Esposito[50], O. Estrada Pastor[170], A.I. Etienvre[138], E. Etzion[155], H. Evans[64], A. Ezhilov[125], M. Ezzi[137e], F. Fabbri[22a,22b], L. Fabbri[22a,22b], V. Fabiani[108], G. Facini[33], R.M. Fakhrutdinov[132], S. Falciano[134a], R.J. Falla[81], J. Faltova[32], Y. Fang[35a], M. Fanti[94a,94b], A. Farbin[8], A. Farilla[136a], C. Farina[127], E.M. Farina[123a,123b], T. Farooque[93], S. Farrell[16], S.M. Farrington[173], P. Farthouat[32], F. Fassi[137e], P. Fassnacht[32], D. Fassouliotis[9], M. Faucci Giannelli[80], A. Favareto[53a,53b], W.J. Fawcett[122], L. Fayard[119], O.L. Fedin[125,q], W. Fedorko[171], S. Feigl[121], L. Feligioni[88], C. Feng[36b], E.J. Feng[32], H. Feng[92], M.J. Fenton[56], A.B. Fenyuk[132], L. Feremenga[8], P. Fernandez Martinez[170], S. Fernandez Perez[13], J. Ferrando[45], A. Ferrari[168], P. Ferrari[109], R. Ferrari[123a], D.E. Ferreira de Lima[60b], A. Ferrer[170], D. Ferrere[52], C. Ferretti[92], F. Fiedler[86], A. Filipčič[78], M. Filipuzzi[45], F. Filthaut[108], M. Fincke-Keeler[172], K.D. Finelli[152], M.C.N. Fiolhais[128a,128c,r], L. Fiorini[170], A. Fischer[2], C. Fischer[13], J. Fischer[178], W.C. Fisher[93], N. Flaschel[45], I. Fleck[143], P. Fleischmann[92], R.R.M. Fletcher[124], T. Flick[178], B.M. Flierl[102], L.R. Flores Castillo[62a], M.J. Flowerdew[103], G.T. Forcolin[87], A. Formica[138], F.A. Förster[13], A. Forti[87], A.G. Foster[19], D. Fournier[119], H. Fox[75], S. Fracchia[141], P. Francavilla[83], M. Franchini[22a,22b], S. Franchino[60a], D. Francis[32], L. Franconi[121], M. Franklin[59], M. Frate[166], M. Fraternali[123a,123b], D. Freeborn[81], S.M. Fressard-Batraneanu[32], B. Freund[97], D. Froidevaux[32], J.A. Frost[122], C. Fukunaga[158], T. Fusayasu[104], J. Fuster[170], C. Gabaldon[58], O. Gabizon[154], A. Gabrielli[22a,22b], A. Gabrielli[16], G.P. Gach[41a], S. Gadatsch[32], S. Gadomski[80], G. Gagliardi[53a,53b], L.G. Gagnon[97], C. Galea[108], B. Galhardo[128a,128c], E.J. Gallas[122], B.J. Gallop[133], P. Gallus[130], G. Galster[39], K.K. Gan[113], S. Ganguly[37], Y. Gao[77], Y.S. Gao[145,g], F.M. Garay Walls[49], C. García[170], J.E. García Navarro[170], J.A. García Pascual[35a], M. Garcia-Sciveres[16], R.W. Gardner[33], N. Garelli[145], V. Garonne[121], A. Gascon Bravo[45], K. Gasnikova[45], C. Gatti[50], A. Gaudiello[53a,53b], G. Gaudio[123a], I.L. Gavrilenko[98], C. Gay[171], G. Gaycken[23], E.N. Gazis[10], C.N.P. Gee[133], J. Geisen[57], M. Geisen[86], M.P. Geisler[60a], K. Gellerstedt[148a,148b], C. Gemme[53a], M.H. Genest[58], C. Geng[92], S. Gentile[134a,134b], C. Gentsos[156], S. George[80], D. Gerbaudo[13], A. Gershon[155], G. Geßner[46],

JHEP09(2017)088

S. Ghasemi[143], M. Ghneimat[23], B. Giacobbe[22a], S. Giagu[134a,134b], P. Giannetti[126a,126b], S.M. Gibson[80], M. Gignac[171], M. Gilchriese[16], D. Gillberg[31], G. Gilles[178], D.M. Gingrich[3,d], N. Giokaris[9,*], M.P. Giordani[167a,167c], F.M. Giorgi[22a], P.F. Giraud[138], P. Giromini[59], D. Giugni[94a], F. Giuli[122], C. Giuliani[103], M. Giulini[60b], B.K. Gjelsten[121], S. Gkaitatzis[156], I. Gkialas[9,s], E.L. Gkougkousis[139], P. Gkountoumis[10], L.K. Gladilin[101], C. Glasman[85], J. Glatzer[13], P.C.F. Glaysher[45], A. Glazov[45], M. Goblirsch-Kolb[25], J. Godlewski[42], S. Goldfarb[91], T. Golling[52], D. Golubkov[132], A. Gomes[128a,128b,128d], R. Gonçalo[128a], R. Goncalves Gama[26a], J. Goncalves Pinto Firmino Da Costa[138], G. Gonella[51], L. Gonella[19], A. Gongadze[68], S. González de la Hoz[170], S. Gonzalez-Sevilla[52], L. Goossens[32], P.A. Gorbounov[99], H.A. Gordon[27], I. Gorelov[107], B. Gorini[32], E. Gorini[76a,76b], A. Gorišek[78], A.T. Goshaw[48], C. Gössling[46], M.I. Gostkin[68], C.A. Gottardo[23], C.R. Goudet[119], D. Goujdami[137c], A.G. Goussiou[140], N. Govender[147b,t], E. Gozani[154], L. Graber[57], I. Grabowska-Bold[41a], P.O.J. Gradin[168], J. Gramling[166], E. Gramstad[121], S. Grancagnolo[17], V. Gratchev[125], P.M. Gravila[28f], C. Gray[56], H.M. Gray[16], Z.D. Greenwood[82,u], C. Grefe[23], K. Gregersen[81], I.M. Gregor[45], P. Grenier[145], K. Grevtsov[5], J. Griffiths[8], A.A. Grillo[139], K. Grimm[75], S. Grinstein[13,v], Ph. Gris[37], J.-F. Grivaz[119], S. Groh[86], E. Gross[175], J. Grosse-Knetter[57], G.C. Grossi[82], Z.J. Grout[81], A. Grummer[107], L. Guan[92], W. Guan[176], J. Guenther[65], F. Guescini[163a], D. Guest[166], O. Gueta[155], B. Gui[113], E. Guido[53a,53b], T. Guillemin[5], S. Guindon[2], U. Gul[56], C. Gumpert[32], J. Guo[36c], W. Guo[92], Y. Guo[36a], R. Gupta[43], S. Gupta[122], G. Gustavino[134a,134b], P. Gutierrez[115], N.G. Gutierrez Ortiz[81], C. Gutschow[81], C. Guyot[138], M.P. Guzik[41a], C. Gwenlan[122], C.B. Gwilliam[77], A. Haas[112], C. Haber[16], H.K. Hadavand[8], N. Haddad[137e], A. Hadef[88], S. Hageböck[23], M. Hagihara[164], H. Hakobyan[180,*], M. Haleem[45], J. Haley[116], G. Halladjian[93], G.D. Hallewell[88], K. Hamacher[178], P. Hamal[117], K. Hamano[172], A. Hamilton[147a], G.N. Hamity[141], P.G. Hamnett[45], L. Han[36a], S. Han[35a], K. Hanagaki[69,w], K. Hanawa[157], M. Hance[139], B. Haney[124], P. Hanke[60a], J.B. Hansen[39], J.D. Hansen[39], M.C. Hansen[23], P.H. Hansen[39], K. Hara[164], A.S. Hard[176], T. Harenberg[178], F. Hariri[119], S. Harkusha[95], R.D. Harrington[49], P.F. Harrison[173], N.M. Hartmann[102], M. Hasegawa[70], Y. Hasegawa[142], A. Hasib[49], S. Hassani[138], S. Haug[18], R. Hauser[93], L. Hauswald[47], L.B. Havener[38], M. Havranek[130], C.M. Hawkes[19], R.J. Hawkings[32], D. Hayakawa[159], D. Hayden[93], C.P. Hays[122], J.M. Hays[79], H.S. Hayward[77], S.J. Haywood[133], S.J. Head[19], T. Heck[86], V. Hedberg[84], L. Heelan[8], S. Heer[23], K.K. Heidegger[51], S. Heim[45], T. Heim[16], B. Heinemann[45,x], J.J. Heinrich[102], L. Heinrich[112], C. Heinz[55], J. Hejbal[129], L. Helary[32], A. Held[171], S. Hellman[148a,148b], C. Helsens[32], R.C.W. Henderson[75], Y. Heng[176], S. Henkelmann[171], A.M. Henriques Correia[32], S. Henrot-Versille[119], G.H. Herbert[17], H. Herde[25], V. Herget[177], Y. Hernández Jiménez[147c], H. Herr[86], G. Herten[51], R. Hertenberger[102], L. Hervas[32], T.C. Herwig[124], G.G. Hesketh[81], N.P. Hessey[163a], J.W. Hetherly[43], S. Higashino[69], E. Higón-Rodriguez[170], K. Hildebrand[33], E. Hill[172], J.C. Hill[30], K.H. Hiller[45], S.J. Hillier[19], M. Hils[47], I. Hinchliffe[16], M. Hirose[51], D. Hirschbuehl[178], B. Hiti[78], O. Hladik[129], X. Hoad[49], J. Hobbs[150], N. Hod[163a], M.C. Hodgkinson[141], P. Hodgson[141], A. Hoecker[32], M.R. Hoeferkamp[107], F. Hoenig[102], D. Hohn[23], T.R. Holmes[33], M. Homann[46], S. Honda[164], T. Honda[69], T.M. Hong[127], B.H. Hooberman[169], W.H. Hopkins[118], Y. Horii[105], A.J. Horton[144], J-Y. Hostachy[58], S. Hou[153], A. Hoummada[137a], J. Howarth[87], J. Hoya[74], M. Hrabovsky[117], J. Hrdinka[32], I. Hristova[17], J. Hrivnac[119], T. Hryn'ova[5], A. Hrynevich[96], P.J. Hsu[63], S.-C. Hsu[140], Q. Hu[36a], S. Hu[36c], Y. Huang[35a], Z. Hubacek[130], F. Hubaut[88], F. Huegging[23], T.B. Huffman[122], E.W. Hughes[38], G. Hughes[75], M. Huhtinen[32], P. Huo[150], N. Huseynov[68,b], J. Huston[93], J. Huth[59], G. Iacobucci[52], G. Iakovidis[27], I. Ibragimov[143], L. Iconomidou-Fayard[119], Z. Idrissi[137e], P. Iengo[32], O. Igonkina[109,y], T. Iizawa[174], Y. Ikegami[69], M. Ikeno[69], Y. Ilchenko[11,z], D. Iliadis[156], N. Ilic[145], G. Introzzi[123a,123b], P. Ioannou[9,*], M. Iodice[136a], K. Iordanidou[38], V. Ippolito[59], M.F. Isacson[168], N. Ishijima[120], M. Ishino[157], M. Ishitsuka[159], C. Issever[122], S. Istin[20a], F. Ito[164], J.M. Iturbe Ponce[87], R. Iuppa[162a,162b], H. Iwasaki[69], J.M. Izen[44], V. Izzo[106a], S. Jabbar[3], P. Jackson[1], R.M. Jacobs[23], V. Jain[2], K.B. Jakobi[86], K. Jakobs[51], S. Jakobsen[65], T. Jakoubek[129], D.O. Jamin[116], D.K. Jana[82], R. Jansky[52], J. Janssen[23], M. Janus[57], P.A. Janus[41a], G. Jarlskog[84], N. Javadov[68,b], T. Javůrek[51], M. Javurkova[51], F. Jeanneau[138], L. Jeanty[16], J. Jejelava[54a,aa],

JHEP09(2017)088

A. Jelinskas[173], P. Jenni[51,ab], C. Jeske[173], S. Jézéquel[5], H. Ji[176], J. Jia[150], H. Jiang[67], Y. Jiang[36a], Z. Jiang[145], S. Jiggins[81], J. Jimenez Pena[170], S. Jin[35a], A. Jinaru[28b], O. Jinnouchi[159], H. Jivan[147c], P. Johansson[141], K.A. Johns[7], C.A. Johnson[64], W.J. Johnson[140], K. Jon-And[148a,148b], R.W.L. Jones[75], S.D. Jones[151], S. Jones[7], T.J. Jones[77], J. Jongmanns[60a], P.M. Jorge[128a,128b], J. Jovicevic[163a], X. Ju[176], A. Juste Rozas[13,v], M.K. Köhler[175], A. Kaczmarska[42], M. Kado[119], H. Kagan[113], M. Kagan[145], S.J. Kahn[88], T. Kaji[174], E. Kajomovitz[48], C.W. Kalderon[84], A. Kaluza[86], S. Kama[43], A. Kamenshchikov[132], N. Kanaya[157], L. Kanjir[78], V.A. Kantserov[100], J. Kanzaki[69], B. Kaplan[112], L.S. Kaplan[176], D. Kar[147c], K. Karakostas[10], N. Karastathis[10], M.J. Kareem[57], E. Karentzos[10], S.N. Karpov[68], Z.M. Karpova[68], K. Karthik[112], V. Kartvelishvili[75], A.N. Karyukhin[132], K. Kasahara[164], L. Kashif[176], R.D. Kass[113], A. Kastanas[149], Y. Kataoka[157], C. Kato[157], A. Katre[52], J. Katzy[45], K. Kawade[70], K. Kawagoe[73], T. Kawamoto[157], G. Kawamura[57], E.F. Kay[77], V.F. Kazanin[111,c], R. Keeler[172], R. Kehoe[43], J.S. Keller[31], J.J. Kempster[80], J Kendrick[19], H. Keoshkerian[161], O. Kepka[129], B.P. Kerševan[78], S. Kersten[178], R.A. Keyes[90], M. Khader[169], F. Khalil-zada[12], A. Khanov[116], A.G. Kharlamov[111,c], T. Kharlamova[111,c], A. Khodinov[160], T.J. Khoo[52], V. Khovanskiy[99,*], E. Khramov[68], J. Khubua[54b,ac], S. Kido[70], C.R. Kilby[80], H.Y. Kim[8], S.H. Kim[164], Y.K. Kim[33], N. Kimura[156], O.M. Kind[17], B.T. King[77], D. Kirchmeier[47], J. Kirk[133], A.E. Kiryunin[103], T. Kishimoto[157], D. Kisielewska[41a], V. Kitali[45], K. Kiuchi[164], O. Kivernyk[5], E. Kladiva[146b], T. Klapdor-Kleingrothaus[51], M.H. Klein[38], M. Klein[77], U. Klein[77], K. Kleinknecht[86], P. Klimek[110], A. Klimentov[27], R. Klingenberg[46], T. Klingl[23], T. Klioutchnikova[32], E.-E. Kluge[60a], P. Kluit[109], S. Kluth[103], E. Kneringer[65], E.B.F.G. Knoops[88], A. Knue[103], A. Kobayashi[157], D. Kobayashi[159], T. Kobayashi[157], M. Kobel[47], M. Kocian[145], P. Kodys[131], T. Koffas[31], E. Koffeman[109], N.M. Köhler[103], T. Koi[145], M. Kolb[60b], I. Koletsou[5], A.A. Komar[98,*], Y. Komori[157], T. Kondo[69], N. Kondrashova[36c], K. Köneke[51], A.C. König[108], T. Kono[69,ad], R. Konoplich[112,ae], N. Konstantinidis[81], R. Kopeliansky[64], S. Koperny[41a], A.K. Kopp[51], K. Korcyl[42], K. Kordas[156], A. Korn[81], A.A. Korol[111,c], I. Korolkov[13], E.V. Korolkova[141], O. Kortner[103], S. Kortner[103], T. Kosek[131], V.V. Kostyukhin[23], A. Kotwal[48], A. Koulouris[10], A. Kourkoumeli-Charalampidi[123a,123b], C. Kourkoumelis[9], E. Kourlitis[141], V. Kouskoura[27], A.B. Kowalewska[42], R. Kowalewski[172], T.Z. Kowalski[41a], C. Kozakai[157], W. Kozanecki[138], A.S. Kozhin[132], V.A. Kramarenko[101], G. Kramberger[78], D. Krasnopevtsev[100], M.W. Krasny[83], A. Krasznahorkay[32], D. Krauss[103], J.A. Kremer[41a], J. Kretzschmar[77], K. Kreutzfeldt[55], P. Krieger[161], K. Krizka[33], K. Kroeninger[46], H. Kroha[103], J. Kroll[129], J. Kroll[124], J. Kroseberg[23], J. Krstic[14], U. Kruchonak[68], H. Krüger[23], N. Krumnack[67], M.C. Kruse[48], T. Kubota[91], H. Kucuk[81], S. Kuday[4b], J.T. Kuechler[178], S. Kuehn[32], A. Kugel[60a], F. Kuger[177], T. Kuhl[45], V. Kukhtin[68], R. Kukla[88], Y. Kulchitsky[95], S. Kuleshov[34b], Y.P. Kulinich[169], M. Kuna[134a,134b], T. Kunigo[71], A. Kupco[129], T. Kupfer[46], O. Kuprash[155], H. Kurashige[70], L.L. Kurchaninov[163a], Y.A. Kurochkin[95], M.G. Kurth[35a], V. Kus[129], E.S. Kuwertz[172], M. Kuze[159], J. Kvita[117], T. Kwan[172], D. Kyriazopoulos[141], A. La Rosa[103], J.L. La Rosa Navarro[26d], L. La Rotonda[40a,40b], F. La Ruffa[40a,40b], C. Lacasta[170], F. Lacava[134a,134b], J. Lacey[45], H. Lacker[17], D. Lacour[83], E. Ladygin[68], R. Lafaye[5], B. Laforge[83], T. Lagouri[179], S. Lai[57], S. Lammers[64], W. Lampl[7], E. Lançon[27], U. Landgraf[51], M.P.J. Landon[79], M.C. Lanfermann[52], V.S. Lang[60a], J.C. Lange[13], R.J. Langenberg[32], A.J. Lankford[166], F. Lanni[27], K. Lantzsch[23], A. Lanza[123a], A. Lapertosa[53a,53b], S. Laplace[83], J.F. Laporte[138], T. Lari[94a], F. Lasagni Manghi[22a,22b], M. Lassnig[32], P. Laurelli[50], W. Lavrijsen[16], A.T. Law[139], P. Laycock[77], T. Lazovich[59], M. Lazzaroni[94a,94b], B. Le[91], O. Le Dortz[83], E. Le Guirriec[88], E.P. Le Quilleuc[138], M. LeBlanc[172], T. LeCompte[6], F. Ledroit-Guillon[58], C.A. Lee[27], G.R. Lee[133,af], S.C. Lee[153], L. Lee[59], B. Lefebvre[90], G. Lefebvre[83], M. Lefebvre[172], F. Legger[102], C. Leggett[16], G. Lehmann Miotto[32], X. Lei[7], W.A. Leight[45], M.A.L. Leite[26d], R. Leitner[131], D. Lellouch[175], B. Lemmer[57], K.J.C. Leney[81], T. Lenz[23], B. Lenzi[32], R. Leone[7], S. Leone[126a,126b], C. Leonidopoulos[49], G. Lerner[151], C. Leroy[97], A.A.J. Lesage[138], C.G. Lester[30], M. Levchenko[125], J. Levêque[5], D. Levin[92], L.J. Levinson[175], M. Levy[19], D. Lewis[79], B. Li[36a,ag], Changqiao Li[36a], H. Li[150], L. Li[36c], Q. Li[35a], S. Li[48], X. Li[36c], Y. Li[143], Z. Liang[35a], B. Liberti[135a], A. Liblong[161],

JHEP09(2017)088

K. Lie[62c], J. Liebal[23], W. Liebig[15], A. Limosani[152], S.C. Lin[183], T.H. Lin[86], B.E. Lindquist[150], A.E. Lionti[52], E. Lipeles[124], A. Lipniacka[15], M. Lisovyi[60b], T.M. Liss[169,ah], A. Lister[171], A.M. Litke[139], B. Liu[153,ai], H. Liu[92], H. Liu[27], J.K.K. Liu[122], J. Liu[36b], J.B. Liu[36a], K. Liu[88], L. Liu[169], M. Liu[36a], Y.L. Liu[36a], Y. Liu[36a], M. Livan[123a,123b], A. Lleres[58], J. Llorente Merino[35a], S.L. Lloyd[79], C.Y. Lo[62b], F. Lo Sterzo[153], E.M. Lobodzinska[45], P. Loch[7], F.K. Loebinger[87], A. Loesle[51], K.M. Loew[25], A. Loginov[179,*], T. Lohse[17], K. Lohwasser[45], M. Lokajicek[129], B.A. Long[24], J.D. Long[169], R.E. Long[75], L. Longo[76a,76b], K.A. Looper[113], J.A. Lopez[34b], D. Lopez Mateos[59], I. Lopez Paz[13], A. Lopez Solis[83], J. Lorenz[102], N. Lorenzo Martinez[5], M. Losada[21], P.J. Lösel[102], X. Lou[35a], A. Lounis[119], J. Love[6], P.A. Love[75], H. Lu[62a], N. Lu[92], Y.J. Lu[63], H.J. Lubatti[140], C. Luci[134a,134b], A. Lucotte[58], C. Luedtke[51], F. Luehring[64], W. Lukas[65], L. Luminari[134a], O. Lundberg[148a,148b], B. Lund-Jensen[149], P.M. Luzi[83], D. Lynn[27], R. Lysak[129], E. Lytken[84], F. Lyu[35a], V. Lyubushkin[68], H. Ma[27], L.L. Ma[36b], Y. Ma[36b], G. Maccarrone[50], A. Macchiolo[103], C.M. Macdonald[141], B. Maček[78], J. Machado Miguens[124,128b], D. Madaffari[170], R. Madar[37], W.F. Mader[47], A. Madsen[45], J. Maeda[70], S. Maeland[15], T. Maeno[27], A.S. Maevskiy[101], V. Magerl[51], J. Mahlstedt[109], C. Maiani[119], C. Maidantchik[26a], A.A. Maier[103], T. Maier[102], A. Maio[128a,128b,128d], O. Majersky[146a], S. Majewski[118], Y. Makida[69], N. Makovec[119], B. Malaescu[83], Pa. Malecki[42], V.P. Maleev[125], F. Malek[58], U. Mallik[66], D. Malon[6], C. Malone[30], S. Maltezos[10], S. Malyukov[32], J. Mamuzic[170], G. Mancini[50], I. Mandić[78], J. Maneira[128a,128b], L. Manhaes de Andrade Filho[26b], J. Manjarres Ramos[47], A. Mann[102], A. Manousos[32], B. Mansoulie[138], J.D. Mansour[35a], R. Mantifel[90], M. Mantoani[57], S. Manzoni[94a,94b], L. Mapelli[32], G. Marceca[29], L. March[52], L. Marchese[122], G. Marchiori[83], M. Marcisovsky[129], M. Marjanovic[37], D.E. Marley[92], F. Marroquim[26a], S.P. Marsden[87], Z. Marshall[16], M.U.F Martensson[168], S. Marti-Garcia[170], C.B. Martin[113], T.A. Martin[173], V.J. Martin[49], B. Martin dit Latour[15], M. Martinez[13,v], V.I. Martinez Outschoorn[169], S. Martin-Haugh[133], V.S. Martoiu[28b], A.C. Martyniuk[81], A. Marzin[32], L. Masetti[86], T. Mashimo[157], R. Mashinistov[98], J. Masik[87], A.L. Maslennikov[111,c], L. Massa[135a,135b], P. Mastrandrea[5], A. Mastroberardino[40a,40b], T. Masubuchi[157], P. Mättig[178], J. Maurer[28b], S.J. Maxfield[77], D.A. Maximov[111,c], R. Mazini[153], I. Maznas[156], S.M. Mazza[94a,94b], N.C. Mc Fadden[107], G. Mc Goldrick[161], S.P. Mc Kee[92], A. McCarn[92], R.L. McCarthy[150], T.G. McCarthy[103], L.I. McClymont[81], E.F. McDonald[91], J.A. Mcfayden[81], G. Mchedlidze[57], S.J. McMahon[133], P.C. McNamara[91], R.A. McPherson[172,o], S. Meehan[140], T.J. Megy[51], S. Mehlhase[102], A. Mehta[77], T. Meideck[58], K. Meier[60a], B. Meirose[44], D. Melini[170,aj], B.R. Mellado Garcia[147c], J.D. Mellenthin[57], M. Melo[146a], F. Meloni[18], A. Melzer[23], S.B. Menary[87], L. Meng[77], X.T. Meng[92], A. Mengarelli[22a,22b], S. Menke[103], E. Meoni[40a,40b], S. Mergelmeyer[17], P. Mermod[52], L. Merola[106a,106b], C. Meroni[94a], F.S. Merritt[33], A. Messina[134a,134b], J. Metcalfe[6], A.S. Mete[166], C. Meyer[124], J-P. Meyer[138], J. Meyer[109], H. Meyer Zu Theenhausen[60a], F. Miano[151], R.P. Middleton[133], S. Miglioranzi[53a,53b], L. Mijović[49], G. Mikenberg[175], M. Mikestikova[129], M. Mikuž[78], M. Milesi[91], A. Milic[161], D.W. Miller[33], C. Mills[49], A. Milov[175], D.A. Milstead[148a,148b], A.A. Minaenko[132], Y. Minami[157], I.A. Minashvili[68], A.I. Mincer[112], B. Mindur[41a], M. Mineev[68], Y. Minegishi[157], Y. Ming[176], L.M. Mir[13], K.P. Mistry[124], T. Mitani[174], J. Mitrevski[102], V.A. Mitsou[170], A. Miucci[18], P.S. Miyagawa[141], A. Mizukami[69], J.U. Mjörnmark[84], T. Mkrtchyan[180], M. Mlynarikova[131], T. Moa[148a,148b], K. Mochizuki[97], P. Mogg[51], S. Mohapatra[38], S. Molander[148a,148b], R. Moles-Valls[23], R. Monden[71], M.C. Mondragon[93], K. Mönig[45], J. Monk[39], E. Monnier[88], A. Montalbano[150], J. Montejo Berlingen[32], F. Monticelli[74], S. Monzani[94a,94b], R.W. Moore[3], N. Morange[119], D. Moreno[21], M. Moreno Llácer[32], P. Morettini[53a], S. Morgenstern[32], D. Mori[144], T. Mori[157], M. Morii[59], M. Morinaga[157], V. Morisbak[121], A.K. Morley[32], G. Mornacchi[32], J.D. Morris[79], L. Morvaj[150], P. Moschovakos[10], M. Mosidze[54b], H.J. Moss[141], J. Moss[145,ak], K. Motohashi[159], R. Mount[145], E. Mountricha[27], E.J.W. Moyse[89], S. Muanza[88], F. Mueller[103], J. Mueller[127], R.S.P. Mueller[102], D. Muenstermann[75], P. Mullen[56], G.A. Mullier[18], F.J. Munoz Sanchez[87], W.J. Murray[173,133], H. Musheghyan[181], M. Muškinja[78], A.G. Myagkov[132,al], M. Myska[130], B.P. Nachman[16], O. Nackenhorst[52], K. Nagai[122], R. Nagai[69,ad], K. Nagano[69], Y. Nagasaka[61], K. Nagata[164], M. Nagel[51], E. Nagy[88], A.M. Nairz[32],

JHEP09(2017)088

Y. Nakahama[105], K. Nakamura[69], T. Nakamura[157], I. Nakano[114], R.F. Naranjo Garcia[45], R. Narayan[11], D.I. Narrias Villar[60a], I. Naryshkin[125], T. Naumann[45], G. Navarro[21], R. Nayyar[7], H.A. Neal[92], P.Yu. Nechaeva[98], T.J. Neep[138], A. Negri[123a,123b], M. Negrini[22a], S. Nektarijevic[108], C. Nellist[119], A. Nelson[166], M.E. Nelson[122], S. Nemecek[129], P. Nemethy[112], M. Nessi[32,am], M.S. Neubauer[169], M. Neumann[178], P.R. Newman[19], T.Y. Ng[62c], T. Nguyen Manh[97], R.B. Nickerson[122], R. Nicolaidou[138], J. Nielsen[139], V. Nikolaenko[132,al], I. Nikolic-Audit[83], K. Nikolopoulos[19], J.K. Nilsen[121], P. Nilsson[27], Y. Ninomiya[157], A. Nisati[134a], N. Nishu[35c], R. Nisius[103], I. Nitsche[46], T. Nobe[157], Y. Noguchi[71], M. Nomachi[120], I. Nomidis[31], M.A. Nomura[27], T. Nooney[79], M. Nordberg[32], N. Norjoharuddeen[122], O. Novgorodova[47], S. Nowak[103], M. Nozaki[69], L. Nozka[117], K. Ntekas[166], E. Nurse[81], F. Nuti[91], K. O'connor[25], D.C. O'Neil[144], A.A. O'Rourke[45], V. O'Shea[56], F.G. Oakham[31,d], H. Oberlack[103], T. Obermann[23], J. Ocariz[83], A. Ochi[70], I. Ochoa[38], J.P. Ochoa-Ricoux[34a], S. Oda[73], S. Odaka[69], A. Oh[87], S.H. Oh[48], C.C. Ohm[16], H. Ohman[168], H. Oide[53a,53b], H. Okawa[164], Y. Okumura[157], T. Okuyama[69], A. Olariu[28b], L.F. Oleiro Seabra[128a], S.A. Olivares Pino[49], D. Oliveira Damazio[27], A. Olszewski[42], J. Olszowska[42], A. Onofre[128a,128e], K. Onogi[105], P.U.E. Onyisi[11,z], H. Oppen[121], M.J. Oreglia[33], Y. Oren[155], D. Orestano[136a,136b], N. Orlando[62b], R.S. Orr[161], B. Osculati[53a,53b,*], R. Ospanov[36a], G. Otero y Garzon[29], H. Otono[73], M. Ouchrif[137d], F. Ould-Saada[121], A. Ouraou[138], K.P. Oussoren[109], Q. Ouyang[35a], M. Owen[56], R.E. Owen[19], V.E. Ozcan[20a], N. Ozturk[8], K. Pachal[144], A. Pacheco Pages[13], L. Pacheco Rodriguez[138], C. Padilla Aranda[13], S. Pagan Griso[16], M. Paganini[179], F. Paige[27], G. Palacino[64], S. Palazzo[40a,40b], S. Palestini[32], M. Palka[41b], D. Pallin[37], E.St. Panagiotopoulou[10], I. Panagoulias[10], C.E. Pandini[83], J.G. Panduro Vazquez[80], P. Pani[32], S. Panitkin[27], D. Pantea[28b], L. Paolozzi[52], Th.D. Papadopoulou[10], K. Papageorgiou[9,s], A. Paramonov[6], D. Paredes Hernandez[179], A.J. Parker[75], M.A. Parker[30], K.A. Parker[45], F. Parodi[53a,53b], J.A. Parsons[38], U. Parzefall[51], V.R. Pascuzzi[161], J.M. Pasner[139], E. Pasqualucci[134a], S. Passaggio[53a], Fr. Pastore[80], S. Pataraia[86], J.R. Pater[87], T. Pauly[32], B. Pearson[103], S. Pedraza Lopez[170], R. Pedro[128a,128b], S.V. Peleganchuk[111,c], O. Penc[129], C. Peng[35a], H. Peng[36a], J. Penwell[64], B.S. Peralva[26b], M.M. Perego[138], D.V. Perepelitsa[27], L. Perini[94a,94b], H. Pernegger[32], S. Perrella[106a,106b], R. Peschke[45], V.D. Peshekhonov[68,*], K. Peters[45], R.F.Y. Peters[87], B.A. Petersen[32], T.C. Petersen[39], E. Petit[58], A. Petridis[1], C. Petridou[156], P. Petroff[119], E. Petrolo[134a], M. Petrov[122], F. Petrucci[136a,136b], N.E. Pettersson[89], A. Peyaud[138], R. Pezoa[34b], F.H. Phillips[93], P.W. Phillips[133], G. Piacquadio[150], E. Pianori[173], A. Picazio[89], E. Piccaro[79], M.A. Pickering[122], R. Piegaia[29], J.E. Pilcher[33], A.D. Pilkington[87], A.W.J. Pin[87], M. Pinamonti[135a,135b], J.L. Pinfold[3], H. Pirumov[45], M. Pitt[175], L. Plazak[146a], M.-A. Pleier[27], V. Pleskot[86], E. Plotnikova[68], D. Pluth[67], P. Podberezko[111], R. Poettgen[148a,148b], R. Poggi[123a,123b], L. Poggioli[119], D. Pohl[23], G. Polesello[123a], A. Poley[45], A. Policicchio[40a,40b], R. Polifka[32], A. Polini[22a], C.S. Pollard[56], V. Polychronakos[27], K. Pommès[32], D. Ponomarenko[100], L. Pontecorvo[134a], G.A. Popeneciu[28d], A. Poppleton[32], S. Pospisil[130], K. Potamianos[16], I.N. Potrap[68], C.J. Potter[30], G. Poulard[32], T. Poulsen[84], J. Poveda[32], M.E. Pozo Astigarraga[32], P. Pralavorio[88], A. Pranko[16], S. Prell[67], D. Price[87], M. Primavera[76a], S. Prince[90], N. Proklova[100], K. Prokofiev[62c], F. Prokoshin[34b], S. Protopopescu[27], J. Proudfoot[6], M. Przybycien[41a], A. Puri[169], P. Puzo[119], J. Qian[92], G. Qin[56], Y. Qin[87], A. Quadt[57], M. Queitsch-Maitland[45], D. Quilty[56], S. Raddum[121], V. Radeka[27], V. Radescu[122], S.K. Radhakrishnan[150], P. Radloff[118], P. Rados[91], F. Ragusa[94a,94b], G. Rahal[182], J.A. Raine[87], S. Rajagopalan[27], C. Rangel-Smith[168], T. Rashid[119], S. Raspopov[5], M.G. Ratti[94a,94b], D.M. Rauch[45], F. Rauscher[102], S. Rave[86], I. Ravinovich[175], J.H. Rawling[87], M. Raymond[32], A.L. Read[121], N.P. Readioff[58], M. Reale[76a,76b], D.M. Rebuzzi[123a,123b], A. Redelbach[177], G. Redlinger[27], R. Reece[139], R.G. Reed[147c], K. Reeves[44], L. Rehnisch[17], J. Reichert[124], A. Reiss[86], C. Rembser[32], H. Ren[35a], M. Rescigno[134a], S. Resconi[94a], E.D. Resseguie[124], S. Rettie[171], E. Reynolds[19], O.L. Rezanova[111,c], P. Reznicek[131], R. Rezvani[97], R. Richter[103], S. Richter[81], E. Richter-Was[41b], O. Ricken[23], M. Ridel[83], P. Rieck[103], C.J. Riegel[178], J. Rieger[57], O. Rifki[115], M. Rijssenbeek[150], A. Rimoldi[123a,123b], M. Rimoldi[18], L. Rinaldi[22a], G. Ripellino[149], B. Ristić[32], E. Ritsch[32], I. Riu[13], F. Rizatdinova[116], E. Rizvi[79],

JHEP09(2017)088

C. Rizzi[13], R.T. Roberts[87], S.H. Robertson[90,o], A. Robichaud-Veronneau[90], D. Robinson[30], J.E.M. Robinson[45], A. Robson[56], E. Rocco[86], C. Roda[126a,126b], Y. Rodina[88,an], S. Rodriguez Bosca[170], A. Rodriguez Perez[13], D. Rodriguez Rodriguez[170], S. Roe[32], C.S. Rogan[59], O. Røhne[121], J. Roloff[59], A. Romaniouk[100], M. Romano[22a,22b], S.M. Romano Saez[37], E. Romero Adam[170], N. Rompotis[77], M. Ronzani[51], L. Roos[83], S. Rosati[134a], K. Rosbach[51], P. Rose[139], N.-A. Rosien[57], E. Rossi[106a,106b], L.P. Rossi[53a], J.H.N. Rosten[30], R. Rosten[140], M. Rotaru[28b], J. Rothberg[140], D. Rousseau[119], A. Rozanov[88], Y. Rozen[154], X. Ruan[147c], F. Rubbo[145], F. Rühr[51], A. Ruiz-Martinez[31], Z. Rurikova[51], N.A. Rusakovich[68], H.L. Russell[90], J.P. Rutherfoord[7], N. Ruthmann[32], Y.F. Ryabov[125], M. Rybar[169], G. Rybkin[119], S. Ryu[6], A. Ryzhov[132], G.F. Rzehorz[57], A.F. Saavedra[152], G. Sabato[109], S. Sacerdoti[29], H.F-W. Sadrozinski[139], R. Sadykov[68], F. Safai Tehrani[134a], P. Saha[110], M. Sahinsoy[60a], M. Saimpert[45], M. Saito[157], T. Saito[157], H. Sakamoto[157], Y. Sakurai[174], G. Salamanna[136a,136b], J.E. Salazar Loyola[34b], D. Salek[109], P.H. Sales De Bruin[168], D. Salihagic[103], A. Salnikov[145], J. Salt[170], D. Salvatore[40a,40b], F. Salvatore[151], A. Salvucci[62a,62b,62c], A. Salzburger[32], D. Sammel[51], D. Sampsonidis[156], D. Sampsonidou[156], J. Sánchez[170], V. Sanchez Martinez[170], A. Sanchez Pineda[167a,167c], H. Sandaker[121], R.L. Sandbach[79], C.O. Sander[45], M. Sandhoff[178], C. Sandoval[21], D.P.C. Sankey[133], M. Sannino[53a,53b], Y. Sano[105], A. Sansoni[50], C. Santoni[37], H. Santos[128a], I. Santoyo Castillo[151], A. Sapronov[68], J.G. Saraiva[128a,128d], B. Sarrazin[23], O. Sasaki[69], K. Sato[164], E. Sauvan[5], G. Savage[80], P. Savard[161,d], N. Savic[103], C. Sawyer[133], L. Sawyer[82,u], J. Saxon[33], C. Sbarra[22a], A. Sbrizzi[22a,22b], T. Scanlon[81], D.A. Scannicchio[166], M. Scarcella[152], J. Schaarschmidt[140], P. Schacht[103], B.M. Schachtner[102], D. Schaefer[32], L. Schaefer[124], R. Schaefer[45], J. Schaeffer[86], S. Schaepe[23], S. Schaetzel[60b], U. Schäfer[86], A.C. Schaffer[119], D. Schaile[102], R.D. Schamberger[150], V.A. Schegelsky[125], D. Scheirich[131], M. Schernau[166], C. Schiavi[53a,53b], S. Schier[139], L.K. Schildgen[23], C. Schillo[51], M. Schioppa[40a,40b], S. Schlenker[32], K.R. Schmidt-Sommerfeld[103], K. Schmieden[32], C. Schmitt[86], S. Schmitt[45], S. Schmitz[86], U. Schnoor[51], L. Schoeffel[138], A. Schoening[60b], B.D. Schoenrock[93], E. Schopf[23], M. Schott[86], J.F.P. Schouwenberg[108], J. Schovancova[181], S. Schramm[52], N. Schuh[86], A. Schulte[86], M.J. Schultens[23], H.-C. Schultz-Coulon[60a], H. Schulz[17], M. Schumacher[51], B.A. Schumm[139], Ph. Schune[138], A. Schwartzman[145], T.A. Schwarz[92], H. Schweiger[87], Ph. Schwemling[138], R. Schwienhorst[93], J. Schwindling[138], A. Sciandra[23], G. Sciolla[25], M. Scornajenghi[40a,40b], F. Scuri[126a,126b], F. Scutti[91], J. Searcy[92], P. Seema[23], S.C. Seidel[107], A. Seiden[139], J.M. Seixas[26a], G. Sekhniaidze[106a], K. Sekhon[92], S.J. Sekula[43], N. Semprini-Cesari[22a,22b], S. Senkin[37], C. Serfon[121], L. Serin[119], L. Serkin[167a,167b], M. Sessa[136a,136b], R. Seuster[172], H. Severini[115], T. Sfiligoj[78], F. Sforza[32], A. Sfyrla[52], E. Shabalina[57], N.W. Shaikh[148a,148b], L.Y. Shan[35a], R. Shang[169], J.T. Shank[24], M. Shapiro[16], P.B. Shatalov[99], K. Shaw[167a,167b], S.M. Shaw[87], A. Shcherbakova[148a,148b], C.Y. Shehu[151], Y. Shen[115], N. Sherafati[31], P. Sherwood[81], L. Shi[153,ao], S. Shimizu[70], C.O. Shimmin[179], M. Shimojima[104], I.P.J. Shipsey[122], S. Shirabe[73], M. Shiyakova[68,ap], J. Shlomi[175], A. Shmeleva[98], D. Shoaleh Saadi[97], M.J. Shochet[33], S. Shojaii[94a], D.R. Shope[115], S. Shrestha[113], E. Shulga[100], M.A. Shupe[7], P. Sicho[129], A.M. Sickles[169], P.E. Sidebo[149], E. Sideras Haddad[147c], O. Sidiropoulou[177], A. Sidoti[22a,22b], F. Siegert[47], Dj. Sijacki[14], J. Silva[128a,128d], S.B. Silverstein[148a], V. Simak[130], Lj. Simic[14], S. Simion[119], E. Simioni[86], B. Simmons[81], M. Simon[86], P. Sinervo[161], N.B. Sinev[118], M. Sioli[22a,22b], G. Siragusa[177], I. Siral[92], S.Yu. Sivoklokov[101], J. Sjölin[148a,148b], M.B. Skinner[75], P. Skubic[115], M. Slater[19], T. Slavicek[130], M. Slawinska[42], K. Sliwa[165], R. Slovak[131], V. Smakhtin[175], B.H. Smart[5], J. Smiesko[146a], N. Smirnov[100], S.Yu. Smirnov[100], Y. Smirnov[100], L.N. Smirnova[101,aq], O. Smirnova[84], J.W. Smith[57], M.N.K. Smith[38], R.W. Smith[38], M. Smizanska[75], K. Smolek[130], A.A. Snesarev[98], I.M. Snyder[118], S. Snyder[27], R. Sobie[172,o], F. Socher[47], A. Soffer[155], A. Søgaard[49], D.A. Soh[153], G. Sokhrannyi[78], C.A. Solans Sanchez[32], M. Solar[130], E.Yu. Soldatov[100], U. Soldevila[170], A.A. Solodkov[132], A. Soloshenko[68], O.V. Solovyanov[132], V. Solovyev[125], P. Sommer[51], H. Son[165], A. Sopczak[130], D. Sosa[60b], C.L. Sotiropoulou[126a,126b], R. Soualah[167a,167c], A.M. Soukharev[111,c], D. South[45], B.C. Sowden[80], S. Spagnolo[76a,76b], M. Spalla[126a,126b], M. Spangenberg[173], F. Spanò[80], D. Sperlich[17],

JHEP09(2017)088

F. Spettel[103], T.M. Spieker[60a], R. Spighi[22a], G. Spigo[32], L.A. Spiller[91], M. Spousta[131], R.D. St. Denis[56,*], A. Stabile[94a], R. Stamen[60a], S. Stamm[17], E. Stanecka[42], R.W. Stanek[6], C. Stanescu[136a], M.M. Stanitzki[45], B.S. Stapf[109], S. Stapnes[121], E.A. Starchenko[132], G.H. Stark[33], J. Stark[58], S.H Stark[39], P. Staroba[129], P. Starovoitov[60a], S. Stärz[32], R. Staszewski[42], P. Steinberg[27], B. Stelzer[144], H.J. Stelzer[32], O. Stelzer-Chilton[163a], H. Stenzel[55], G.A. Stewart[56], M.C. Stockton[118], M. Stoebe[90], G. Stoicea[28b], P. Stolte[57], S. Stonjek[103], A.R. Stradling[8], A. Straessner[47], M.E. Stramaglia[18], J. Strandberg[149], S. Strandberg[148a,148b], M. Strauss[115], P. Strizenec[146b], R. Ströhmer[177], D.M. Strom[118], R. Stroynowski[43], A. Strubig[49], S.A. Stucci[27], B. Stugu[15], N.A. Styles[45], D. Su[145], J. Su[127], S. Suchek[60a], Y. Sugaya[120], M. Suk[130], V.V. Sulin[98], DMS Sultan[162a,162b], S. Sultansoy[4c], T. Sumida[71], S. Sun[59], X. Sun[3], K. Suruliz[151], C.J.E. Suster[152], M.R. Sutton[151], S. Suzuki[69], M. Svatos[129], M. Swiatlowski[33], S.P. Swift[2], I. Sykora[146a], T. Sykora[131], D. Ta[51], K. Tackmann[45], J. Taenzer[155], A. Taffard[166], R. Tafirout[163a], N. Taiblum[155], H. Takai[27], R. Takashima[72], E.H. Takasugi[103], T. Takeshita[142], Y. Takubo[69], M. Talby[88], A.A. Talyshev[111,c], J. Tanaka[157], M. Tanaka[159], R. Tanaka[119], S. Tanaka[69], R. Tanioka[70], B.B. Tannenwald[113], S. Tapia Araya[34b], S. Tapprogge[86], S. Tarem[154], G.F. Tartarelli[94a], P. Tas[131], M. Tasevsky[129], T. Tashiro[71], E. Tassi[40a,40b], A. Tavares Delgado[128a,128b], Y. Tayalati[137e], A.C. Taylor[107], G.N. Taylor[91], P.T.E. Taylor[91], W. Taylor[163b], P. Teixeira-Dias[80], D. Temple[144], H. Ten Kate[32], P.K. Teng[153], J.J. Teoh[120], F. Tepel[178], S. Terada[69], K. Terashi[157], J. Terron[85], S. Terzo[13], M. Testa[50], R.J. Teuscher[161,o], T. Theveneaux-Pelzer[88], J.P. Thomas[19], J. Thomas-Wilsker[80], P.D. Thompson[19], A.S. Thompson[56], L.A. Thomsen[179], E. Thomson[124], M.J. Tibbetts[16], R.E. Ticse Torres[88], V.O. Tikhomirov[98,ar], Yu.A. Tikhonov[111,c], S. Timoshenko[100], P. Tipton[179], S. Tisserant[88], K. Todome[159], S. Todorova-Nova[5], S. Todt[47], J. Tojo[73], S. Tokár[146a], K. Tokushuku[69], E. Tolley[59], L. Tomlinson[87], M. Tomoto[105], L. Tompkins[145,as], K. Toms[107], B. Tong[59], P. Tornambe[51], E. Torrence[118], H. Torres[144], E. Torró Pastor[140], J. Toth[88,at], F. Touchard[88], D.R. Tovey[141], C.J. Treado[112], T. Trefzger[177], F. Tresoldi[151], A. Tricoli[27], I.M. Trigger[163a], S. Trincaz-Duvoid[83], M.F. Tripiana[13], W. Trischuk[161], B. Trocmé[58], A. Trofymov[45], C. Troncon[94a], M. Trottier-McDonald[16], M. Trovatelli[172], L. Truong[147b], M. Trzebinski[42], A. Trzupek[42], K.W. Tsang[62a], J.C-L. Tseng[122], P.V. Tsiareshka[95], G. Tsipolitis[10], N. Tsirintanis[9], S. Tsiskaridze[13], V. Tsiskaridze[51], E.G. Tskhadadze[54a], K.M. Tsui[62a], I.I. Tsukerman[99], V. Tsulaia[16], S. Tsuno[69], D. Tsybychev[150], Y. Tu[62b], A. Tudorache[28b], V. Tudorache[28b], T.T. Tulbure[28a], A.N. Tuna[59], S.A. Tupputi[22a,22b], S. Turchikhin[68], D. Turgeman[175], I. Turk Cakir[4b,au], R. Turra[94a], P.M. Tuts[38], G. Ucchielli[22a,22b], I. Ueda[69], M. Ughetto[148a,148b], F. Ukegawa[164], G. Unal[32], A. Undrus[27], G. Unel[166], F.C. Ungaro[91], Y. Unno[69], C. Unverdorben[102], J. Urban[146b], P. Urquijo[91], P. Urrejola[86], G. Usai[8], J. Usui[69], L. Vacavant[88], V. Vacek[130], B. Vachon[90], A. Vaidya[81], C. Valderanis[102], E. Valdes Santurio[148a,148b], S. Valentinetti[22a,22b], A. Valero[170], L. Valéry[13], S. Valkar[131], A. Vallier[5], J.A. Valls Ferrer[170], W. Van Den Wollenberg[109], H. van der Graaf[109], P. van Gemmeren[6], J. Van Nieuwkoop[144], I. van Vulpen[109], M.C. van Woerden[109], M. Vanadia[135a,135b], W. Vandelli[32], A. Vaniachine[160], P. Vankov[109], G. Vardanyan[180], R. Vari[134a], E.W. Varnes[7], C. Varni[53a,53b], T. Varol[43], D. Varouchas[119], A. Vartapetian[8], K.E. Varvell[152], J.G. Vasquez[179], G.A. Vasquez[34b], F. Vazeille[37], T. Vazquez Schroeder[90], J. Veatch[57], V. Veeraraghavan[7], L.M. Veloce[161], F. Veloso[128a,128c], S. Veneziano[134a], A. Ventura[76a,76b], M. Venturi[172], N. Venturi[32], A. Venturini[25], V. Vercesi[123a], M. Verducci[136a,136b], W. Verkerke[109], A.T. Vermeulen[109], J.C. Vermeulen[109], M.C. Vetterli[144,d], N. Viaux Maira[34b], O. Viazlo[84], I. Vichou[169,*], T. Vickey[141], O.E. Vickey Boeriu[141], G.H.A. Viehhauser[122], S. Viel[16], L. Vigani[122], M. Villa[22a,22b], M. Villaplana Perez[94a,94b], E. Vilucchi[50], M.G. Vincter[31], V.B. Vinogradov[68], A. Vishwakarma[45], C. Vittori[22a,22b], I. Vivarelli[151], S. Vlachos[10], M. Vogel[178], P. Vokac[130], G. Volpi[126a,126b], H. von der Schmitt[103], E. von Toerne[23], V. Vorobel[131], K. Vorobev[100], M. Vos[170], R. Voss[32], J.H. Vossebeld[77], N. Vranjes[14], M. Vranjes Milosavljevic[14], V. Vrba[130], M. Vreeswijk[109], R. Vuillermet[32], I. Vukotic[33], P. Wagner[23], W. Wagner[178], J. Wagner-Kuhr[102], H. Wahlberg[74], S. Wahrmund[47], J. Wakabayashi[105], J. Walder[75], R. Walker[102], W. Walkowiak[143],

JHEP09(2017)088

V. Wallangen[148a,148b], C. Wang[35b], C. Wang[36b,av], F. Wang[176], H. Wang[16], H. Wang[3], J. Wang[45], J. Wang[152], Q. Wang[115], R. Wang[6], S.M. Wang[153], T. Wang[38], W. Wang[153,aw], W. Wang[36a], Z. Wang[36c], C. Wanotayaroj[118], A. Warburton[90], C.P. Ward[30], D.R. Wardrope[81], A. Washbrook[49], P.M. Watkins[19], A.T. Watson[19], M.F. Watson[19], G. Watts[140], S. Watts[87], B.M. Waugh[81], A.F. Webb[11], S. Webb[86], M.S. Weber[18], S.W. Weber[177], S.A. Weber[31], J.S. Webster[6], A.R. Weidberg[122], B. Weinert[64], J. Weingarten[57], M. Weirich[86], C. Weiser[51], H. Weits[109], P.S. Wells[32], T. Wenaus[27], T. Wengler[32], S. Wenig[32], N. Wermes[23], M.D. Werner[67], P. Werner[32], M. Wessels[60a], K. Whalen[118], N.L. Whallon[140], A.M. Wharton[75], A.S. White[92], A. White[8], M.J. White[1], R. White[34b], D. Whiteson[166], B.W. Whitmore[75], F.J. Wickens[133], W. Wiedenmann[176], M. Wielers[133], C. Wiglesworth[39], L.A.M. Wiik-Fuchs[51], A. Wildauer[103], F. Wilk[87], H.G. Wilkens[32], H.H. Williams[124], S. Williams[109], C. Willis[93], S. Willocq[89], J.A. Wilson[19], I. Wingerter-Seez[5], E. Winkels[151], F. Winklmeier[118], O.J. Winston[151], B.T. Winter[23], M. Wittgen[145], M. Wobisch[82,u], T.M.H. Wolf[109], R. Wolff[88], M.W. Wolter[42], H. Wolters[128a,128c], V.W.S. Wong[171], S.D. Worm[19], B.K. Wosiek[42], J. Wotschack[32], K.W. Wozniak[42], M. Wu[33], S.L. Wu[176], X. Wu[52], Y. Wu[92], T.R. Wyatt[87], B.M. Wynne[49], S. Xella[39], Z. Xi[92], L. Xia[35c], D. Xu[35a], L. Xu[27], T. Xu[138], B. Yabsley[152], S. Yacoob[147a], D. Yamaguchi[159], Y. Yamaguchi[120], A. Yamamoto[69], S. Yamamoto[157], T. Yamanaka[157], M. Yamatani[157], K. Yamauchi[105], Y. Yamazaki[70], Z. Yan[24], H. Yang[36c], H. Yang[16], Y. Yang[153], Z. Yang[15], W-M. Yao[16], Y.C. Yap[83], Y. Yasu[69], E. Yatsenko[5], K.H. Yau Wong[23], J. Ye[43], S. Ye[27], I. Yeletskikh[68], E. Yigitbasi[24], E. Yildirim[86], K. Yorita[174], K. Yoshihara[124], C. Young[145], C.J.S. Young[32], J. Yu[8], J. Yu[67], S.P.Y. Yuen[23], I. Yusuff[30,ax], B. Zabinski[42], G. Zacharis[10], R. Zaidan[13], A.M. Zaitsev[132,al], N. Zakharchuk[45], J. Zalieckas[15], A. Zaman[150], S. Zambito[59], D. Zanzi[91], C. Zeitnitz[178], G. Zemaityte[122], A. Zemla[41a], J.C. Zeng[169], Q. Zeng[145], O. Zenin[132], T. Ženiš[146a], D. Zerwas[119], D. Zhang[92], F. Zhang[176], G. Zhang[36a,ay], H. Zhang[35b], J. Zhang[6], L. Zhang[51], L. Zhang[36a], M. Zhang[169], P. Zhang[35b], R. Zhang[23], R. Zhang[36a,av], X. Zhang[36b], Y. Zhang[35a], Z. Zhang[119], X. Zhao[43], Y. Zhao[36b,az], Z. Zhao[36a], A. Zhemchugov[68], B. Zhou[92], C. Zhou[176], L. Zhou[43], M. Zhou[35a], M. Zhou[150], N. Zhou[35c], C.G. Zhu[36b], H. Zhu[35a], J. Zhu[92], Y. Zhu[36a], X. Zhuang[35a], K. Zhukov[98], A. Zibell[177], D. Zieminska[64], N.I. Zimine[68], C. Zimmermann[86], S. Zimmermann[51], Z. Zinonos[103], M. Zinser[86], M. Ziolkowski[143], L. Živković[14], G. Zobernig[176], A. Zoccoli[22a,22b], R. Zou[33], M. zur Nedden[17], L. Zwalinski[32]

[1] Department of Physics, University of Adelaide, Adelaide, Australia
[2] Physics Department, SUNY Albany, Albany NY, U.S.A.
[3] Department of Physics, University of Alberta, Edmonton AB, Canada
[4] [(a)] Department of Physics, Ankara University, Ankara; [(b)] Istanbul Aydin University, Istanbul; [(c)] Division of Physics, TOBB University of Economics and Technology, Ankara, Turkey
[5] LAPP, CNRS/IN2P3 and Université Savoie Mont Blanc, Annecy-le-Vieux, France
[6] High Energy Physics Division, Argonne National Laboratory, Argonne IL, U.S.A.
[7] Department of Physics, University of Arizona, Tucson AZ, U.S.A.
[8] Department of Physics, The University of Texas at Arlington, Arlington TX, U.S.A.
[9] Physics Department, National and Kapodistrian University of Athens, Athens, Greece
[10] Physics Department, National Technical University of Athens, Zografou, Greece
[11] Department of Physics, The University of Texas at Austin, Austin TX, U.S.A.
[12] Institute of Physics, Azerbaijan Academy of Sciences, Baku, Azerbaijan
[13] Institut de Física d'Altes Energies (IFAE), The Barcelona Institute of Science and Technology, Barcelona, Spain
[14] Institute of Physics, University of Belgrade, Belgrade, Serbia
[15] Department for Physics and Technology, University of Bergen, Bergen, Norway
[16] Physics Division, Lawrence Berkeley National Laboratory and University of California, Berkeley CA, U.S.A.
[17] Department of Physics, Humboldt University, Berlin, Germany
[18] Albert Einstein Center for Fundamental Physics and Laboratory for High Energy Physics, University of Bern, Bern, Switzerland

JHEP09(2017)088

[19] School of Physics and Astronomy, University of Birmingham, Birmingham, United Kingdom
[20] [(a)] Department of Physics, Bogazici University, Istanbul; [(b)] Department of Physics Engineering, Gaziantep University, Gaziantep; [(d)] Istanbul Bilgi University, Faculty of Engineering and Natural Sciences, Istanbul; [(e)] Bahcesehir University, Faculty of Engineering and Natural Sciences, Istanbul, Turkey
[21] Centro de Investigaciones, Universidad Antonio Narino, Bogota, Colombia
[22] [(a)] INFN Sezione di Bologna; [(b)] Dipartimento di Fisica e Astronomia, Università di Bologna, Bologna, Italy
[23] Physikalisches Institut, University of Bonn, Bonn, Germany
[24] Department of Physics, Boston University, Boston MA, U.S.A.
[25] Department of Physics, Brandeis University, Waltham MA, U.S.A.
[26] [(a)] Universidade Federal do Rio De Janeiro COPPE/EE/IF, Rio de Janeiro; [(b)] Electrical Circuits Department, Federal University of Juiz de Fora (UFJF), Juiz de Fora; [(c)] Federal University of Sao Joao del Rei (UFSJ), Sao Joao del Rei; [(d)] Instituto de Fisica, Universidade de Sao Paulo, Sao Paulo, Brazil
[27] Physics Department, Brookhaven National Laboratory, Upton NY, U.S.A.
[28] [(a)] Transilvania University of Brasov, Brasov; [(b)] Horia Hulubei National Institute of Physics and Nuclear Engineering, Bucharest; [(c)] Department of Physics, Alexandru Ioan Cuza University of Iasi, Iasi; [(d)] National Institute for Research and Development of Isotopic and Molecular Technologies, Physics Department, Cluj Napoca; [(e)] University Politehnica Bucharest, Bucharest; [(f)] West University in Timisoara, Timisoara, Romania
[29] Departamento de Física, Universidad de Buenos Aires, Buenos Aires, Argentina
[30] Cavendish Laboratory, University of Cambridge, Cambridge, United Kingdom
[31] Department of Physics, Carleton University, Ottawa ON, Canada
[32] CERN, Geneva, Switzerland
[33] Enrico Fermi Institute, University of Chicago, Chicago IL, U.S.A.
[34] [(a)] Departamento de Física, Pontificia Universidad Católica de Chile, Santiago; [(b)] Departamento de Física, Universidad Técnica Federico Santa María, Valparaíso, Chile
[35] [(a)] Institute of High Energy Physics, Chinese Academy of Sciences, Beijing; [(b)] Department of Physics, Nanjing University, Jiangsu; [(c)] Physics Department, Tsinghua University, Beijing 100084, China
[36] [(a)] Department of Modern Physics and State Key Laboratory of Particle Detection and Electronics, University of Science and Technology of China, Anhui; [(b)] School of Physics, Shandong University, Shandong; [(c)] Department of Physics and Astronomy, Key Laboratory for Particle Physics, Astrophysics and Cosmology, Ministry of Education; Shanghai Key Laboratory for Particle Physics and Cosmology, Shanghai Jiao Tong University, Shanghai(also at PKU-CHEP);, China
[37] Université Clermont Auvergne, CNRS/IN2P3, LPC, Clermont-Ferrand, France
[38] Nevis Laboratory, Columbia University, Irvington NY, U.S.A.
[39] Niels Bohr Institute, University of Copenhagen, Kobenhavn, Denmark
[40] [(a)] INFN Gruppo Collegato di Cosenza, Laboratori Nazionali di Frascati; [(b)] Dipartimento di Fisica, Università della Calabria, Rende, Italy
[41] [(a)] AGH University of Science and Technology, Faculty of Physics and Applied Computer Science, Krakow; [(b)] Marian Smoluchowski Institute of Physics, Jagiellonian University, Krakow, Poland
[42] Institute of Nuclear Physics Polish Academy of Sciences, Krakow, Poland
[43] Physics Department, Southern Methodist University, Dallas TX, U.S.A.
[44] Physics Department, University of Texas at Dallas, Richardson TX, U.S.A.
[45] DESY, Hamburg and Zeuthen, Germany
[46] Lehrstuhl für Experimentelle Physik IV, Technische Universität Dortmund, Dortmund, Germany
[47] Institut für Kern- und Teilchenphysik, Technische Universität Dresden, Dresden, Germany
[48] Department of Physics, Duke University, Durham NC, U.S.A.
[49] SUPA - School of Physics and Astronomy, University of Edinburgh, Edinburgh, United Kingdom
[50] INFN e Laboratori Nazionali di Frascati, Frascati, Italy

JHEP09(2017)088

[51] Fakultät für Mathematik und Physik, Albert-Ludwigs-Universität, Freiburg, Germany
[52] Departement de Physique Nucleaire et Corpusculaire, Université de Genève, Geneva, Switzerland
[53] [(a)] INFN Sezione di Genova; [(b)] Dipartimento di Fisica, Università di Genova, Genova, Italy
[54] [(a)] E. Andronikashvili Institute of Physics, Iv. Javakhishvili Tbilisi State University, Tbilisi; [(b)] High Energy Physics Institute, Tbilisi State University, Tbilisi, Georgia
[55] II Physikalisches Institut, Justus-Liebig-Universität Giessen, Giessen, Germany
[56] SUPA - School of Physics and Astronomy, University of Glasgow, Glasgow, United Kingdom
[57] II Physikalisches Institut, Georg-August-Universität, Göttingen, Germany
[58] Laboratoire de Physique Subatomique et de Cosmologie, Université Grenoble-Alpes, CNRS/IN2P3, Grenoble, France
[59] Laboratory for Particle Physics and Cosmology, Harvard University, Cambridge MA, U.S.A.
[60] [(a)] Kirchhoff-Institut für Physik, Ruprecht-Karls-Universität Heidelberg, Heidelberg; [(b)] Physikalisches Institut, Ruprecht-Karls-Universität Heidelberg, Heidelberg, Germany
[61] Faculty of Applied Information Science, Hiroshima Institute of Technology, Hiroshima, Japan
[62] [(a)] Department of Physics, The Chinese University of Hong Kong, Shatin, N.T., Hong Kong; [(b)] Department of Physics, The University of Hong Kong, Hong Kong; [(c)] Department of Physics and Institute for Advanced Study, The Hong Kong University of Science and Technology, Clear Water Bay, Kowloon, Hong Kong, China
[63] Department of Physics, National Tsing Hua University, Taiwan, Taiwan
[64] Department of Physics, Indiana University, Bloomington IN, U.S.A.
[65] Institut für Astro- und Teilchenphysik, Leopold-Franzens-Universität, Innsbruck, Austria
[66] University of Iowa, Iowa City IA, U.S.A.
[67] Department of Physics and Astronomy, Iowa State University, Ames IA, U.S.A.
[68] Joint Institute for Nuclear Research, JINR Dubna, Dubna, Russia
[69] KEK, High Energy Accelerator Research Organization, Tsukuba, Japan
[70] Graduate School of Science, Kobe University, Kobe, Japan
[71] Faculty of Science, Kyoto University, Kyoto, Japan
[72] Kyoto University of Education, Kyoto, Japan
[73] Research Center for Advanced Particle Physics and Department of Physics, Kyushu University, Fukuoka, Japan
[74] Instituto de Física La Plata, Universidad Nacional de La Plata and CONICET, La Plata, Argentina
[75] Physics Department, Lancaster University, Lancaster, United Kingdom
[76] [(a)] INFN Sezione di Lecce; [(b)] Dipartimento di Matematica e Fisica, Università del Salento, Lecce, Italy
[77] Oliver Lodge Laboratory, University of Liverpool, Liverpool, United Kingdom
[78] Department of Experimental Particle Physics, Jožef Stefan Institute and Department of Physics, University of Ljubljana, Ljubljana, Slovenia
[79] School of Physics and Astronomy, Queen Mary University of London, London, United Kingdom
[80] Department of Physics, Royal Holloway University of London, Surrey, United Kingdom
[81] Department of Physics and Astronomy, University College London, London, United Kingdom
[82] Louisiana Tech University, Ruston LA, U.S.A.
[83] Laboratoire de Physique Nucléaire et de Hautes Energies, UPMC and Université Paris-Diderot and CNRS/IN2P3, Paris, France
[84] Fysiska institutionen, Lunds universitet, Lund, Sweden
[85] Departamento de Fisica Teorica C-15, Universidad Autonoma de Madrid, Madrid, Spain
[86] Institut für Physik, Universität Mainz, Mainz, Germany
[87] School of Physics and Astronomy, University of Manchester, Manchester, United Kingdom
[88] CPPM, Aix-Marseille Université and CNRS/IN2P3, Marseille, France
[89] Department of Physics, University of Massachusetts, Amherst MA, U.S.A.
[90] Department of Physics, McGill University, Montreal QC, Canada
[91] School of Physics, University of Melbourne, Victoria, Australia
[92] Department of Physics, The University of Michigan, Ann Arbor MI, U.S.A.

JHEP09(2017)088

[93] Department of Physics and Astronomy, Michigan State University, East Lansing MI, U.S.A.
[94] [(a)] INFN Sezione di Milano; [(b)] Dipartimento di Fisica, Università di Milano, Milano, Italy
[95] B.I. Stepanov Institute of Physics, National Academy of Sciences of Belarus, Minsk, Republic of Belarus
[96] Research Institute for Nuclear Problems of Byelorussian State University, Minsk, Republic of Belarus
[97] Group of Particle Physics, University of Montreal, Montreal QC, Canada
[98] P.N. Lebedev Physical Institute of the Russian Academy of Sciences, Moscow, Russia
[99] Institute for Theoretical and Experimental Physics (ITEP), Moscow, Russia
[100] National Research Nuclear University MEPhI, Moscow, Russia
[101] D.V. Skobeltsyn Institute of Nuclear Physics, M.V. Lomonosov Moscow State University, Moscow, Russia
[102] Fakultät für Physik, Ludwig-Maximilians-Universität München, München, Germany
[103] Max-Planck-Institut für Physik (Werner-Heisenberg-Institut), München, Germany
[104] Nagasaki Institute of Applied Science, Nagasaki, Japan
[105] Graduate School of Science and Kobayashi-Maskawa Institute, Nagoya University, Nagoya, Japan
[106] [(a)] INFN Sezione di Napoli; [(b)] Dipartimento di Fisica, Università di Napoli, Napoli, Italy
[107] Department of Physics and Astronomy, University of New Mexico, Albuquerque NM, U.S.A.
[108] Institute for Mathematics, Astrophysics and Particle Physics, Radboud University Nijmegen/Nikhef, Nijmegen, Netherlands
[109] Nikhef National Institute for Subatomic Physics and University of Amsterdam, Amsterdam, Netherlands
[110] Department of Physics, Northern Illinois University, DeKalb IL, U.S.A.
[111] Budker Institute of Nuclear Physics, SB RAS, Novosibirsk, Russia
[112] Department of Physics, New York University, New York NY, U.S.A.
[113] Ohio State University, Columbus OH, U.S.A.
[114] Faculty of Science, Okayama University, Okayama, Japan
[115] Homer L. Dodge Department of Physics and Astronomy, University of Oklahoma, Norman OK, U.S.A.
[116] Department of Physics, Oklahoma State University, Stillwater OK, U.S.A.
[117] Palacký University, RCPTM, Olomouc, Czech Republic
[118] Center for High Energy Physics, University of Oregon, Eugene OR, U.S.A.
[119] LAL, Univ. Paris-Sud, CNRS/IN2P3, Université Paris-Saclay, Orsay, France
[120] Graduate School of Science, Osaka University, Osaka, Japan
[121] Department of Physics, University of Oslo, Oslo, Norway
[122] Department of Physics, Oxford University, Oxford, United Kingdom
[123] [(a)] INFN Sezione di Pavia; [(b)] Dipartimento di Fisica, Università di Pavia, Pavia, Italy
[124] Department of Physics, University of Pennsylvania, Philadelphia PA, U.S.A.
[125] National Research Centre "Kurchatov Institute" B.P.Konstantinov Petersburg Nuclear Physics Institute, St. Petersburg, Russia
[126] [(a)] INFN Sezione di Pisa; [(b)] Dipartimento di Fisica E. Fermi, Università di Pisa, Pisa, Italy
[127] Department of Physics and Astronomy, University of Pittsburgh, Pittsburgh PA, U.S.A.
[128] [(a)] Laboratório de Instrumentação e Física Experimental de Partículas - LIP, Lisboa; [(b)] Faculdade de Ciências, Universidade de Lisboa, Lisboa; [(c)] Department of Physics, University of Coimbra, Coimbra; [(d)] Centro de Física Nuclear da Universidade de Lisboa, Lisboa; [(e)] Departamento de Fisica, Universidade do Minho, Braga; [(f)] Departamento de Fisica Teorica y del Cosmos and CAFPE, Universidad de Granada, Granada; [(g)] Dep Fisica and CEFITEC of Faculdade de Ciencias e Tecnologia, Universidade Nova de Lisboa, Caparica, Portugal
[129] Institute of Physics, Academy of Sciences of the Czech Republic, Praha, Czech Republic
[130] Czech Technical University in Prague, Praha, Czech Republic
[131] Charles University, Faculty of Mathematics and Physics, Prague, Czech Republic
[132] State Research Center Institute for High Energy Physics (Protvino), NRC KI, Russia

JHEP09(2017)088

[133] Particle Physics Department, Rutherford Appleton Laboratory, Didcot, United Kingdom
[134] [(a)] INFN Sezione di Roma; [(b)] Dipartimento di Fisica, Sapienza Università di Roma, Roma, Italy
[135] [(a)] INFN Sezione di Roma Tor Vergata; [(b)] Dipartimento di Fisica, Università di Roma Tor Vergata, Roma, Italy
[136] [(a)] INFN Sezione di Roma Tre; [(b)] Dipartimento di Matematica e Fisica, Università Roma Tre, Roma, Italy
[137] [(a)] Faculté des Sciences Ain Chock, Réseau Universitaire de Physique des Hautes Energies - Université Hassan II, Casablanca; [(b)] Centre National de l'Energie des Sciences Techniques Nucleaires, Rabat; [(c)] Faculté des Sciences Semlalia, Université Cadi Ayyad, LPHEA-Marrakech; [(d)] Faculté des Sciences, Université Mohamed Premier and LPTPM, Oujda; [(e)] Faculté des sciences, Université Mohammed V, Rabat, Morocco
[138] DSM/IRFU (Institut de Recherches sur les Lois Fondamentales de l'Univers), CEA Saclay (Commissariat à l'Energie Atomique et aux Energies Alternatives), Gif-sur-Yvette, France
[139] Santa Cruz Institute for Particle Physics, University of California Santa Cruz, Santa Cruz CA, U.S.A.
[140] Department of Physics, University of Washington, Seattle WA, U.S.A.
[141] Department of Physics and Astronomy, University of Sheffield, Sheffield, United Kingdom
[142] Department of Physics, Shinshu University, Nagano, Japan
[143] Department Physik, Universität Siegen, Siegen, Germany
[144] Department of Physics, Simon Fraser University, Burnaby BC, Canada
[145] SLAC National Accelerator Laboratory, Stanford CA, U.S.A.
[146] [(a)] Faculty of Mathematics, Physics & Informatics, Comenius University, Bratislava; [(b)] Department of Subnuclear Physics, Institute of Experimental Physics of the Slovak Academy of Sciences, Kosice, Slovak Republic
[147] [(a)] Department of Physics, University of Cape Town, Cape Town; [(b)] Department of Physics, University of Johannesburg, Johannesburg; [(c)] School of Physics, University of the Witwatersrand, Johannesburg, South Africa
[148] [(a)] Department of Physics, Stockholm University; [(b)] The Oskar Klein Centre, Stockholm, Sweden
[149] Physics Department, Royal Institute of Technology, Stockholm, Sweden
[150] Departments of Physics & Astronomy and Chemistry, Stony Brook University, Stony Brook NY, U.S.A.
[151] Department of Physics and Astronomy, University of Sussex, Brighton, United Kingdom
[152] School of Physics, University of Sydney, Sydney, Australia
[153] Institute of Physics, Academia Sinica, Taipei, Taiwan
[154] Department of Physics, Technion: Israel Institute of Technology, Haifa, Israel
[155] Raymond and Beverly Sackler School of Physics and Astronomy, Tel Aviv University, Tel Aviv, Israel
[156] Department of Physics, Aristotle University of Thessaloniki, Thessaloniki, Greece
[157] International Center for Elementary Particle Physics and Department of Physics, The University of Tokyo, Tokyo, Japan
[158] Graduate School of Science and Technology, Tokyo Metropolitan University, Tokyo, Japan
[159] Department of Physics, Tokyo Institute of Technology, Tokyo, Japan
[160] Tomsk State University, Tomsk, Russia
[161] Department of Physics, University of Toronto, Toronto ON, Canada
[162] [(a)] INFN-TIFPA; [(b)] University of Trento, Trento, Italy
[163] [(a)] TRIUMF, Vancouver BC; [(b)] Department of Physics and Astronomy, York University, Toronto ON, Canada
[164] Faculty of Pure and Applied Sciences, and Center for Integrated Research in Fundamental Science and Engineering, University of Tsukuba, Tsukuba, Japan
[165] Department of Physics and Astronomy, Tufts University, Medford MA, U.S.A.
[166] Department of Physics and Astronomy, University of California Irvine, Irvine CA, U.S.A.
[167] [(a)] INFN Gruppo Collegato di Udine, Sezione di Trieste, Udine; [(b)] ICTP, Trieste; [(c)] Dipartimento di Chimica, Fisica e Ambiente, Università di Udine, Udine, Italy

JHEP09(2017)088

[168] Department of Physics and Astronomy, University of Uppsala, Uppsala, Sweden
[169] Department of Physics, University of Illinois, Urbana IL, U.S.A.
[170] Instituto de Fisica Corpuscular (IFIC), Centro Mixto Universidad de Valencia - CSIC, Spain
[171] Department of Physics, University of British Columbia, Vancouver BC, Canada
[172] Department of Physics and Astronomy, University of Victoria, Victoria BC, Canada
[173] Department of Physics, University of Warwick, Coventry, United Kingdom
[174] Waseda University, Tokyo, Japan
[175] Department of Particle Physics, The Weizmann Institute of Science, Rehovot, Israel
[176] Department of Physics, University of Wisconsin, Madison WI, U.S.A.
[177] Fakultät für Physik und Astronomie, Julius-Maximilians-Universität, Würzburg, Germany
[178] Fakultät für Mathematik und Naturwissenschaften, Fachgruppe Physik, Bergische Universität Wuppertal, Wuppertal, Germany
[179] Department of Physics, Yale University, New Haven CT, U.S.A.
[180] Yerevan Physics Institute, Yerevan, Armenia
[181] CH-1211 Geneva 23, Switzerland
[182] Centre de Calcul de l'Institut National de Physique Nucléaire et de Physique des Particules (IN2P3), Villeurbanne, France
[183] Academia Sinica Grid Computing, Institute of Physics, Academia Sinica, Taipei, Taiwan

[a] Also at Department of Physics, King's College London, London, United Kingdom
[b] Also at Institute of Physics, Azerbaijan Academy of Sciences, Baku, Azerbaijan
[c] Also at Novosibirsk State University, Novosibirsk, Russia
[d] Also at TRIUMF, Vancouver BC, Canada
[e] Also at Department of Physics & Astronomy, University of Louisville, Louisville, KY, U.S.A.
[f] Also at Physics Department, An-Najah National University, Nablus, Palestine
[g] Also at Department of Physics, California State University, Fresno CA, U.S.A.
[h] Also at Department of Physics, University of Fribourg, Fribourg, Switzerland
[i] Also at II Physikalisches Institut, Georg-August-Universität, Göttingen, Germany
[j] Also at Departament de Fisica de la Universitat Autonoma de Barcelona, Barcelona, Spain
[k] Also at Departamento de Fisica e Astronomia, Faculdade de Ciencias, Universidade do Porto, Portugal
[l] Also at Tomsk State University, Tomsk, Russia
[m] Also at The Collaborative Innovation Center of Quantum Matter (CICQM), Beijing, China
[n] Also at Universita di Napoli Parthenope, Napoli, Italy
[o] Also at Institute of Particle Physics (IPP), Canada
[p] Also at Horia Hulubei National Institute of Physics and Nuclear Engineering, Bucharest, Romania
[q] Also at Department of Physics, St. Petersburg State Polytechnical University, St. Petersburg, Russia
[r] Also at Borough of Manhattan Community College, City University of New York, New York City, U.S.A.
[s] Also at Department of Financial and Management Engineering, University of the Aegean, Chios, Greece
[t] Also at Centre for High Performance Computing, CSIR Campus, Rosebank, Cape Town, South Africa
[u] Also at Louisiana Tech University, Ruston LA, U.S.A.
[v] Also at Institucio Catalana de Recerca i Estudis Avancats, ICREA, Barcelona, Spain
[w] Also at Graduate School of Science, Osaka University, Osaka, Japan
[x] Also at Fakultät für Mathematik und Physik, Albert-Ludwigs-Universität, Freiburg, Germany
[y] Also at Institute for Mathematics, Astrophysics and Particle Physics, Radboud University Nijmegen/Nikhef, Nijmegen, Netherlands
[z] Also at Department of Physics, The University of Texas at Austin, Austin TX, U.S.A.
[aa] Also at Institute of Theoretical Physics, Ilia State University, Tbilisi, Georgia

JHEP09(2017)088

[ab] Also at CERN, Geneva, Switzerland
[ac] Also at Georgian Technical University (GTU),Tbilisi, Georgia
[ad] Also at Ochadai Academic Production, Ochanomizu University, Tokyo, Japan
[ae] Also at Manhattan College, New York NY, U.S.A.
[af] Also at Departamento de Física, Pontificia Universidad Católica de Chile, Santiago, Chile
[ag] Also at Department of Physics, The University of Michigan, Ann Arbor MI, U.S.A.
[ah] Also at The City College of New York, New York NY, U.S.A.
[ai] Also at School of Physics, Shandong University, Shandong, China
[aj] Also at Departamento de Fisica Teorica y del Cosmos and CAFPE, Universidad de Granada, Granada, Portugal
[ak] Also at Department of Physics, California State University, Sacramento CA, U.S.A.
[al] Also at Moscow Institute of Physics and Technology State University, Dolgoprudny, Russia
[am] Also at Departement de Physique Nucleaire et Corpusculaire, Université de Genève, Geneva, Switzerland
[an] Also at Institut de Física d'Altes Energies (IFAE), The Barcelona Institute of Science and Technology, Barcelona, Spain
[ao] Also at School of Physics, Sun Yat-sen University, Guangzhou, China
[ap] Also at Institute for Nuclear Research and Nuclear Energy (INRNE) of the Bulgarian Academy of Sciences, Sofia, Bulgaria
[aq] Also at Faculty of Physics, M.V.Lomonosov Moscow State University, Moscow, Russia
[ar] Also at National Research Nuclear University MEPhI, Moscow, Russia
[as] Also at Department of Physics, Stanford University, Stanford CA, U.S.A.
[at] Also at Institute for Particle and Nuclear Physics, Wigner Research Centre for Physics, Budapest, Hungary
[au] Also at Giresun University, Faculty of Engineering, Turkey
[av] Also at CPPM, Aix-Marseille Université and CNRS/IN2P3, Marseille, France
[aw] Also at Department of Physics, Nanjing University, Jiangsu, China
[ax] Also at University of Malaya, Department of Physics, Kuala Lumpur, Malaysia
[ay] Also at Institute of Physics, Academia Sinica, Taipei, Taiwan
[az] Also at LAL, Univ. Paris-Sud, CNRS/IN2P3, Université Paris-Saclay, Orsay, France
[*] Deceased

JHEP09(2017)088